

RESTRICTED

**Energy/Geological Survey of
the Netherlands**

Princetonlaan 6
3584 CB Utrecht
P.O. Box 80015
3508 TA Utrecht
The Netherlands

www.tno.nl

T +31 88 866 42 56
F +31 88 866 44 75

TNO report

TNO 2014 R11703

**Recent developments of the Groningen field in
2014 and, specifically, the southwest
periphery of the field**

Date	9 December 2014
Author(s)	Karin van Thienen-Visser, Manuel Nepveu, Bart van Kempen, Marloes Kortekaas, Jenny Hettelaar, Lies Peters, Serge van Gessel, Jaap Breunese
Copy no	
No. of copies	
Number of pages	96 (incl. appendices)
Number of appendices	6
Sponsor	Ministry of Economic Affairs
Project name	C1 Trillingen - Groningen
Project number	060.07751/01.02

All rights reserved.

No part of this publication may be reproduced and/or published by print, photoprint, microfilm or any other means without the previous written consent of TNO.

In case this report was drafted on instructions, the rights and obligations of contracting parties are subject to either the General Terms and Conditions for commissions to TNO, or the relevant agreement concluded between the contracting parties. Submitting the report for inspection to parties who have a direct interest is permitted.

© 2014 TNO

RESTRICTED

Nederlandse samenvatting

Titel : Recent developments of the Groningen field in 2014 and, specifically, the southwest periphery of the field
Auteur(s) : Karin van Thienen-Visser, Manuel Nepveu, Bart van Kempen, Marloes Kortekaas, Jenny Hettelaar, Lies Peters, Serge van Gessel, Jaap Breunese
Datum : 9 december 2014
Rapportnr. : TNO 2014 R11703

Doel en achtergrond

Op 17 januari 2014 besloot de minister van Economische zaken om een plafond voor de productie van het Groningen veld vast te stellen van 42.5 miljard Nm³ voor 2014 en 2015 en 40 miljard Nm³ voor 2016 en daarnaast om de productie van de vijf Loppersum clusters in het Groningen veld met 80% te verminderen voor de periode van januari 2014 tot januari 2017. De motivatie van deze reductie is het verlagen van de seismische dreiging in het centrale deel van het veld.

De NAM heeft hier meteen gehoor aan gegeven door de productie van de vijf Loppersum clusters terug te draaien op 17 januari 2014. Een beving van magnitude 2.8 bij Ten Boer op 30 september 2014 leidde tot kamervragen. Hierop kwam het verzoek van de minister aan NAM om de bevingsgevoeligheid voor de zuidwest periferie van het Groningen gasveld te analyseren (nabij het Eemskanaal cluster). Aan het Staatstoezicht op de Mijnen (SodM) is gevraagd om over deze analyse te adviseren. SodM heeft in dit kader aan TNO gevraagd om een technisch rapport op te stellen. Daarbij zijn de nieuwe gegevens gebruikt, die sinds het ontwerpbesluit ter beschikking zijn gekomen.

Dit rapport richt zich op:

- Zijn er aanwijzingen dat de productiebeperking effect heeft?
- Analyse van het ondergrondmodel van de de zuidwestelijke periferie.
- Review van de analyse van NAM over de zuidwestelijke periferie.
- Actualisatie van het rapport (TNO 2014a, b).

De belangrijkste bevindingen op bovengenoemde punten zijn hier samengevat:

- Er zijn aanwijzingen dat de productiebeperking effect heeft op de seismiciteit. Op dit moment zijn nog onvoldoende monitoringsdata beschikbaar om hier statistisch sterke uitspraken over te doen.
- De productie van de Eemskanaal (EKL) cluster in 2014 is hoger dan eerder in de modellen aangenomen. De compactie in de zuidwestelijke periferie is groter dan tot nu toe werd aangenomen en past beter bij de gemeten bodemdaling. Dit is in lijn met de NAM analyse, waarin een tweetal compactiemodellen worden meegenomen. TNO verwacht dat verlaging van productie van de Eemskanaal cluster een tijdelijk effect op de druk in het zuidwestelijke deel van het Groningen veld zal hebben van circa twee jaar.
- NAM heeft voor de zuidwestelijke periferie naar een voldoende breed spectrum aan modellen gekeken. Echter, bekende onzekerheden in het ondergrondmodel worden niet meegenomen in de calibratie van het seismologisch model. Ook in deze analyse van NAM wordt de ruimtelijke differentiatie van de seismische dreiging slechts beperkt meegenomen.

- De ruimtelijke verdeling van de indicator voor seismische dreiging is vergelijkbaar met het (waargenomen) verschil in aardbevingsdichtheid voor de jaren 2013 en 2014. De (gemodelleerde) indicator suggereert een lokale respons op de gemeten seismiciteit (in het bijzonder de locatie van bevingen).

Summary

Titel : Recent developments of the Groningen field in 2014 and, specifically, the southwest periphery of the field

Auteur(s): Karin van Thienen-Visser, Serge van Gessel, Jenny Hettelaar, Bart van Kempen, Marloes Kortekaas, Manuel Nepveu, Lies Peters, Jaap Breunese

Datum : 5 december 2014

Rapportnr. : TNO 2014 R11703

Goal and background

On the 17th of January 2014 the Minister of Economic Affairs decided to impose a production cap of 42.5 billion Nm³ for 2014, 2015 and 40 billion Nm³ for 2016. Additionally, production of the five central Loppersum clusters in the Groningen field was reduced by 80% for the period from January 2014 until January 2017. This reduction had the objective to reduce seismic hazard in the central part of the field.

NAM has complied with this decision on January 17th 2014 by reducing production of the five Loppersum clusters. A $M_L=2.8$ event near Ten Boer on the 30th of September 2014 led to new questions from the Second Chamber of Parliament. In response, the Minister has requested NAM to assess the specific seismic hazard for the south-west periphery of the Groningen field (near the Eemskanaal cluster). SodM (State Supervision of Mines) was asked to give advice on the outcomes of this assessment. Subsequently, SodM commissioned TNO to provide a technical report. This TNO report uses all new data which have become available since the decision of January 2014 and addresses the following topics:

- Are there indications of an effect on seismicity due to the production reduction as imposed on January 17th 2014?
- Analysis of the subsurface model, focusing on the south-west periphery.
- Review of the analysis of NAM (2014) report on the seismic hazard of the Eemskanaal area.
- Actualization of the TNO report (2014a, b).

Important findings on the abovementioned points are summarized as follows:

- There are indications that the reduction of production since January 17th 2014 has had influence on the seismicity in the field. However, at this moment insufficient data is available for any degree of statistical significance.
- The actual production of the EKL cluster in 2014 is higher than assumed before. Also, the compaction in the south-west periphery is larger which gives a better match to the observed subsidence. This finding is in agreement with the NAM analysis, where two compaction models have been taken into account. TNO expects that a reduction in production of the Eemskanaal cluster will have a temporary effect of about two years in the southwestern periphery of the Groningen field.
- NAM has looked at a broad spectrum of models for the southwest periphery. However, known uncertainties of the subsurface model are not taken into account in the calibration of the seismological model of NAM. Also, in the NAM analysis spatial differentiation is only partially taken into account.

- The spatial distribution of the seismic hazard indicator is similar to the difference in earthquake density as observed for the years 2013 and 2014. The seismic hazard indicator suggests a local response in terms of seismicity (i.e. location of seismic events).

Contents

	Nederlandse samenvatting	2
	Summary	4
1	Introduction	12
2	Recent developments in 2014	14
2.1	Introduction	14
2.2	Gas production 2013 versus 2014.....	14
2.3	Observed seismic events 2013 versus 2014.....	16
2.4	Correlation between gas production and event density	22
2.5	Statistics of the induced seismicity of the Groningen field	24
3	Geological evaluation and petrophysical analysis Eemskanaal area	29
3.1	Introduction	29
3.2	Geological setting	29
3.3	Petrophysical evaluation.....	30
3.4	Compaction coefficient	31
3.5	Modelled porosity distribution	31
3.6	Summary of findings.....	37
4	Possible delay effect on compaction of reducing Eemskanaal production	38
5	Review of report on Eemskanaal area of NAM	40
5.1	Introduction	40
5.2	Reservoir compaction in the Eemskanaal area.....	40
5.3	Seismic hazard of the Eemskanaal area	49
5.4	Overall findings on the NAM (2014) report.....	52
6	TNOs seismic hazard indicator	54
7	Main Findings	56
8	References	58
9	Signature	60
	Appendices	
	A Derivation of relation time-distance of pressure wave	
	B Bayesian Statistical method	
	C Petrophysical analysis	
	D Geological information at location Eemskanaal based on static model	
	GFR2012	
	E Reservoir dynamics	
	F Earthquake density maps for 2003 to 2012	

List of Figures

Figure 2-1. The production of each cluster in the Groningen field in the time from April 1 st to November 1 st in 2013 and 2014.	15
Figure 2-2. Left: The distance a pressure wave has travelled through the reservoir since the time of the production change (17 th January 2014) in the case of a permeability of 350 mD. The lower limit is the distance for 99% of the effect, the higher limit gives the wave front. The effect of permeability on the distance travelled (time*permeability \propto distance ²).....	16
Figure 2-3. Distance travelled (mid November 2014) by the pressure wave from the five clusters where production was lowered on 17 th January 2014, top: 2.2 km (99% of pressure wave), bottom: 6.7 km (first arrival pressure wave). Background is the cumulative compaction of January 2014 according to TNO (2014).....	18
Figure 2-4. Earthquake density (number of events per km ²) from April 1 st 2013 to November 1 st 2013. The observed events in the same period and their magnitudes are indicated by the coloured small circles.	19
Figure 2-5. Earthquake density (number of events per km ²) from April 1 st 2014 to November 1 st 2014. The circles indicate and area of 3.5 km in which the pressure wave has travelled in 10 months (with an average permeability of 150 mD). The observed events in the same period and their magnitudes are indicated by the coloured small circles. The colour scale is the same as Figure 2-4 to allow for comparison.	20
Figure 2-6. Difference in earthquake density (number of events per km ²) between April 1 st and November 1 st in 2013 and 2014. A positive (green) difference indicates a lower earthquake density in 2014 compared to 2013. The circles indicate and area of 3.5 km in which the pressure wave has travelled in 10 months (with an average permeability of 150 mD).....	21
Figure 2-7. Difference in production (in 10 ⁵ Nm ³) from April 1 st to November 1 st in 2013 compared to the same period in 2014. A positive (green) difference indicates a smaller production in 2014 compared to 2013.	23
Figure 2-8. Number of events in time (top), with in colour the magnitude of the seismic events. In 2014, only the events up to November 1 st have been taken into account. Bottom: production in billion cubic meters (bcm) per year.	24
Figure 2-9. Definition of the SW and Central area. The background colour is the cumulative compaction, calculated with the RTiCM model (Rate Type Compaction Model in Isotach formulation) as described in TNO (2013, 2014b) for January 2014. In red the contours of the Central area and the SW area.	25
Figure 2-10. Probability density functions for the time constant in the increase models for Central, SW and Other. The Bayesian prior probability used in the calculations is Jeffrey's prior. See the Appendix B.....	27
Figure 3-1. Outline Groningen field (red) on depth map Top Rotliegend surface. Modelled faults are indicated in grey and the main well locations and production clusters in black (Petrel GFR2012 model). A blue circle indicates the location of production cluster Eemskanaal (EKL).....	33
Figure 3-2. Structural map of Top Rotliegend showing the location of the Eemskanaal cluster wells (based on Petrel GFR2012 model).	34

Figure 3-3. Average porosity for the USS.2.res zone based on the GFR2012 porosity model at the Eemskanaal location.	35
Figure 3-4. Porosity trend map of the USS2.res zone as used in the interpolation process for calculating average porosity maps. Wells indicated with white squares are used to create this trend map.	36
Figure 4-1. Time it would take for the first arrival of a pressure wave in the reservoir to travel 2, 4, 6, 8 and 10 km from the EKL cluster.	39
Figure 5-1. Results from compaction tests on Groningen cores: compaction coefficient vs porosity of the sample.	42
Figure 5-2. Permeability multipliers as applied in the STR38 and STR40 model (left) and water saturation (right).	44
Figure 5-3. Pressure history match of wells HRS-2A, EKL-13, KHM-1 and TBR-4 for STR38, STR40 and the 2013 production plan model (NAM 2013) with updated 2013 production data (all geological model G1).	45
Figure 5-4. Cumulative compaction (January 2014) according to model STR40 (NAM), left, and model STR38 (NAM 2014), right. The contour of the Groningen field is in black as well as the topography, and a number of cities have been indicated (GRO=Groningen, LOP=Loppersum, SPK=Spijk, SDB=Siddeburen, HGZ=Hoogezand, WIN=Winschoten, DLZ=Delfzijl).	46
Figure 5-5. Difference (cm) between measured and modelled subsidence with STR40 (left)/STR38 (right). A negative difference indicates subsidence is underpredicted in the modelled subsidence.	46
Figure 5-6. Difference between measured and modelled subsidence (in m) of model STR40 (left) and model STR38 (right) for measurements over the whole field. Compaction is calculated using the RTICM model (TNO 2013, Pruiksma et al., <i>submitted</i> 2014).	47
Figure 5-7. Difference in cumulative compaction (m) between the model F524_Lsum3 (TNO 2014a) and model STR40 (NAM 2014), left. Right, difference in cumulative compaction between the model F524_Lsum3 (TNO 2014a) and model STR38 (NAM 2014). A negative difference indicates areas where the 'new' model (STR40/STR38) gives less compaction than the 'old' model (F425_Lsum3). The background is similar to Figure 5-4.	48
Figure 5-8. Difference in cumulative compaction (m) in January 2014 between the model STR38 (NAM 2014) and the model STR40 (NAM 2014). A positive difference indicates areas where the STR38 model gives more compaction than the STR40 model. The background is similar to Figure 5-4.	48
Figure 5-9. Actual and modelled production of the Eemskanaal (EKL) cluster in 2014 per month (January to September).	49
Figure 6-1. Partitioning coefficient for the relationship described in (TNO, 2014b) for the two models of NAM (2014): STR38 (left) and STR40 (right). The background is similar to Figure 5-4.	54
Figure 6-2. Seismic hazard indicator for the STR38 model with 8 mln Nm ³ /day production of EKL compared to a scenario that follows the market demand.	55
Figure C-1. Porosity vs permeability measured on core plug samples from the Slochteren Sandstone in wells EKL-12.	2
Figure C-2. Contour plot of data-point density based on black data points. Black point set represents EKL-12 core porosity measurements versus bulk density. The black line is defined by TNO and represents the linear trend through this	

set. The purple point set represents porosity values from NAM’s porosity profile versus bulk density. The purple line, defined by NAM, represents the trend through this set.5

Figure C-3. NAM Porosity from maps at well locations (blue) and average porosity from NAM’s porosity logs (red) for the USS3 reservoir.8

Figure C-4. NAM Porosity from maps at well locations (blue) and average porosity from NAM’s porosity logs (red) for the USS2 reservoir.8

Figure C-5. NAM Porosity from maps at well locations (blue) and average porosity from NAM’s porosity logs (red) for the USS1 reservoir.8

Figure C-6. NAM Porosity from maps at well locations (blue) and average porosity from NAM’s porosity logs (red) for the LSS2 reservoir9

Figure C-7. EKL-09 porosity log (left) and compaction coefficient log (right). Above about 17-18% porosity the compaction coefficient increases significantly.....11

Figure C-8. Well panel from West to East through 6 wells in the Eemskanaal cluster, representing Cm logs.12

Figure D-1 Position of Eemskanaal cluster wells on Top Rotliegend depth surface (GFR2012).2

Figure D-2 Close-up of position of Eemskanaal cluster wells EKL-1 to EKL-12 on Top Rotliegend depth surface (GFR2012).3

Figure D-3 Transect showing the different FWL at the EKL-13 location (Harkstede block) at 3016 mTVD in the Upper Slochteren 1 zone vs the 2995mTVD at the Eemskanaal cluster location (FWL in the Carboniferous).3

Figure D-4 Transect through Eemskanaal cluster shows lower porosity in downthrown blocks.4

Figure D-5 Porosity trend map for the Upper Slochteren 3 reservoir zone (USS3.res). The white squares indicate the wells NAM considered to be relevant to create the trend map (GFR2012). From the GFR2012 report it is unclear which Eemskanaal was chosen apart from the EKL-13 well.5

Figure D-6 Average porosity map for the USS3.res zone based on the GFR2012 porosity model at the Eemskanaal location.6

Figure D-7 Porosity trend map for the Upper Slochteren 2 reservoir zone (USS2.res). The white squares indicate the wells NAM considered to be relevant to create the trend map (GFR2012). From the GFR2012 report it is unclear which Eemskanaal was chosen apart from the EKL-13 well.7

Figure D-8 Average porosity for the USS2.res zone based on the GFR2012 porosity model at the Eemskanaal location.8

Figure D-9 Porosity trend map for the Upper Slochteren 1 reservoir zone (USS1.res). The white squares indicate the wells NAM considered to be relevant to create the trend map (GFR2012). From the GFR2012 report it is unclear which Eemskanaal was chosen apart from the EKL-13 well.9

Figure D-10 Average porosity for the USS1.res zone based on the GFR2012 porosity model at the Eemskanaal location.10

Figure E-1. Pressure in the top of the Upper Slochteren formation (ROSLU, model layer 4) showing the effect of the aquifer in Oct 20141

Figure E-2. Pressure on 1 Oct 2014 in the top of Upper Slochteren formation (ROSLU, model layer 4), for STR 40 (left) and STR40 with viscosity of the Lauwersee aquifer from the production plan model (right).2

Figure E-3. Pressure history match for well HRS-2A for STR40 (left) and STR40 with the viscosity of the Lauwersee aquifer from the production plan model (right).....3

List of Tables

Table 4-1. Time of arrival of the pressure wave in the area of Eemskanaal (average permeability of 100 mD) as a function of the distance to the EKL cluster.	38
Table 5-1. Overview of local causes of uncertainty.	41
Table C-1. Available log data for wells in the Eemskanaal cluster.	1
Table C-2. Overview of core data used for petrophysical evaluation.	2
Table C-3. Overview of determined and calculated porosity values for the USS3.res reservoir interval.	6
Table C-4. Overview of determined and calculated porosity values for the USS2.res reservoir interval.	6
Table C-5. Overview of determined and calculated porosity values for the USS1.res reservoir interval.	7
Table C-6. Overview of determined and calculated porosity values for the LSS2.res reservoir interval.	7
Table C-7. Calculations of the relative increase of compaction coefficient with respect to 1% and 2% porosity increase for well EKL-09.	12
Table D-1. List of wells in the production cluster Eemskanaal with their location (RD reference system) and top Rotliegend in True Vertical Depth (TVD in m) and measured depth (MD in m along hole).	1

1 Introduction

Background

On the 17th of January 2014, the minister of Economic Affairs decided to reduce production from five production clusters in the centre of the Groningen field to 3 bcm per year for the period 2014 - 2016 in order to try to reduce the seismicity in the centre of the field. In addition, total field production was limited to 42.5 bcm for 2014 and 2015 and 40 bcm for 2016 (EZ 2014). Preceding this decision, technical reports (NAM 2013, TNO 2013) concluded that the seismicity is related to the compaction (and hence the production) of the Groningen field. In March 2014, TNO (TNO 2014a, b) analysed various production scenarios to indicate the relative seismic hazard change in the Groningen field, comparing the original production plan scenario and the reduced production plan in accordance with the decision of the Minister. The results indicated a potentially substantial reduction of seismic hazard in the centre of the field and a relatively small increase of seismic hazard just north of Hoogezand (TNO 2014b).

Scope

Recent seismic events that occurred after the decision to reduce production at the Loppersum clusters, including a magnitude 2.8 seismic event (30th of September 2014) close to the Eemskanaal cluster, have raised new questions from the Second Chamber of Parliament concerning the development of the seismic hazard in relation to the adjusted production plan. In response to these questions the Minister of Economic Affairs (MEA) has asked NAM to assess the seismic hazard in the area of the Eemskanaal cluster. State Supervision of Mines (SodM) has been asked for advice regarding the outcomes of NAM's assessment.

TNO has provided SodM with technical support needed for their advice. In this context TNO has carried out technical evaluations with regard to the following issues:

- 1) Are there indications of an effect on seismicity due to the production reduction as imposed on January 17th 2014?
- 2) Analysis of compaction near the Eemskanaal cluster. Is there a geological ground to explain discrepancies between modelled and observed subsidence in terms of porosity and associated compaction coefficient.
- 3) Review of NAMs (2014) report on the hazard of the Eemskanaal area
- 4) Actualization of the report TNO (2014).

Report set up

Chapters 2 to 4 report the key results and findings of TNO's technical evaluations.

- Chapter 2 shows the recent developments in terms of production and observed seismicity in 2014 and the statistical evaluation of the seismic events.
- Chapter 3 describes the petrophysical and geologic results concerning the porosity in the southwest periphery of the Groningen field.
- Chapter 4 discusses the possible effect, should the production of the Eemskanaal be reduced.

Chapter 5 discusses NAM's assessment, thereby using TNO's results as an independent reference.

Chapter 6 covers the actualization of the relative seismic hazard indicator as presented in TNO (2014a, b).

Chapter 7 summarizes the findings with regard to the questions posed by SodM.

Technical background, methodologies and in-depth technical analysis results are reported separately in the Appendices.

2 Recent developments in 2014

2.1 Introduction

The reduction of production in 2014 (Figure 2-1) in the centre of the Groningen field was aimed at reducing seismic hazard. In the studies of 2013 (NAM 2013, TNO 2013), production was directly linked to the compaction of the Groningen field which, in turn, was linked to the occurrence of seismicity. The observed rate of seismicity (number of events per unit of time and unit of area) should, therefore, indicate whether the decrease in production rate has had an effect in 2014.

This chapter presents the results from the following evaluations: 1) analysis of the pressure wave front induced by the decreased production rate at the Loppersum clusters, 2) analysis of the density of seismicity before and after January 2014, and 3) analysis of production versus seismicity and the statistical analysis of the entire history of induced seismicity of the Groningen field.

2.2 Gas production 2013 versus 2014

Figure 2-1 shows per cluster, what the level of gas production has been in 2013 relative to 2014 in the same period of the year (April 1st tot November 1st). Clearly, the gas production in the Loppersum area clusters (LRM, POS, PAU, OVS and ZND) has been strongly reduced, as was requested by the minister of Economic Affairs on January 17th 2014. Some clusters in the eastern fringe have produced somewhat more in 2014, while in the southern fringe production levels have been maintained. In the southwestern area, Eemskanaal has produced somewhat less, whereas Harkstede in 2013 has produced only minor volumes compared to 2013.

The reduction in production will not lead to an immediate response of the reservoir due to the time it takes for a pressure wave (in the gas phase) to travel through the reservoir. In Appendix A an analytical relation is derived between the distance the front of a pressure wave has travelled and the time since production was reduced. Figure 2-2 (left) shows this relation for a (horizontal) permeability of 350 mD. After 10 months (17th of November) the distance travelled of the first pressure wave is 6.7 km. In this period the full (99%) pressure wave has travelled only a third of that distance (2.2 km). Figure 2-2 (right) shows the effect of the permeability on the travelled distance of the first pressure wave.

The permeability in the centre of the Groningen gas field varies between 150 and 500 mD. A permeability of 350 mD was chosen as a reasonable average value for the centre of the field. Given this permeability, the pressure wave from the affected clusters (POS, PAU, OVS, LRM and ZND) will have travelled a few kilometers, i.e. 2.2 km (99% of wave has arrived) and 6.7 km (first arrival of wave), during the period from 17th January 2014 to 17th November 2014 (Figure 2-3).

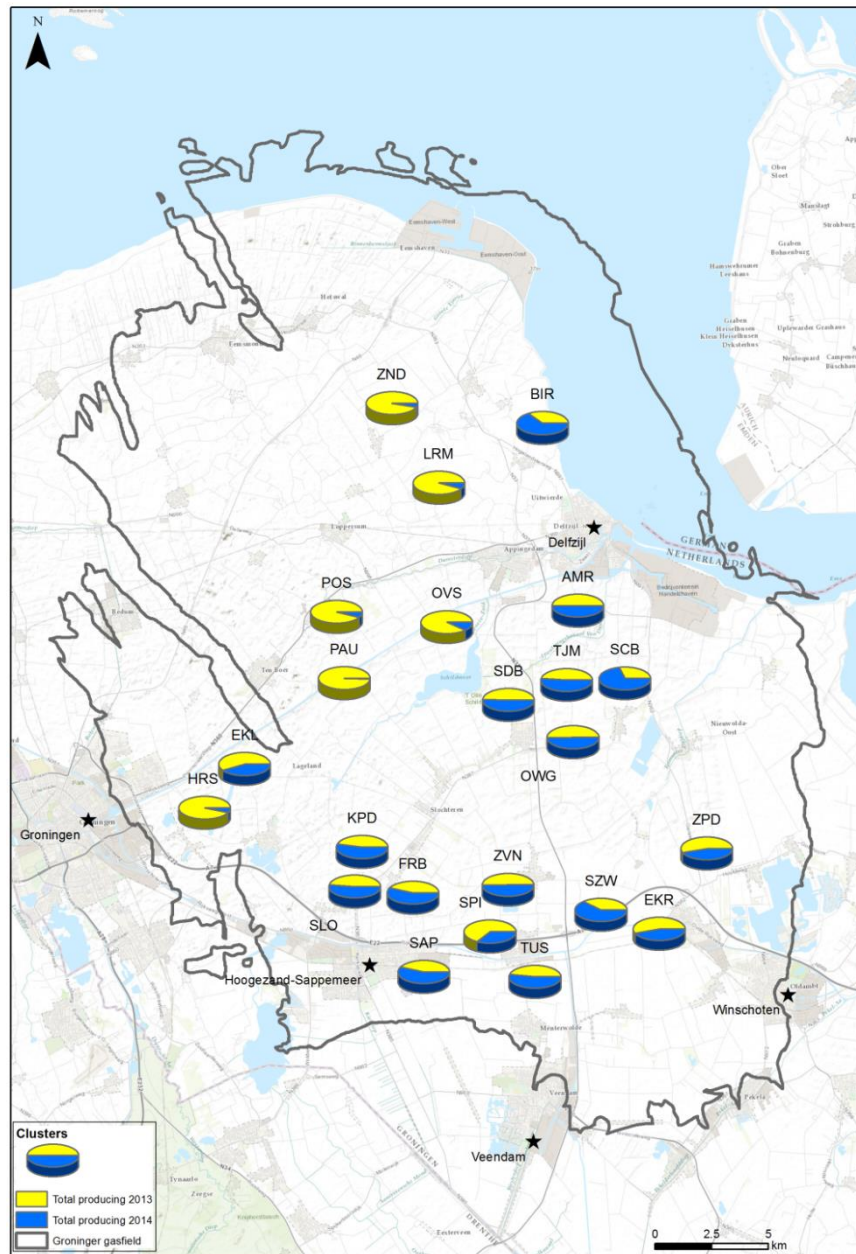


Figure 2-1. The production of each cluster in the Groningen field in the time from April 1st to November 1st in 2013 and 2014.

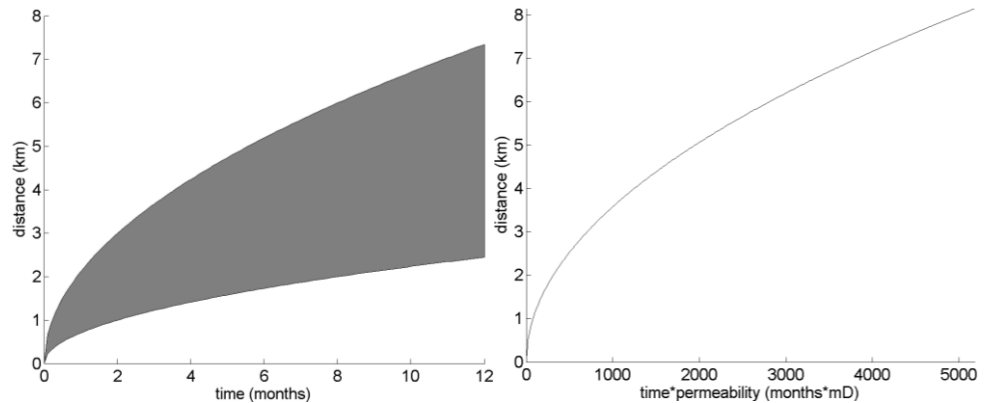


Figure 2-2. Left: The distance a pressure wave has travelled through the reservoir since the time of the production change (17th January 2014) in the case of a permeability of 350 mD. The lower limit is the distance for 99% of the effect, the higher limit gives the wave front. The effect of permeability on the distance travelled ($\text{time} \cdot \text{permeability} \propto \text{distance}^2$).

At any point on the surface, the subsidence at this point is a summation of compaction over a circular area in the reservoir with a radius equal to the depth of the reservoir. The GPS measurements of Ten Post (NAM, 2014b) show a change in subsidence rate around April 2014. This would indicate that the area in the reservoir which is influenced by the reduction of pressure should have a radius of about 3 km. After 3 months (January 17th to April 17th) the pressure wave front could be ranging from 3.7 km to 4.4 km and the full pressure wave (99%) from 1.2 km to 1.4 km depending on the permeability (150 mD and 500 mD, respectively). These values are within the range of the subsidence rate change observation in the GPS signal. GPS measurements are taken every hour and are, thus, well equipped to observe changes in subsidence rate. The measurement time since January 17th 2014 is, however, not extended enough to give firm evidence for a subsidence rate change.

2.3 Observed seismic events 2013 versus 2014

In Appendix F the earthquake density of observed events with magnitudes larger than 1.0 (source: KNMI) is plotted per year from 2003 up to 2013. The earthquake density was determined using a Kernel Density (standard GIS application) with a radius of 5 km and a cell size of 50 m.

The pattern of the earthquake density is quite similar for most years (except maybe 2010), with the highest density in the centre of the field. Again, the pattern of event density of 2014 is quite different from the previous years (2003 to 2013).

In Figure 2-4 and Figure 2-5 the density of observed events is shown for the period April 1st to November 1st in 2013 and 2014, respectively. April 1st corresponds to the date where the pressure wave should have travelled 2 to 4 km since January 17th 2014 (first arrival, depending on permeability). November 1st was chosen as the seismicity database in 2014 was extended up to this date.

Figure 2-4 to Figure 2-6 illustrate that the spatial variation in earthquake density is different between 2013 and 2014. In 2013 (Figure 2-4) the centre of the field and a patch around the south-western part of the field have the highest earthquake densities. In 2014 (Figure 2-5), the overall amplitude of the earthquake density is much lower (by a factor 2) with largest reductions shown for the centre of the field (Figure 2-6). The highest earthquake densities in 2014 are found at the south-western part of the Groningen field, in the patch north of Hoogezand and the area around Tjuchem. For the last two areas more events have been recorded in 2014 than in 2013 (Figure 2-6). The statistical significance of this will be examined in paragraph 2.5.

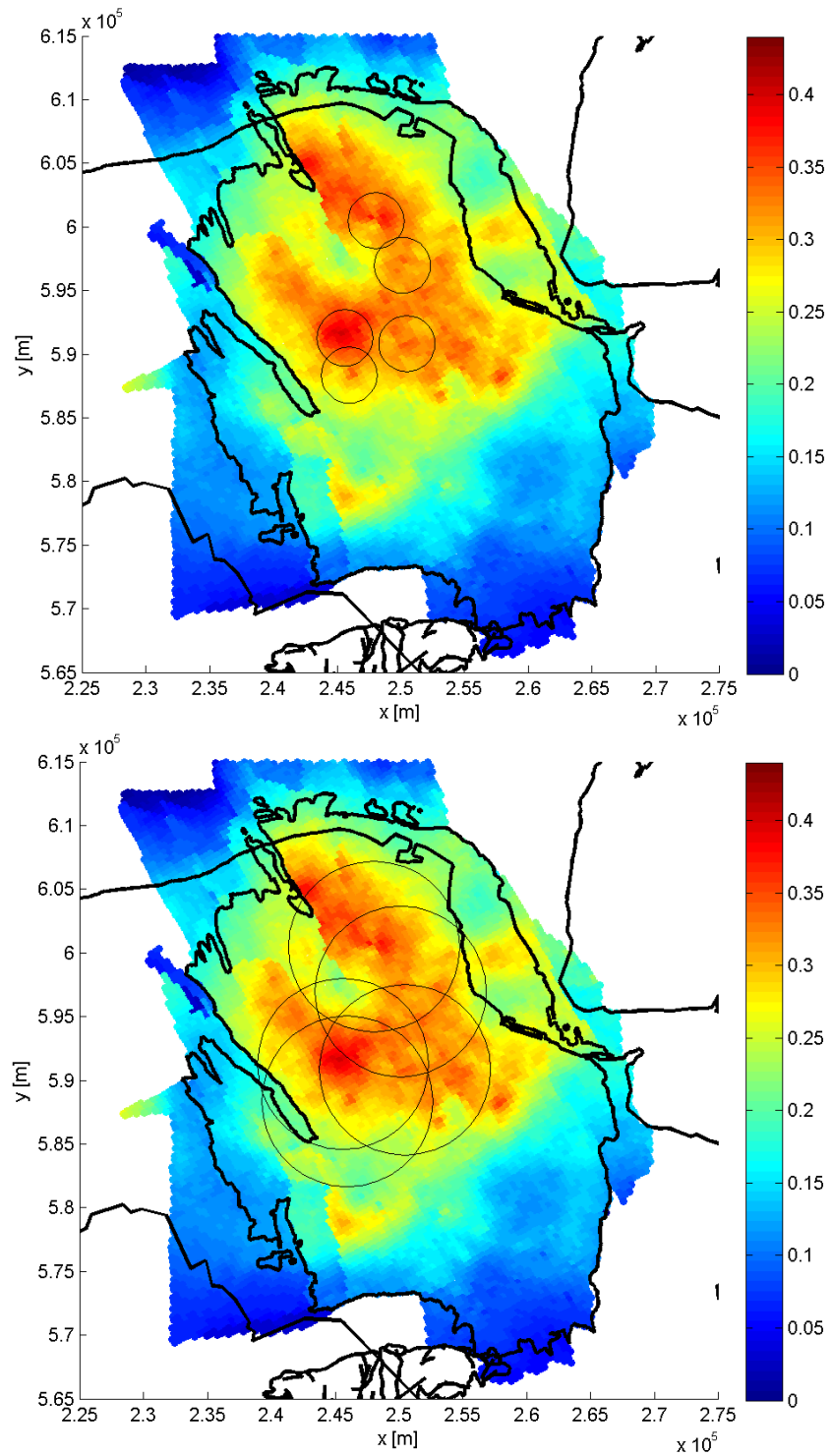


Figure 2-3. Distance travelled (mid November 2014) by the pressure wave from the five clusters where production was lowered on 17th January 2014, top: 2.2 km (99% of pressure wave), bottom: 6.7 km (first arrival pressure wave). Background is the cumulative compaction of January 2014 according to TNO (2014).

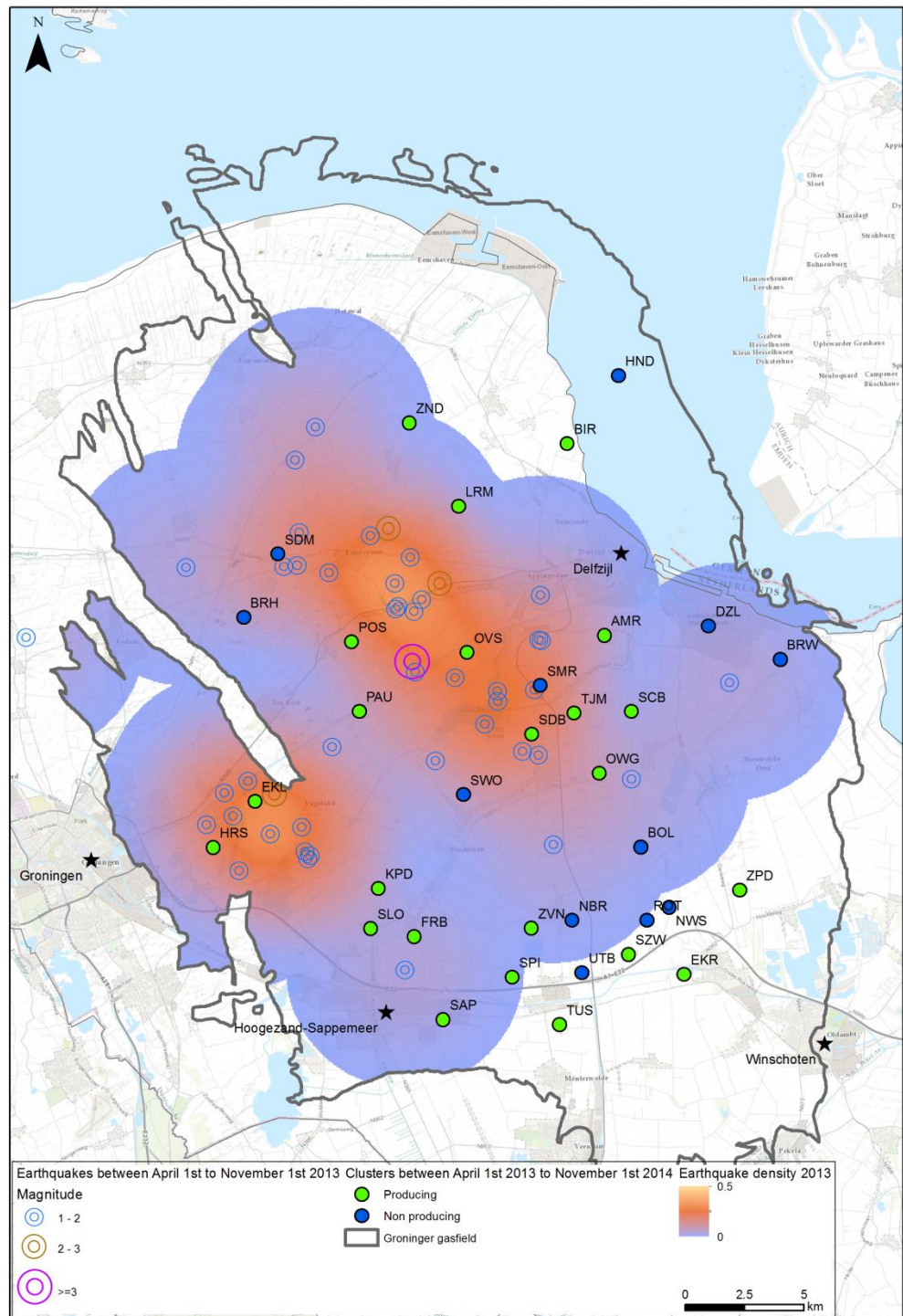


Figure 2-4. Earthquake density (number of events per km²) from April 1st 2013 to November 1st 2013. The observed events in the same period and their magnitudes are indicated by the coloured small circles.

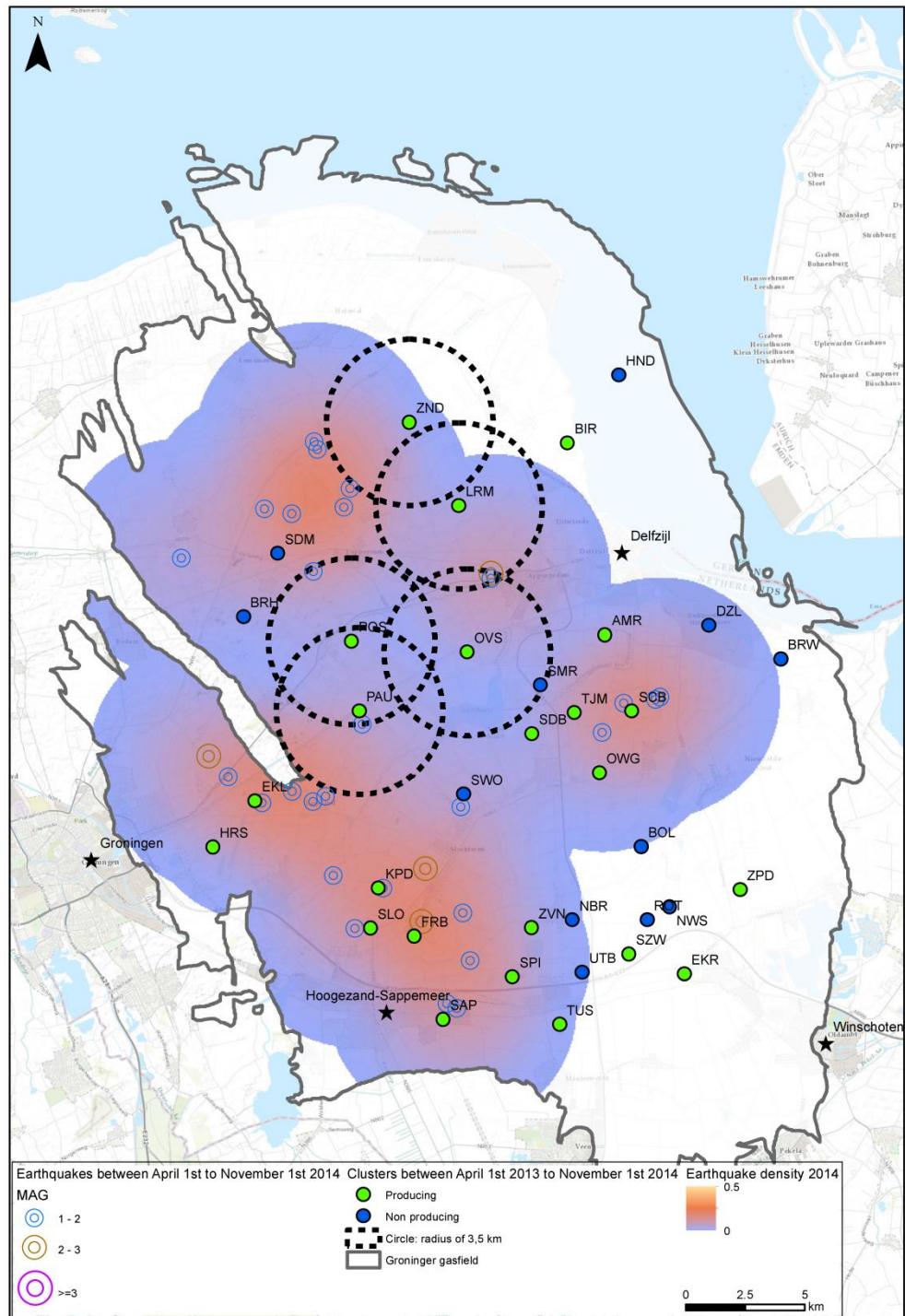


Figure 2-5. Earthquake density (number of events per km²) from April 1st 2014 to November 1st 2014. The circles indicate and area of 3.5 km in which the pressure wave has travelled in 10 months (with an average permeability of 150 mD). The observed events in the same period and their magnitudes are indicated by the coloured small circles. The colour scale is the same as Figure 2-4 to allow for comparison.

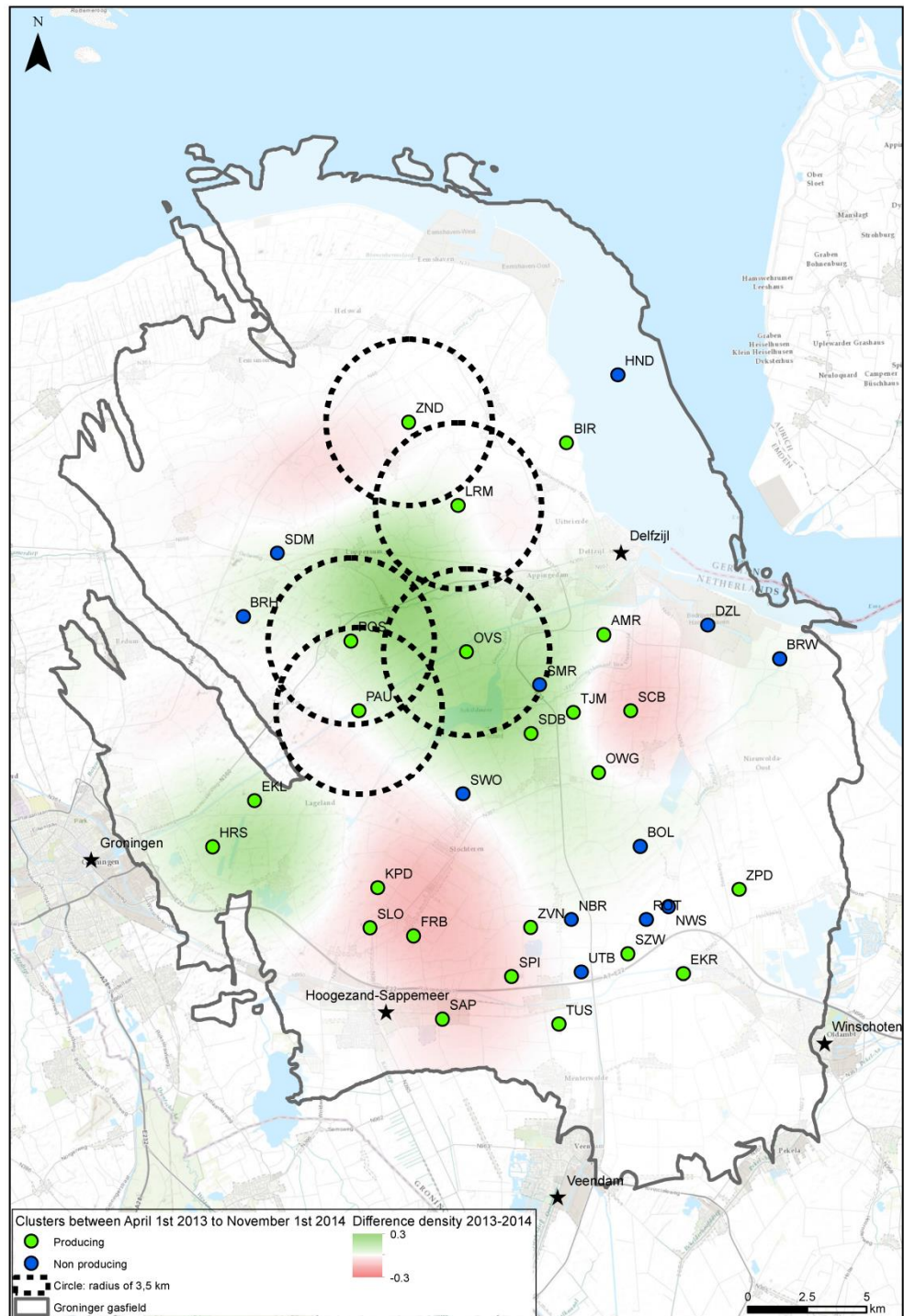


Figure 2-6. Difference in earthquake density (number of events per km²) between April 1st and November 1st in 2013 and 2014. A positive (green) difference indicates a lower earthquake density in 2014 compared to 2013. The circles indicate and area of 3.5 km in which the pressure wave has travelled in 10 months (with an average permeability of 150 mD).

2.4 Correlation between gas production and event density

Figure 2-7 shows the difference in production between April 1st and November 1st for 2013 and 2014. The production per cluster is averaged over an area which corresponds to the distance a pressure wave can travel in 10 months (17th January to 17th November) using a low permeability of 150 mD (3.5 km distance of pressure wave). The largest difference is observed in the centre of the Groningen gas field. By comparing Figure 2-6 with Figure 2-7 there seems to be a correlation between production and seismicity. This would support the link between production and seismicity, as proposed in TNO (2013). Furthermore, the seismic response of the reservoir to a change in production seems to be almost instant with a delay of only a few months. The delay is probably due to the time it takes before the effect is present in a larger area of the reservoir (Appendix A).

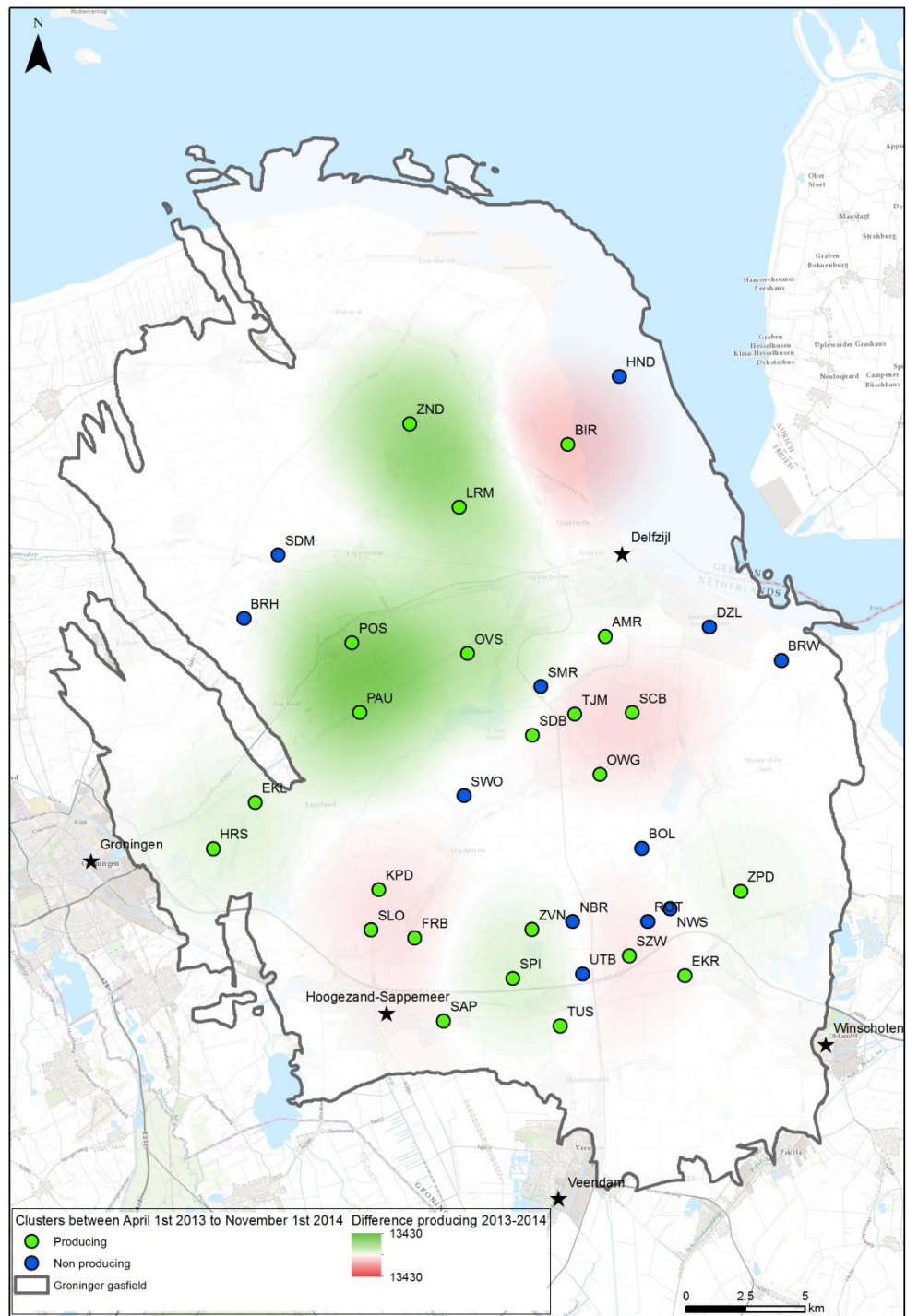


Figure 2-7. Difference in production (in 10^5 Nm^3) from April 1st to November 1st in 2013 compared to the same period in 2014. A positive (green) difference indicates a smaller production in 2014 compared to 2013.

2.5 Statistics of the induced seismicity of the Groningen field

This paragraph discusses the time dependence of seismicity in Groningen using Bayesian Statistics. Figure 2-8 shows the year by year aggregated data on seismicity and production. A change in characteristics for the year 2003 seems visible in the seismicity time series. The frequency of the seismic events seems to increase in the period after 2002 and events with a magnitude of 3 and higher make their appearance as well.

The date of 17th January 2014 is of special interest as at this date the production was reduced at the five Loppersum clusters (PAU, POS, LRM, OVS, and ZND) located in the centre of the Groningen gas field. If the occurrence of seismicity is directly linked to compaction in the reservoir (NAM 2013, TNO 2013), a reduction of production would lead to a change in the observed seismicity over the field. This change would be either almost instantaneous (as in the case for the Rate Type Compaction Model (RTiCM, TNO 2013, 2014, Pruiksma et al., *submitted*) or with some time delay (in the order of 7 years for the Time Decay model of NAM).

From a physical point of view, some time is needed before changes in the pressure field as a result of a change in production are communicated over the Groningen field (Appendix A). In this paragraph we therefore want to investigate:

1. whether there is statistical evidence that seismicity is behaving differently in the period after December 2002 with regard to the period before January 2003 and,
2. Whether statistical analysis supports a significant change in the frequency of seismic events for the period after 17th January 2014.

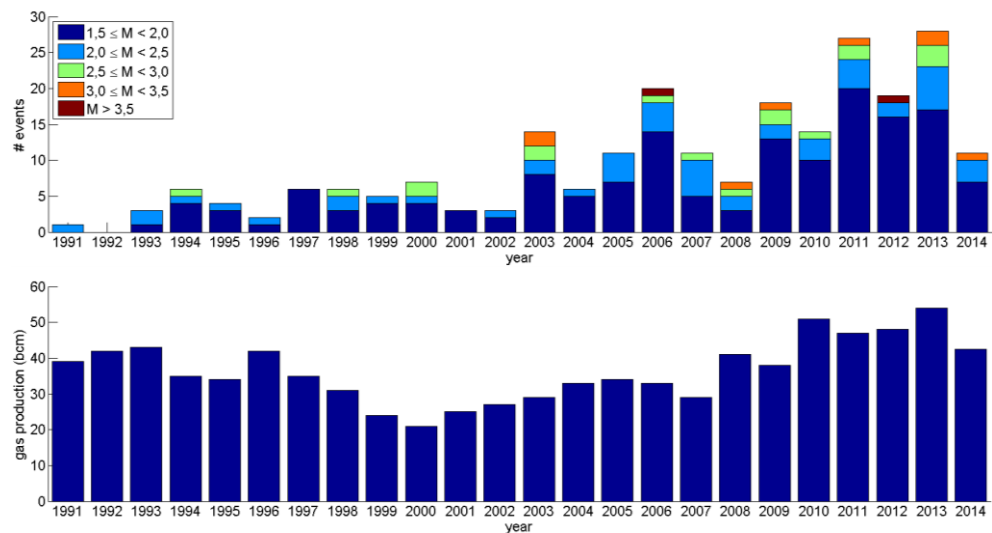


Figure 2-8. Number of events in time (top), with in colour the magnitude of the seismic events. In 2014, only the events up to November 1st have been taken into account. Bottom: production in billion cubic meters (bcm) per year.

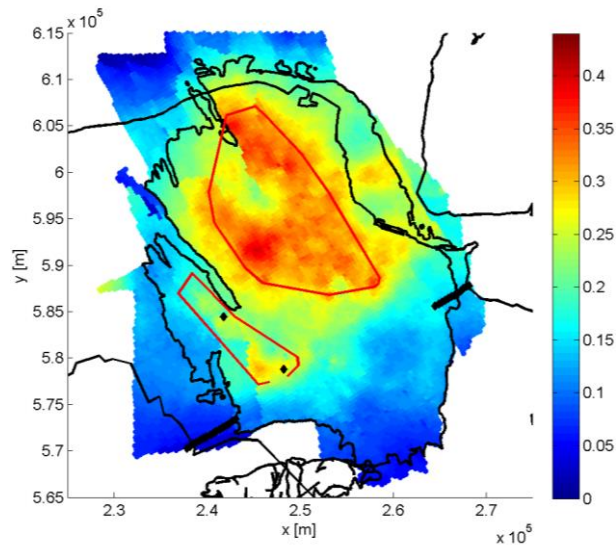


Figure 2-9. Definition of the SW and Central area. The background colour is the cumulative compaction, calculated with the RTiCM model (Rate Type Compaction Model in Isotach formulation) as described in TNO (2013, 2014b) for January 2014. In red the contours of the Central area and the SW area.

2.5.1 Assumptions and definitions

For this statistical analysis, the area over the Groningen field is divided in three subareas (Figure 2-9):

- **Central:** the area in the centre of the Groningen field where cumulative compaction is highest.
- **SW:** the area close to the clusters of EKL and FRB with extension to the northeast of cluster EKL
- **Other:** remaining areas of the Groningen field.

Furthermore the analysis distinguishes the following time periods:

- 1) From December 1991 (time of the first measured event) until November 1st 2014 (entire catalogue)
- 2) from December 1991 (time of the first measured event) up till 1st January 2003
- 3) from 1st January 2003 up till 17th January 2014
- 4) after 17th January 2014

It is assumed that the seismic events can be described as a so-called Poisson process (see Appendix B). In the absence of aftershocks, this is a valid assumption. In the Groningen seismicity database there is some evidence for aftershocks but they do not seem to be too numerous (NAM 2013).

Three statistical models have been investigated in this study:

- 1) **Stationary:** a model assuming that the Poisson process is *stationary*, meaning that the frequency of events is constant in the course of time.
- 2) **Increasing:** a model assuming that the Poisson process is *non-stationary* with an increasing frequency of events over time.
- 3) **Decreasing:** a model assuming that the Poisson process is *non-stationary* with a decreasing frequency of events over time. This model was only applied for the investigation of the seismicity since 17th of January 2014.

The key quantity computed for each time period and each area is the so-called **Bayes factor** of two models we want to compare. The Bayes factor is defined as the quotient of the likelihoods for the two models considered, thereby quantifying a relative preference for the one model over the other. For the determination of the Bayes factors all seismic events with a magnitude larger than or equal to 1.0 are regarded. Although a magnitude of completeness of 1.5 is usually assumed for the Groningen seismicity dataset, a visual inspection of the frequency magnitude curve suggests that the magnitude of completeness could be lower (as low as 1.0). The magnitude of completeness is defined as the minimum magnitude which would have been observed over the entire field. For the conceptual and mathematical details we refer to Appendix B.

2.5.2 Results

Comparison for entire catalogue

For the entire period of December 1991 until November 2014 a total of 315, 60 and 184 events were incorporated for the “Central”, “SW” and “Other” area respectively. It appears that for each of these areas the Bayes factors for the “increasing” model vs “constant” model (i.e. likelihood “increasing” model divided by likelihood “stationary” model) are at least of order $3 \cdot 10^9$, indicating that the “stationary” model has extremely low likelihood and that these outcomes are indisputable.

Comparison for December 1991 up till 1st January 2003

The table below presents the Bayes factors for the “increasing” model vs the “constant” model concerning events monitored from December 1991 up till 1st January 2003.

Name	Bayes Factor	Number of events
Central	0.12	64
SW	0.76	8
Other	0.11	34

From these results it can be concluded that the stationary model is at least as adequate as the “increasing” model. However, an “increasing” model is not ruled out according to a general interpretation on the meaning of the figures (see Appendix B).

Comparison for 1st January 2003 up till 17th January 2014

The table below presents the Bayes factors for the “increasing” model vs the “stationary” model concerning events monitored from 1st January 2003 up till 17th January 2014.

Name	Bayes Factor	Number of events
Central	$5.4 \cdot 10^4$	236
SW	25.4	43
Other	$1.4 \cdot 10^5$	129

From the high Bayes factors it can be concluded that an “increasing” model fits the data best by far. In this case there is hardly any room for a discussion whether the alternative (stationary) model might also work.

The probability density functions for the time constant of the “increasing” model have been determined for this period (Figure 2-10). The time constant represents the period over which a significant change in the frequency of events takes place (represented by τ). From the figure it follows that the time constants for the different areas most probably vary in the range of 5-10 years.

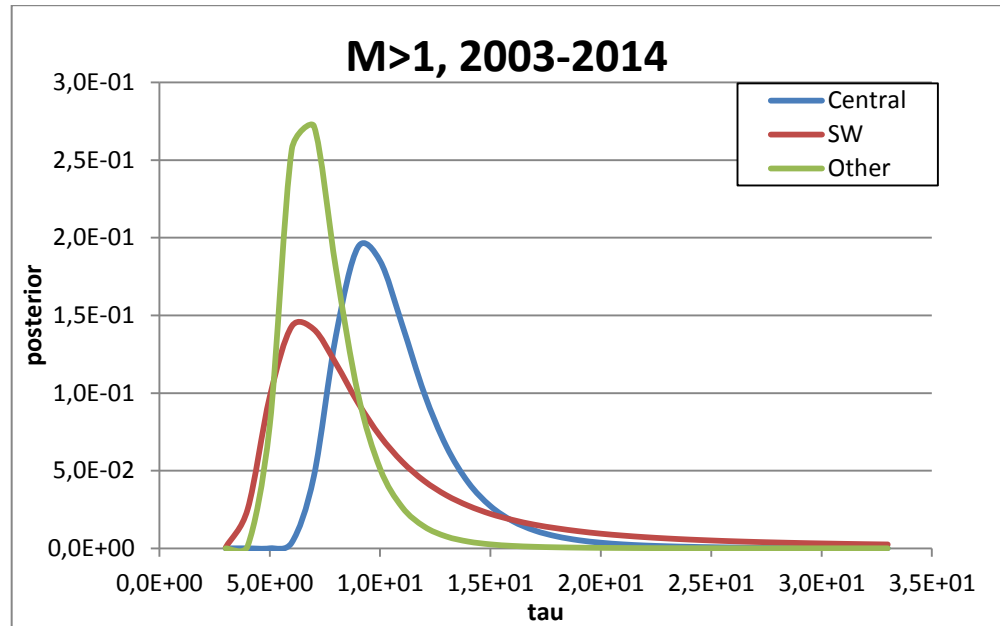


Figure 2-10. Probability density functions for the time constant in the increase models for Central, SW and Other. The Bayesian prior probability used in the calculations is Jeffrey’s prior. See the Appendix B.

It is worth noticing that if only events with at least a magnitude of 1.5 were regarded for this analysis, the Bayes factors would have been considerably lower (Appendix B). “Increasing” models would still be preferred, but the stationary ones would not be excluded.

Comparison after 17th January 2014

For the comparison of the period after 17th January 2014, the finite travel time of the pressure wave (resulting from a sudden production decrease) to any given point in the field, has to be taken into account. The analysis to investigate whether the production decrease might have had an effect on the seismicity only extends to the seismic events in those areas that have actually been reached by the wave. This simple physical consideration necessitates a redefinition of the various areas which are subsequently called “ADAPTED Central”, “ADAPTED SW” and “ADAPTED Other”

The table below lists the Bayes factors both for “increasing” and “decreasing” models compared to the stationary model.

Name	Bayes Factor Increase/ Stationary	Number of events
ADAPTED Central	0.92	6
ADAPTED SW	0.92	12
ADAPTED Other	0.90	28

Name	Bayes Factor Decrease/ Stationary	Number of events
ADAPTED Central	1.19	6
ADAPTED SW	1.14	12
ADAPTED Other	1.15	28

From the results it can be concluded that all three models are acceptable up to this point in time. One will notice that for all three areas the “decreasing” model is a worthy competitor and that it is slightly favored over the other two models. A definite judgment regarding the suitability of the three models for the separate areas can be passed only when more seismicity data have become available (Appendix B), i.e. when we see how seismicity evolves in the time to come.

3 Geological evaluation and petrophysical analysis Eemskanaal area.

3.1 Introduction

The geological input parameters used in the compaction calculations are essential to understand the seismicity at the location of the Eemskanaal production cluster. Seismicity is related to compaction and the compaction coefficient in turn is related to porosity.

As described in TNO (2013), the observed subsidence for the area in the western part of the Groningen field (South of Winsum and Bedum) is higher than the modelled subsidence. The modelled subsidence calculations are based on the porosity distribution and associated compaction coefficient. In this chapter TNO discusses whether there is geological ground for alternative porosity distributions in this area such that the observed discrepancy of measured versus modelled subsidence can be explained. To that end TNO has performed a petrophysical analysis of the wells in the vicinity of the Eemskanaal cluster and evaluated the modelled porosity distribution in the GFR2012 porosity model (NAM 2012) and associated uncertainties.

3.2 Geological setting

The Eemskanaal production cluster is located in the southwestern part of the Groningen field (see Figure 3-1). Wells EKL-1 to 12 produce the reservoir from the near vicinity of the Eemskanaal cluster location, while the deviated EKL-13 well produces the reservoir from the deeper positioned Harkstede Block located further to the South.

The top Rotliegend is relatively shallow in this area (at ~2650 m depth at the Eemskanaal cluster location, and at ~2880m depth at the Harkstede Block). The Slochteren reservoir is approximately 150m thick. The Free Water Level (FWL) at the Eemskanaal cluster location is estimated at 2995m depth (within the Carboniferous interval), and at 3016m depth in the Harkstede block (within the Upper Slochteren reservoir formation at the EKL-13 well location). Figure D-3 in Appendix D provides a reservoir cross section across both areas.

In the GFR2012 (NAM 2012) the Slochteren Sandstone is subdivided in multiple reservoir- and heterogeneous non-reservoir units:

- USS3.1.res
- USS2.2.het
- USS2.1.res
- USS1.2.het
- USS1.1.res
- LSS2.4.het
- LSS2.3.res
- LSS2.2.het
- LSS2.1.res

The three Upper Slochteren reservoir units are characterized by the highest porosities in the Eemskanaal area and thereby contribute mostly to compaction.

The Eemskanaal area is characterized by a relatively high fault density. NW-SE trending faults (including a zone of pop-up structures) and E-W / N-S trending faults cross in this southwestern area of the Groningen field. Figure 3-2 shows the location of the wells at Top Rotliegend level relative to the interpreted faults (NAM 2012). TNO considers the possibility that porosities may have been influenced in the direct vicinity of these faults (e.g. porosity reduction). Within the geological model these influences should then be treated as local phenomena.

3.3 Petrophysical evaluation

In this section TNO evaluates porosity in the wells of the Eemskanaal cluster and compares the methodology and results with the porosity values reported by NAM (2012).

NAM has used two different methods for calculating porosity (NAM 2012).

- Full petrophysical analysis using a complex Waxman-Smiths method is applied for those wells that do have shallow resistivity log data available.
- For most wells in the Eemskanaal cluster a linear bulk density (or sonic slowness) to porosity transform method (RHOB-CPOR) was applied as shallow resistivity data are lacking. This transform is determined for the entire Groningen reservoir and made well-specific by correcting for depth and shale volume.

In order to check and validate NAMs porosity calculations, TNO performed independent petrophysical analyses on a selection of wells using the density log method in combination with the Indonesian formula for gas saturation. In addition a linear transform was constructed specifically for the Eemskanaal cluster wells. TNO's transform is characterized by higher uncertainty than NAM's transform because it is based on the data of a single well only. Compared to NAM's general transform however, it is more specific to the local porosity estimation.

Except for the Lower Slochteren LSS2.res unit only minor differences are observed between NAM's porosity values and results from petrophysical analyses by TNO (Table C-3 to Table C-6 in Appendix C). This consistency supports the validity of the results of NAM.

For the LSS2 unit NAM calculated higher porosities than TNO. This difference may have resulted from:

- The fact that for some wells NAM has applied the RHOB-CPOR method, while TNO performed full petrophysical analysis.
- The different RHOB-CPOR transform used by TNO which generally produce higher porosity values than NAM above 18% porosity and lower porosity values below 18% porosity.

The differences at porosities higher than 18% are most relevant with regard to their effect on compaction. The difference with NAM's transform indicates that there is an uncertainty range of 1-2 porosity units (pu) at porosities higher than 18%. NAM has used the porosity profiles, calculated from well data, as input for the porosity model

and porosity maps (part of the GFR2012 Petrel model, NAM 2012). A comparison by TNO shows that for the LSS2 unit the mapped values are generally lower than the values NAM has determined in the wells (i.e. a mismatch between input data and the model). This is confirmed by the results of the petrophysical analysis by TNO (Appendix C). The effect of the observed differences on compaction coefficient will however be minimal as the differences in porosity occur in the lower porosity ranges (Figure 5-1).

3.4 Compaction coefficient

A sensitivity analysis of the effect of porosity on compaction has been conducted by TNO. By converting NAM's porosity profiles to compaction coefficient logs using the formula for Groningen core samples only on page 86 in TNO 2013, small scale changes in compaction coefficient and localized high compaction zones can be identified. A calculated relative increase in compaction with two steps of increasing porosity (1 and 2 pu increase, see appendix C) shows that the relative increase in compaction coefficient is significantly higher compared to the relative increase in average porosity at higher porosities. In low porosity reservoirs the increase in compaction coefficient is less.

3.5 Modelled porosity distribution

TNO (2013) states that the GFR2012 porosity model does not provide information on alternative porosity distributions in the porosity trend maps. NAM (NAM 2012) mentions that specific steering of interpolation using facies maps or seismic data (acoustic impedance) was not implemented. The GFR2012 porosity model can therefore be considered to represent only one statistical realization of the spatial porosity distribution.

The GFR 2012 Upper Slochteren (main reservoir) porosity maps for the areas West and North-West of the Eemskanaal cluster show a clear Westward trend of decreasing porosity, extending into a large region of distinctively low porosities around Bedum (e.g. Figure D-6). As modelled porosities between the Eemskanaal (EKL) wells and the Ten Boer (TBR) and Bedum (BDM) wells have little or no further well control, the porosity distribution pattern in this area is largely defined by the regional porosity trend maps generated by NAM (e.g. Figure D-5). The Westward decreasing porosity trend is strongly determined by the interpolation of higher porosity values in the Eemskanaal wells and lower porosity values in wells BDM-1 and TBR-4.

TNO observes that well TBR-4 has been drilled near or within one of the faults represented in the GFR-2012 model. Although this has not been proven by petrophysical analysis, TNO considers the possibility that the low porosities in this well may be the result of fault induced porosity reduction, thereby possibly representing a local rather than regional phenomenon. TNO relates this possibility to the observed low porosity in well EKL-2 which is also drilled into or close to a fault. The reduced porosity around this well is markedly present in all other reservoir zones and heterogeneous zones (see Appendix D). The EKL-2 well was apparently not used for modelling the regional trend maps and NAM justly incorporated this

well as a local anomaly in the final average porosity maps (see e.g. Figure D-6 in Appendix D).

The low porosity in well BDM-1 (13%) deviates from the higher (15-17.5%) porosity values in the surrounding other BDM wells. Although the low porosity in BDM-1 cannot be related to one of the faults in the model, TNO considers the possibility that this value represents a local phenomenon in relation to the overall higher values in the nearby other wells.

In summary TNO regards that, in case wells BDM-1 and TBR-4 are indeed representing locally influenced porosity values, the westward trend of decreasing porosity may be less pronounced than currently modelled in the trend maps. In the absence of well control in the area, there may thus be room to extrapolate the higher porosity values of wells EKL-1 to EKL-12 further westward, notably in the area where the top reservoir has a similar depth range. This would imply a possible increase of porosity by 1 to 2 pu, with a maximum of 3 pu in the area where a mismatch has been observed between modelled and measured subsidence. Hereby the porosity in this western area would increase from ca. 14% to maximum 17%, having an increasing effect on the compaction coefficient. NAM reports (NAM 2012) a field wide relative porosity uncertainty of 2.2% (which is one standard deviation). In this part of the field (average porosity of 0.17), two standard deviations would correspond to 0.8 pu change in porosity. TNO considers that porosity variations may indeed be somewhat higher here.

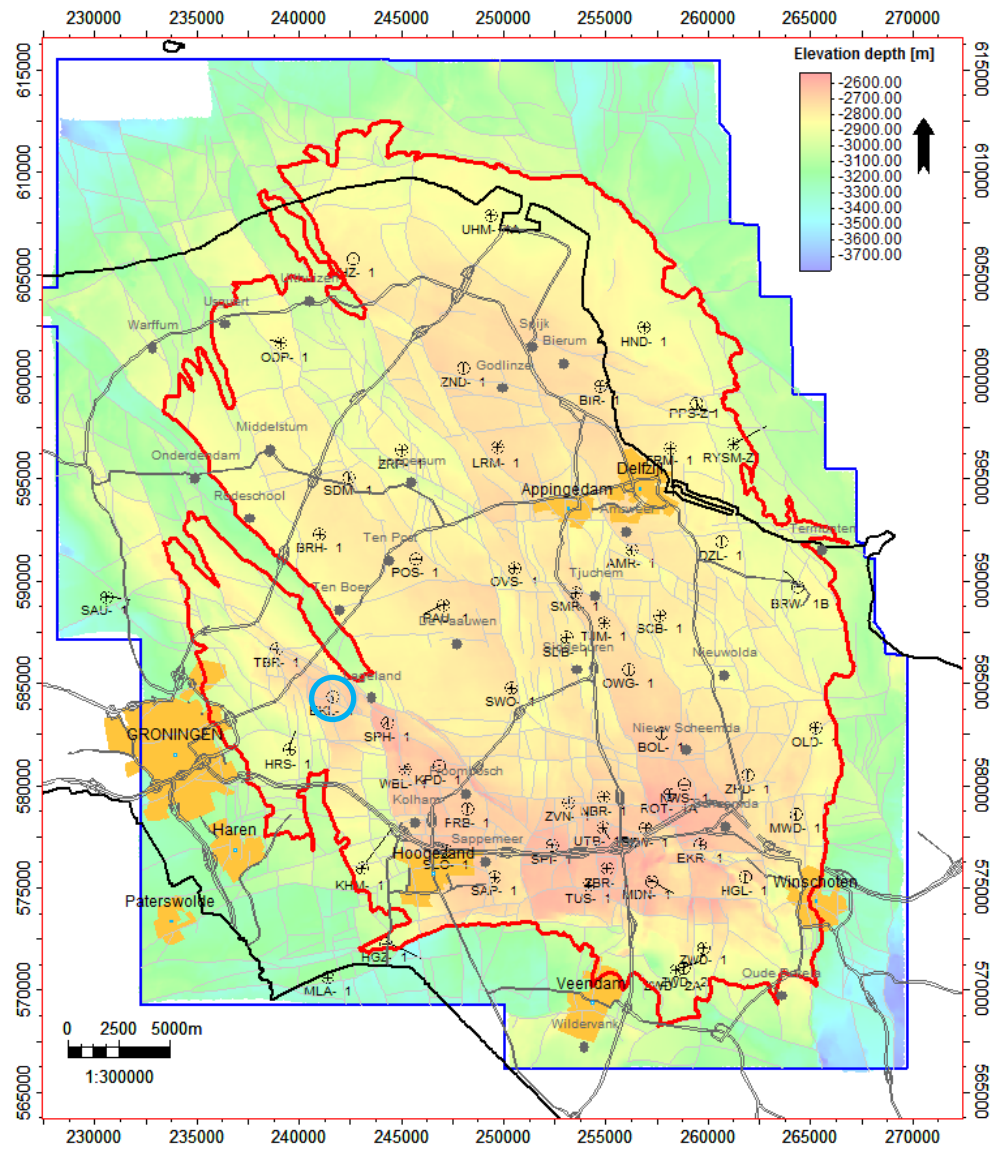


Figure 3-1. Outline Groningen field (red) on depth map Top Rotliegend surface. Modelled faults are indicated in grey and the main well locations and production clusters in black (Petrel GFR2012 model). A blue circle indicates the location of production cluster Emskanaal (EKL).

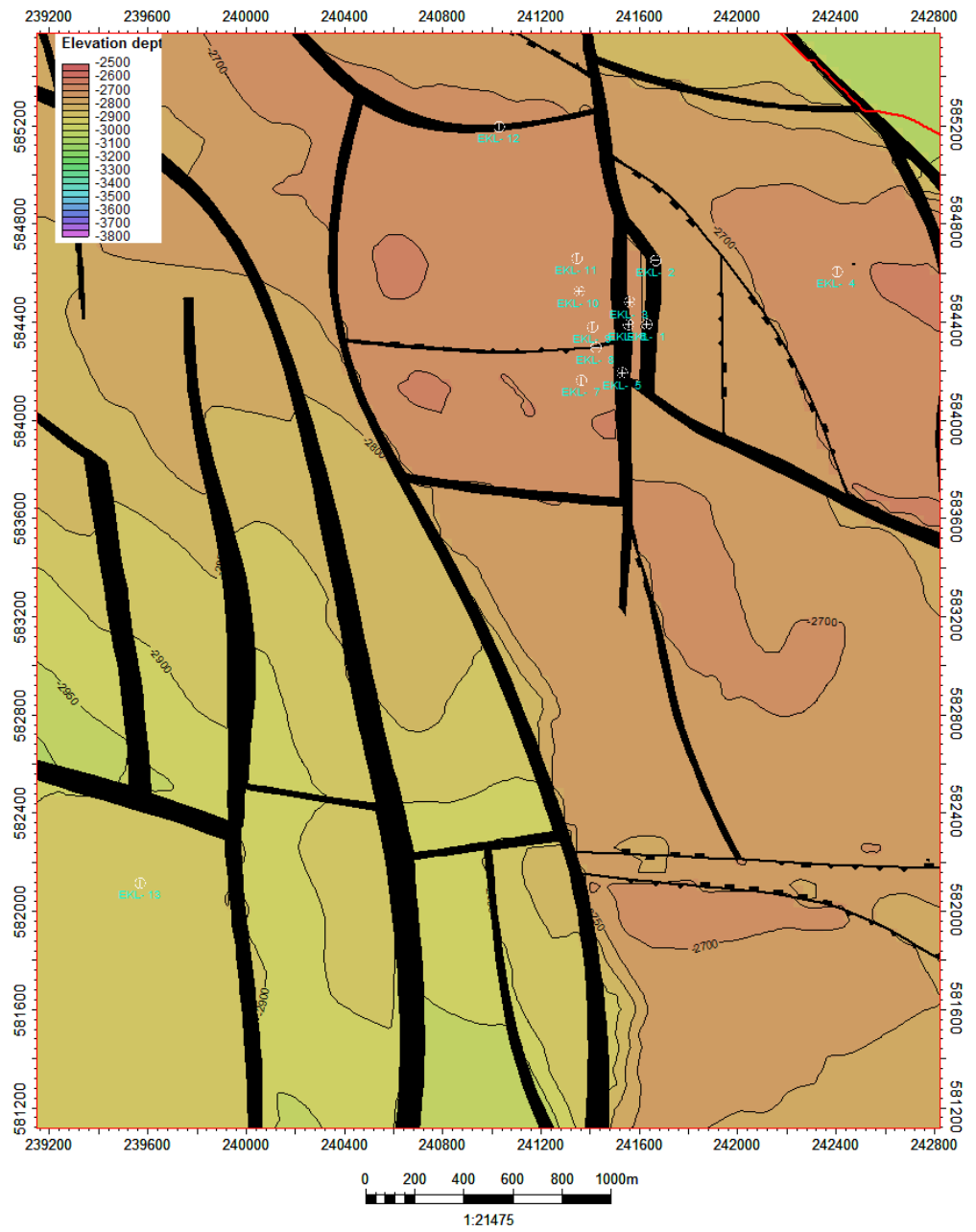


Figure 3-2. Structural map of Top Rotliegend showing the location of the Eemskanaal cluster wells (based on Petrel GFR2012 model).

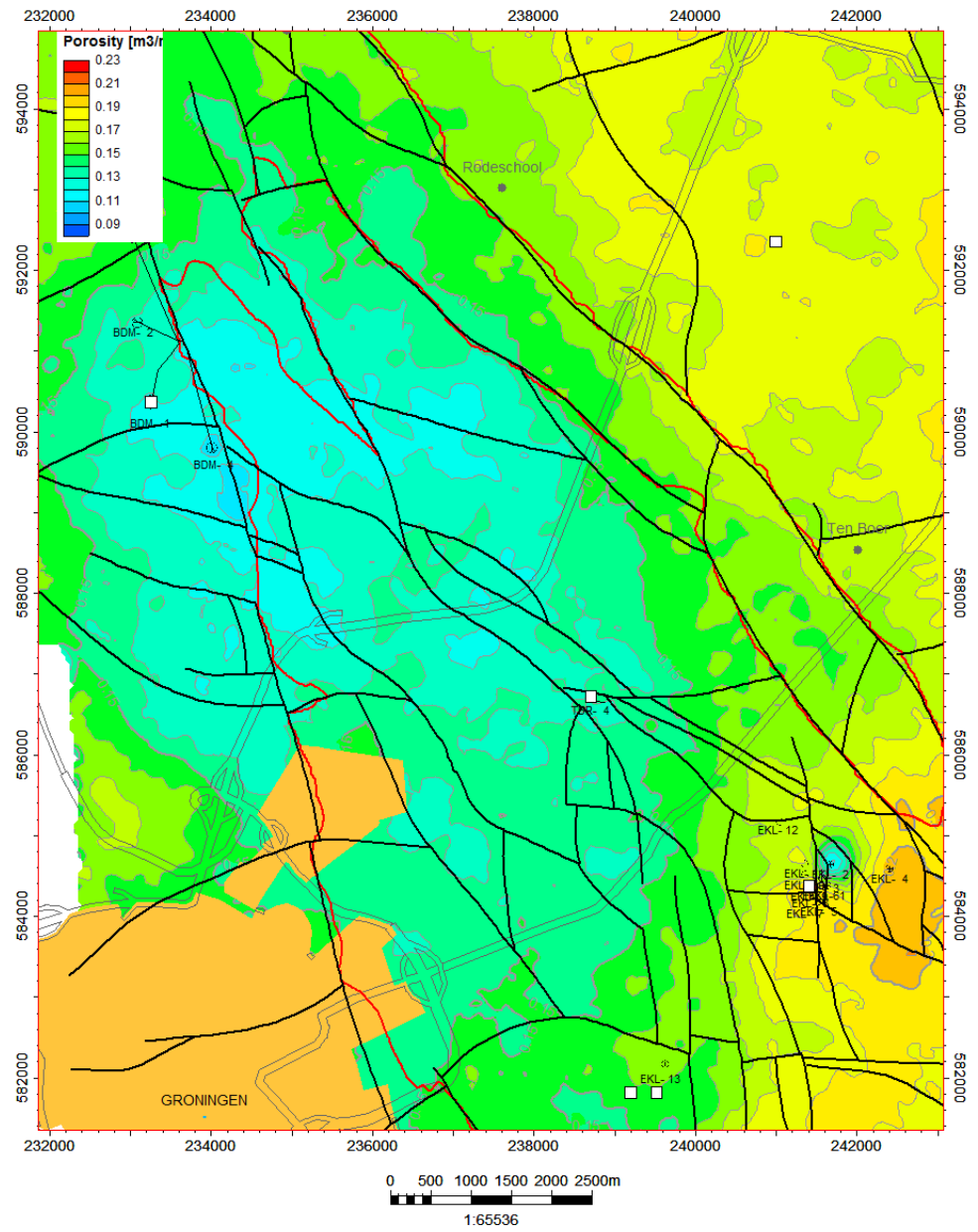


Figure 3-3. Average porosity for the USS.2.res zone based on the GFR2012 porosity model at the Eemskanaal location.

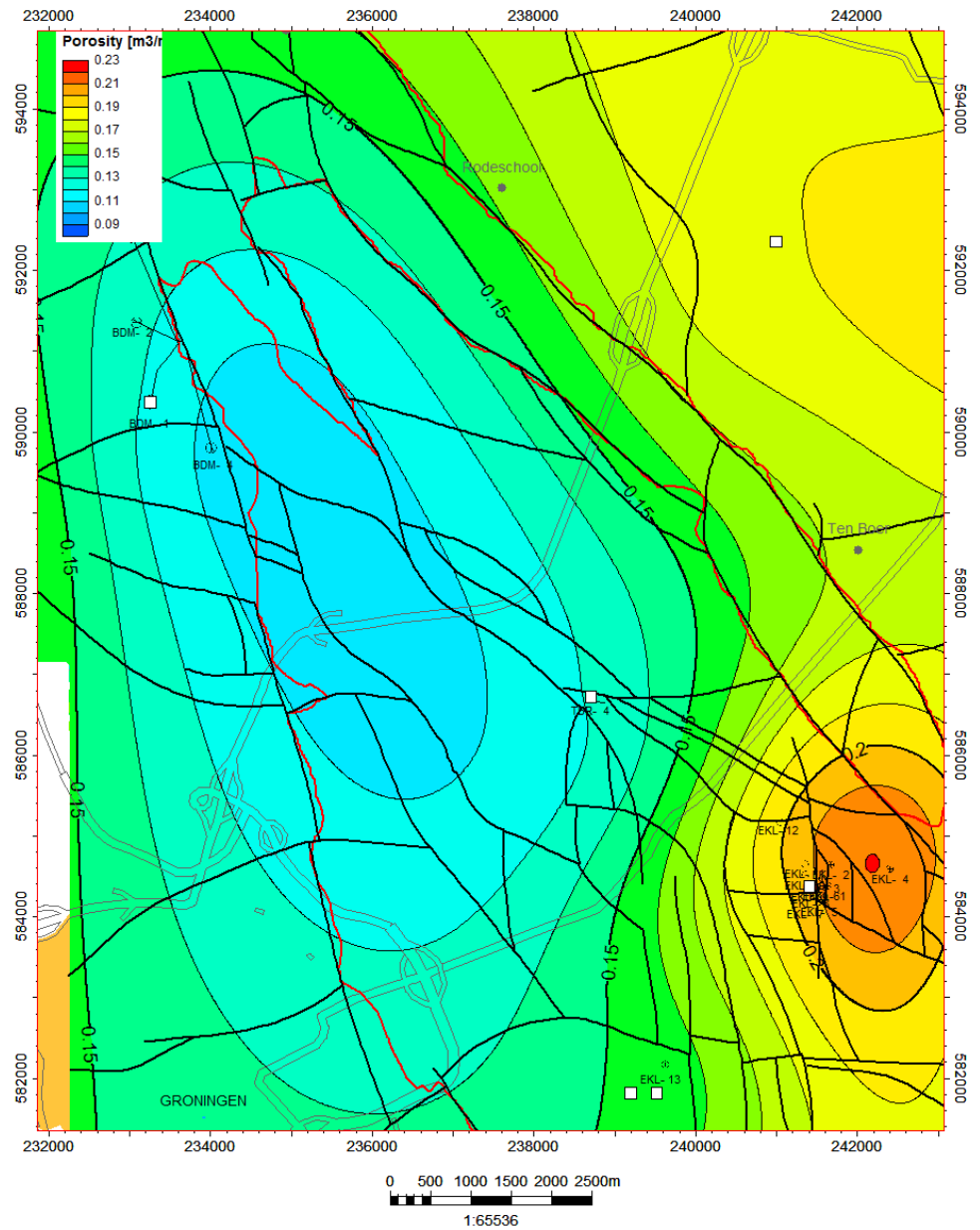


Figure 3-4. Porosity trend map of the USS2.res zone as used in the interpolation process for calculating average porosity maps. Wells indicated with white squares are used to create this trend map.

3.6 Summary of findings

- Petrophysical analyses for a number of Eemskanaal wells performed by TNO generate on average similar porosity log values as the ones reported by NAM in the GFR2012 study.
- Some wells drilled in faults show lower porosities which may be a result of fault induced porosity reduction.
- Low porosity values in the TBR-4 and BDM-1 wells West of Eemskanaal possibly represent more localized phenomena.
- Based on these assumptions TNO considers it is well possible that the average porosity west of the Eemskanaal cluster is higher than modelled in the GFR2012 model with potential increases from 1 to 2 pu up to maximum 3 pu.
- TNO maintains its remarks regarding the porosity modelling process as made in TNO (2013) (i.e. no geologic/seismic steering and no mentioning of alternative porosity distributions in the average porosity maps and trend maps).

4 Possible delay effect on compaction of reducing Eemskanaal production

In case the production would be reduced in the Eemskanaal (EKL) cluster, a temporary situation would develop where pressure would decrease slower in this area and, consequently, compaction rate would also decrease. As mentioned before, the reduction in production will not physically lead to a direct response of the reservoir volume due to the time it takes for a pressure wave (in the gas phase) to travel through the reservoir. In Table 4-1 the relation is shown between the distance to the EKL cluster and the time it takes for the first arrival of the pressure wave and the full (99%) arrival of the pressure wave. The data in Table 4-1 holds for an average permeability in this area of 100 mD and uses the analytical equation derived in Appendix A. As an example: at 4 km distance, the first arrival of the effect of production reduction would be visible in 13 months while the full effect would take 39 months to materialize.

The Eemskanaal region has a lower average permeability (100 mD) than the centre of the field (350 mD, see paragraph 2.2), which causes the pressure wave to travel with a lower velocity: note that the time of a pressure wave to travel a certain distance is inversely proportional to permeability.

Table 4-1. Time of arrival of the pressure wave in the area of Eemskanaal (average permeability of 100 mD) as a function of the distance to the EKL cluster.

Distance to EKL (km)	Time first arrival (months)	Time (99%) of pressure wave (months)
2	3	9
4	13	39
6	28	84
8	51	153
10	79	237

If production would be reduced in the Eemskanaal area, the pressure waves of surrounding producing clusters would at some time arrive in the Eemskanaal area and reduction of the pressures in the reservoir and, therefore, compaction would resume. The producing clusters of Froombosch (FRB), Slochteren (SLO) and Kooipolder (KPD) are between 6 and 8 km distance from the EKL cluster (Figure 4-1). The first arrival of the pressure wave from other clusters would, therefore, take at least 28 months to arrive, while the full arrival (99%) would take at least 84 months.

The values of the arrival time of the pressure wave in the reservoir are based on the analytical equations of Appendix A. It would be more realistic to model the time responses of the reservoir using the numerical reservoir model, that takes into account the spatial distribution for the various parameters and permeability in particular which is critical for wave travel considerations. This was, however, not possible due to the limited time available.

Summarizing, if production were to be reduced in the Eemskanaal area the pressure effects would be temporary (circa 2 years, maybe more) due to the producing clusters nearby and the time it would take for the effect to materialize. A

reduction in the rate of pressure decrease will reduce the rate of compaction in the area (assuming there is a direct response in compaction, as in the RTiCM model; TNO 2013; 2014b) and, consequently, the rate of seismicity.

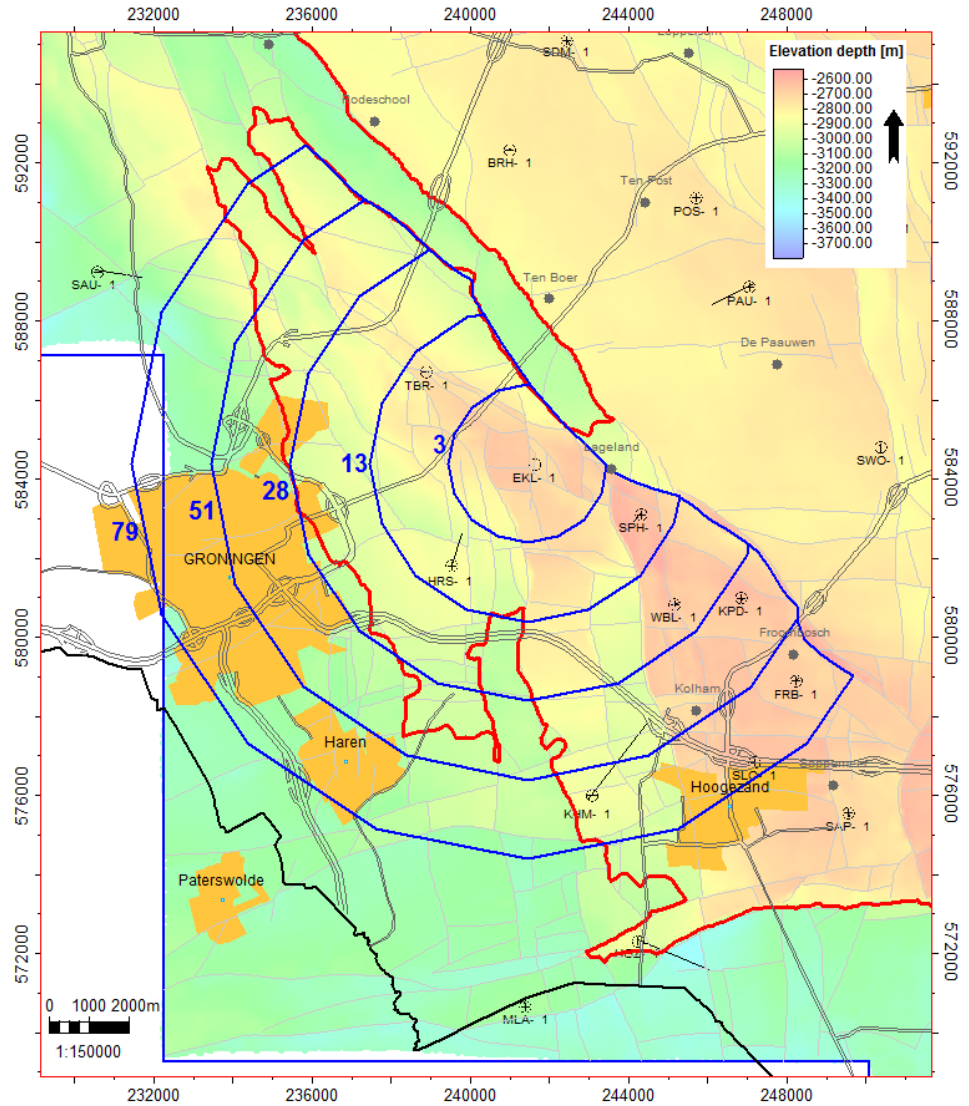


Figure 4-1. Time it would take for the first arrival of a pressure wave in the reservoir to travel 2, 4, 6, 8 and 10 km from the EKL cluster.

5 Review of report on Eemskanaal area of NAM

5.1 Introduction

In this chapter TNO reviews the report 'Hazard Assessment for the Eemskanaal area of the Groningen field' of NAM (2014).

The main body of the review consists of two parts, being 1) reservoir compaction (paragraph 5.2) and 2) hazard (paragraph 5.3). Finally, our findings are presented in paragraph 5.4.

The NAM report covers the main steps that have been taken to arrive at hazard assessment for the Eemskanaal area. As the report itself states, at some places, the time for the work has been very short, leading to compromises and comprehensiveness in some of the workflows and reporting.

In order to better understand and verify the NAM report, supplementary information has been provided on our request by NAM, e.g. the dynamic reservoir models underlying the compaction and hazard assessment. This review is based on the report itself, the additional information provided and our evaluations, including the work that has been presented in the previous chapters.

5.2 Reservoir compaction in the Eemskanaal area

5.2.1 Problem statement

An important driver for the NAM report is the discrepancy that has been observed between modelled and measured subsidence over the south-west periphery of the Groningen field. This discrepancy has been reported both by NAM and by TNO (TNO, 2013), and turns out to be quite independent of the particular compaction model applied (Time Decay or RTiCM). This suggests that assumptions with regard to the reservoir model (static and/or dynamic) in this area are possibly incorrect leading to underestimating of compaction in the south-west periphery.

Both NAM (NAM 2013) and TNO (TNO 2013) have observed that the modelled subsidence (obtained using InSAR and levelling data) is smaller (up to 7 cm) than measured over this area (TNO, 2013; figure 5.23).

Provided the geodetic data are reliable, the actual reservoir compaction is larger than calculated so far. This in turn has an impact on the outcome of the hazard assessment that uses reservoir compaction both for calibrating the seismological model as well as main input for the calculation of seismic hazard.

5.2.2 Framework for uncertainty analysis

Reservoir compaction is calculated using the volume change and the pressure decrease in the field. The static (or geological) reservoir model provides the spatial distribution of the porosity, which is linked to the compaction coefficient by core

measurements in the laboratory (Figure 5-1). The dynamic reservoir model provides the distribution in space and time of the pressure decrease, that has occurred since production start in the gas zone, as well as in water bearing zones (aquifers) connected to the gas zone.

Table 5-1 shows an overview of the areal distribution of the level of uncertainty in compaction for the Groningen field. The areas, where porosity is larger than 18 %, have a higher compaction coefficient due to the strongly non-linear relation between porosity and compaction. Uncertainty in the porosity will have a larger impact on the compaction in these areas, giving rise to higher uncertainty in compaction. The presence of side and bottom aquifers gives an additional uncertainty in compaction due to the limited data available on the aquifer geometry and pressure behaviour. As shown in Table 5-1, the southwest periphery of the field has areas with both a fairly high porosity as well as a side aquifer to the west, rendering this part of the field the most uncertain in terms of determining compaction. In that respect, TNO agrees with NAM's statement that determining the compaction in this part of the field is challenging.

Table 5-1. Overview of local causes of uncertainty.

Porosity (%)	aquifer	Uncertainty of compaction	Region of field
< 18	No	Low	Southeast periphery
< 18	Yes	Medium	Northeast periphery and east periphery
> 18	No	High	Centre and West (Central area)
> 18	Yes	Very high	Southwest periphery

5.2.3 Review of the geological model and porosity evaluation of NAM (2014)

NAMs assessment specifically focuses on the Harkstede block, which is located some 3 km South-West of the Eemskanaal cluster and circa 200 m deeper relative to the Eemskanaal cluster area. NAM concludes that:

- Porosity in the Harkstede Block is unlikely to be more than 1.5 pu (porosity units) higher than in the 'winningsplan' reservoir model;
- Uncertainty in depth of the top of the reservoir could increase away from the Eemskanaal-13 well and the Harkstede-1 well up to some 20 meters, with an areal average of 10 meters.

TNO has the following remarks:

- The uncertainty in porosity of the southwest periphery of 1.5 pu, as indicated by NAM, is realistic at the well locations;
- NAMs geological assessment does however not address the wider area around the Eemskanaal cluster that is also marked by a discrepancy between modelled and measured subsidence.
- Porosity could be up to 3 pu higher, particularly in areas far from well control.
- The increase of some 10 m of compacting height is reasonable.

5.2.4 The relation between porosity and compaction coefficient

NAM has not considered the uncertainty in the relation between porosity and compaction coefficient. Since this relation is vital to the calculation of compaction, TNO has analysed this.

Figure 5-1 shows the compaction coefficients as a function of porosity from compaction experiments on core data taken from the Groningen field. TNO has used the regression line (green) to calculate compaction. Values of the compaction coefficient of the well EKL-12 (red) seem a bit higher than this regression line. A best fit third order polynomial regression line through these points (black line) indicates that the compaction coefficient could be 50% higher (at 15-20% porosity) than used so far. In TNO (2012) the confidence levels of the regression function for Ameland are shown. If the confidence levels of the regression function of Groningen are similar, the EKL regression function is at the high end of the distribution between 67% and 95% confidence level, thus not statistically different from the used relation.

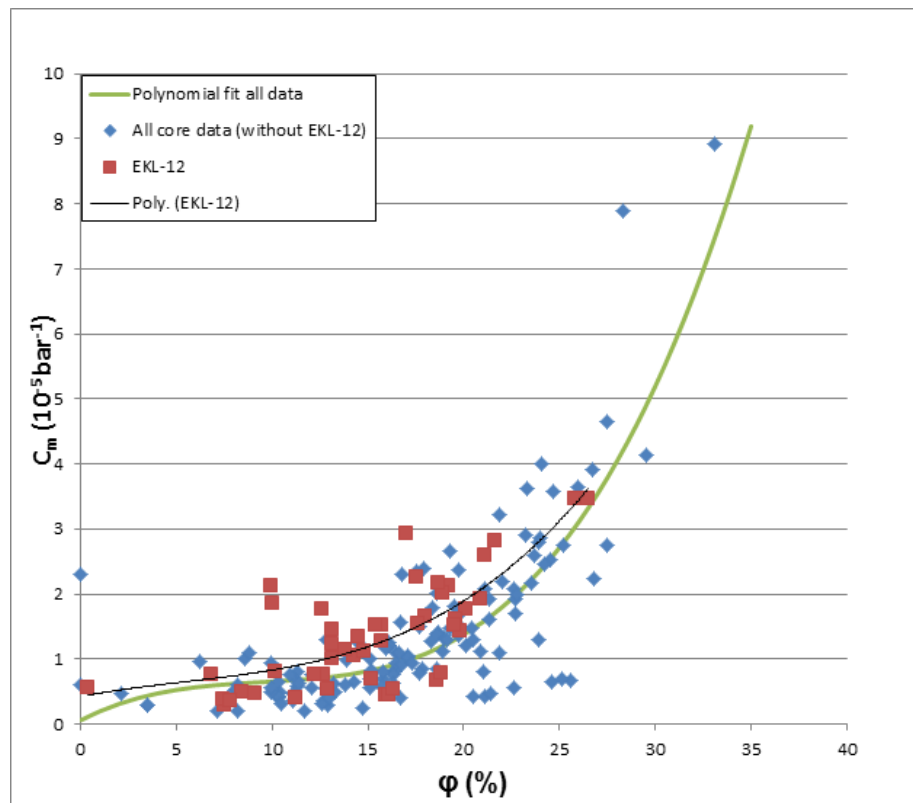


Figure 5-1. Results from compaction tests on Groningen cores: compaction coefficient vs porosity of the sample.

5.2.5 Geodetic information

In the same area, there is an unexplained discrepancy in subsidence rates between the InSAR and levelling data (~ 4 mm/year) on one hand and the GPS data (~ 8.5 mm/year) on the other hand observed at the EKL station for 2014 (NAM, 2014). The difference in subsidence rate is significant with a magnitude of $\sim +4.5$ mm/year, where InSAR and levelling give a much smaller subsidence rate. Although the time

scales of the measurements are very different (GPS: hourly, InSAR: monthly, levelling: yearly at best) which makes comparison difficult, the difference in subsidence rate remains unexplained so far.

5.2.6 *Review of the reservoir dynamics of the south-west periphery of the Groningen gas field*

Model selection

The activity of the west aquifer (Figure 5-2) is difficult to model due to the low well density and scarce data on pressure and water rise. NAM has therefore calculated two end members (strong aquifer: STR40 vs weak aquifer: STR38). Both models show a better history match on measured reservoir pressures in the southwest periphery than the NAM (2013) model, which was based on the so called G1 model. The G1 model considered an unrealistic strong aquifer in the north of the field, which was commented on in TNO (2013). This has not been addressed in the new models.

Reservoir dynamics of the south-west periphery

To improve the history match in the Harkstede block, a number of local adjustments were made in the south-west corner of the dynamic model (NAM 2014). In the original model (NAM 2013), the water inflow to EKL-13 (the only well that produces from the Harkstede block) was overestimated and the pressure in KHM-1 (south of Harkstede) and TBR-4 (north of Harkstede) was a poor match as well. This is in line with the general matching of the Groningen field, which is very good in the central part of the field, but poorer in the margins, where information is sparser. The changes to the model were focused on reducing water inflow to EKL-13 while maintaining pressure support. The following adjustments were made to the model used for the production plan in 2013 (NAM 2013) in the report of NAM 2014:

- The permeability in the aquifer (below the Free Water Level (FWL) of 2995m TVDSS) is decreased in the southwest area by a factor of 10 (Figure 5-2).
- The permeability in the Harkstede block and a block to the north of Harkstede is increased by a factor of 5 (both above and below FWL in these blocks) (Figure 5-2).
- The porosity is increased with 0.015 in the Harkstede block. For an average porosity in this area of 0.15 to 0.2 this is an increase in the order of 10%.
- The FWL in the Harkstede block is decreased from 3016 m depth to 3026 m. This is a quick fix to account for uncertainty in the top structure. The top was possibly too deep. To mimic this effect without having to update the geological model, the FWL is lowered. The net effect is similar, i.e. increasing the gas column height – and therefore compacting height - by 10m.
- The fault sealing of two faults in the south-west has been reduced. Fault M6 (Figure 5-2) which separates the extreme south-west from the rest of the field is made much more sealing. The permeability of this fault is multiplied by 10^{-8} . Fault M25, which defines the Harkstede block on the north side has also been made more sealing as well. For model STR40, the permeability is reduced to approximately 25% and for STR38 the permeability is reduced to approximately 16% of the original permeability.

- For model STR38, the Lauwersee aquifer (Figure 5-2) is turned off (by setting the width of the aquifer to zero).
- For both versions, the viscosity of the Lauwersee aquifer is decreased compared to the production plan model. The history match for the production plan of NAM (2013) included a reduction in the permeability that was implemented by increasing the viscosity. This reduction was removed, decreasing viscosity by a factor $10^{2.78}$. For model version STR38 this is not relevant, but for model STR40 the reduced viscosity increases the inflow and the pressure in this area. In Appendix E the effect of this change in viscosity is described in more detail.

As a result of these changes the history match improves considerably in the Harkstede area, especially for model STR40. The water production in EKL-13 was reduced to a realistic level in both history matched models (STR38 and STR40). For STR40 the history match in the Harkstede block (HRS-2A and EKL-13) is excellent (Figure 5-3). Also the match in KHM-1 and TBR-4 is very good. The main concern for this model is that the match is based on a strong analytical aquifer, which may or may not be realistic. For STR38 the history match has improved considerably compared to the production plan model of NAM (2013), but is not as good as for STR40 (Figure 5-2) especially for HRS-2A and EKL-13. In Appendix E, the pressure distribution is shown for STR38, STR40 and the 2013 production plan model (NAM 2013). This shows large differences in pressure between these 3 different models. Other observations that could help distinguish between the models are the PNL (Pulsed Neutron Lifetime Log) observations which give an indication of the FWL rise. Unfortunately, in this case, they provide little help. In TBR-4, the PNL observations show no change in FWL at all, whereas in all models the GWC rises more than 25m, albeit more in STR40 than in STR38. In HRS-2A, there is a clear indication in the measurements of a rise in FWL. The match of both models to reservoir pressures is improved with respect to the production plan (NAM 2013). Model STR40 gives a better match than model STR38.

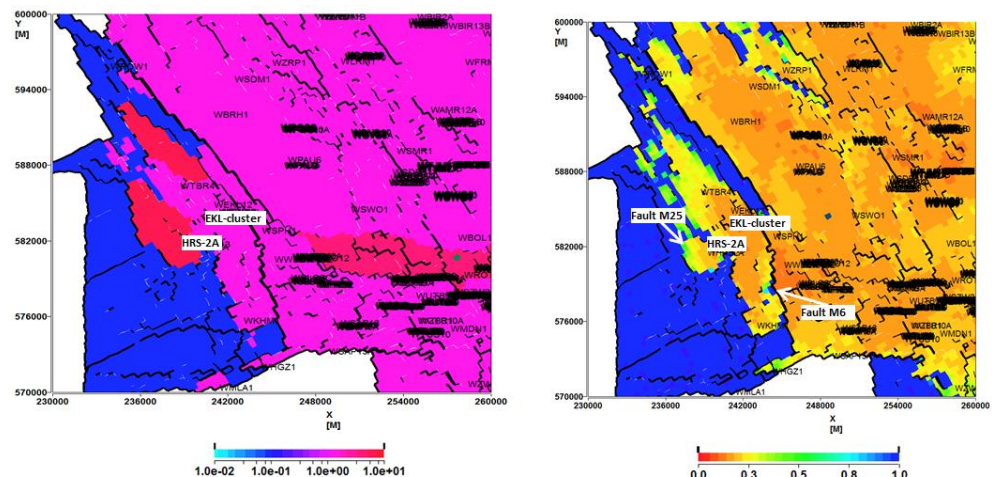


Figure 5-2. Permeability multipliers as applied in the STR38 and STR40 model (left) and water saturation (right).

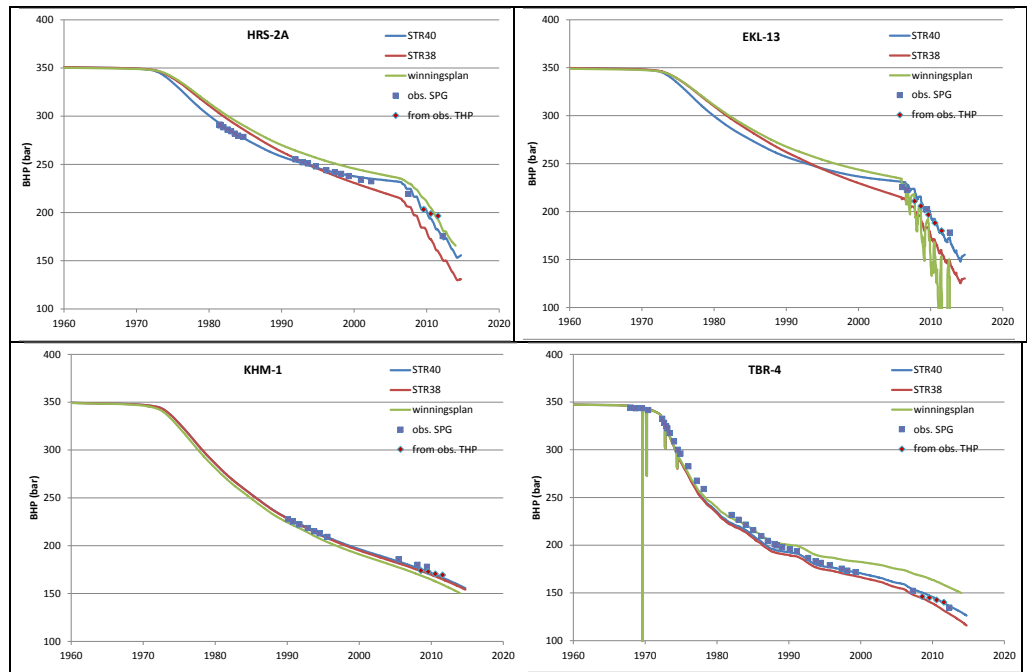


Figure 5-3. Pressure history match of wells HRS-2A, EKL-13, KHM-1 and TBR-4 for STR38, STR40 and the 2013 production plan model (NAM 2013) with updated 2013 production data (all geological model G1).

5.2.7 Explanation of the discrepancy between modelled and measured subsidence

As described in the previous paragraphs, new reservoir models have been introduced by NAM (STR38 and STR40), that match the measured pressures and water production better for the southwest corner of the field. Here we present TNO's compaction and subsidence calculations, using the RTiCM model, based on these new reservoir models in order to see, to what extent the discrepancy between modelled and measured subsidence is explained by these new reservoir models.

Figure 5-4 shows the cumulative compaction in January 2014 for the STR40 and the STR38 model. Figure 5-5 shows the difference between the measured and modelled subsidence in 2013 for the two new models. The pattern of this difference is similar to the pattern of the difference in subsidence shown in TNO (2013, figure 5.23). In the southwest corner of the field, the subsidence is underestimated (up to 10 cm) in the STR 40 model. The STR38 model improves the fit to the measured subsidence in the southwest corner due to the lower pressures in the aquifer of the model (paragraph 5.2.5). Figure 5-6 shows the difference between modelled and measured subsidence at every time step and location. STR38 improves the fit (deviation from the 45 degree (red) line) compared to STR40.

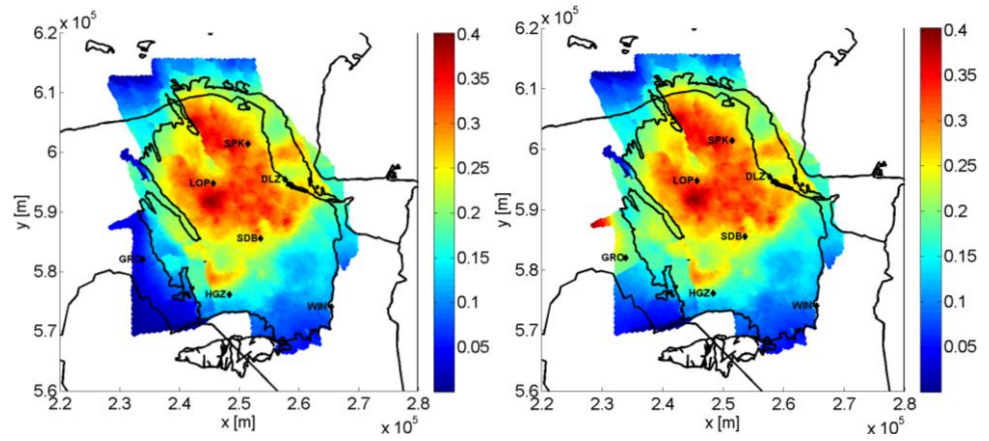


Figure 5-4. Cumulative compaction (January 2014) according to model STR40 (NAM), left, and model STR38 (NAM 2014), right. The contour of the Groningen field is in black as well as the topography, and a number of cities have been indicated (GRO=Groningen, LOP=Loppersum, SPK=Spijk, SDB=Siddeburen, HGZ=Hoogezand, WIN=Winschoten, DLZ=Delfzijl).

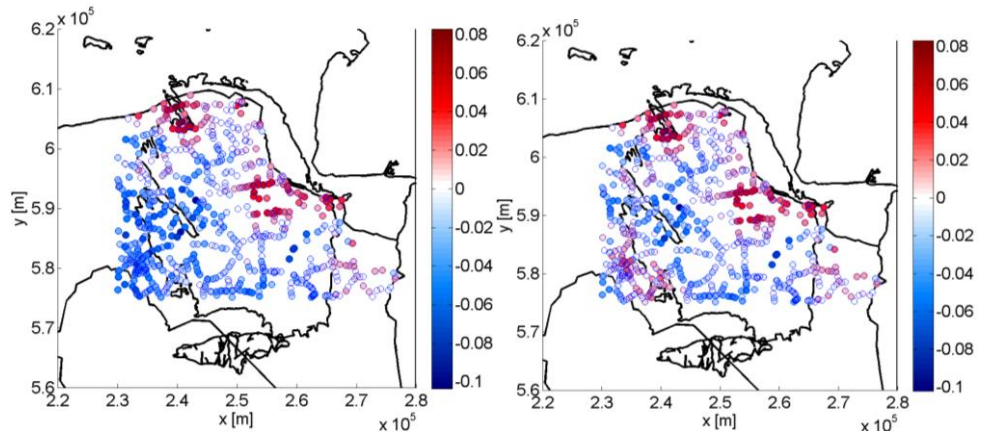


Figure 5-5. Difference (cm) between measured and modelled subsidence with STR40 (left)/STR38 (right). A negative difference indicates subsidence is underpredicted in the modelled subsidence.

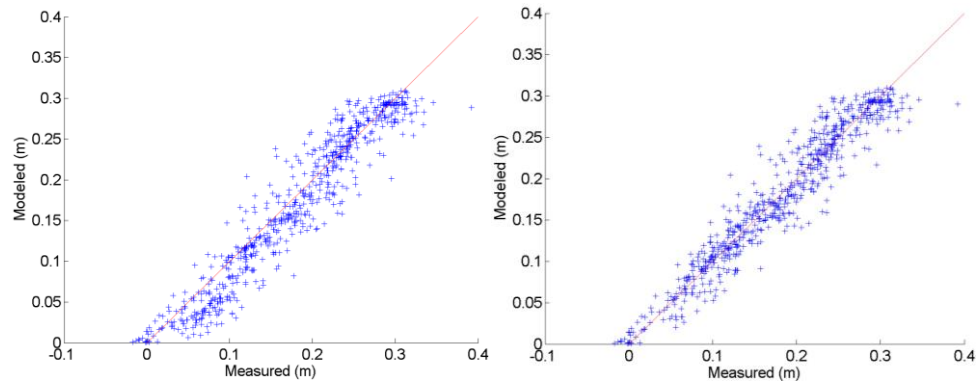


Figure 5-6. Difference between measured and modelled subsidence (in m) of model STR40 (left) and model STR38 (right) for measurements over the whole field. Compaction is calculated using the RTiCM model (TNO 2013, Pruiksmas et al., *submitted* 2014).

Figure 5-7 shows the differences between the compaction models (based on STR40 and STR38, respectively) to the 'old' model F425_Lsum3, which was used in TNO (2014a). Differences in the southwest corner are due to the different pressures in the models in this region, which in turn are caused by the difference in permeability. In the south-west periphery, the new models give a higher compaction due to the increase in permeability with a factor 5. West of the EKL cluster in the aquifer close to the Harkstede block the STR40 model gives lower compaction due to the decrease in permeability with a factor 10 and increase in the viscosity of the aquifer with a factor 100 (see paragraph 5.2.5 for comments on these changes applied by NAM, 2014). In Figure 5-8 the difference in compaction (January 2014) is shown between model STR38 and model STR40.

The two models (STR38 and STR40) only differ in the southwest corner of the field and side aquifer. The compaction calculated with these models differs by ~6 cm in the southwest periphery of the field, which is also reflected in the subsidence. The model STR38 (weak aquifer) fits the subsidence measurements better than the STR40 model.

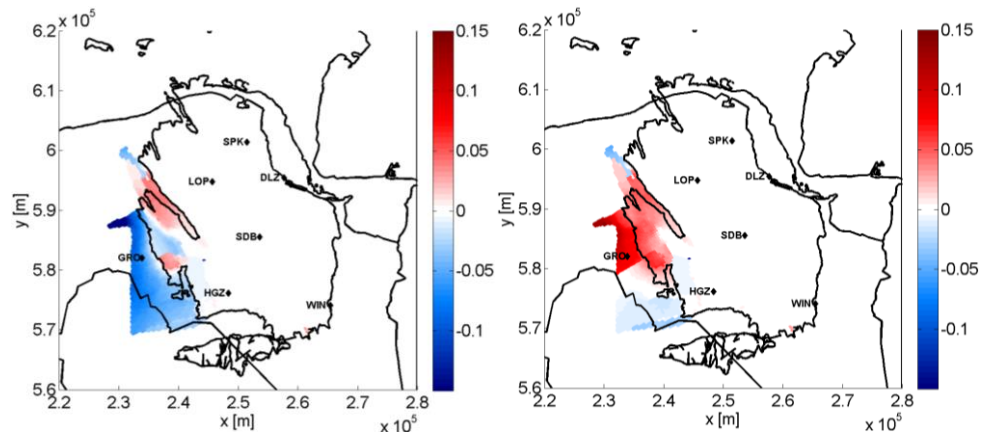


Figure 5-7. Difference in cumulative compaction (m) between the model F524_Lsum3 (TNO 2014a) and model STR40 (NAM 2014), left. Right, difference in cumulative compaction between the model F524_Lsum3 (TNO 2014a) and model STR38 (NAM 2014). A negative difference indicates areas where the 'new' model (STR40/STR38) gives less compaction than the 'old' model (F425_Lsum3). The background is similar to Figure 5-4.

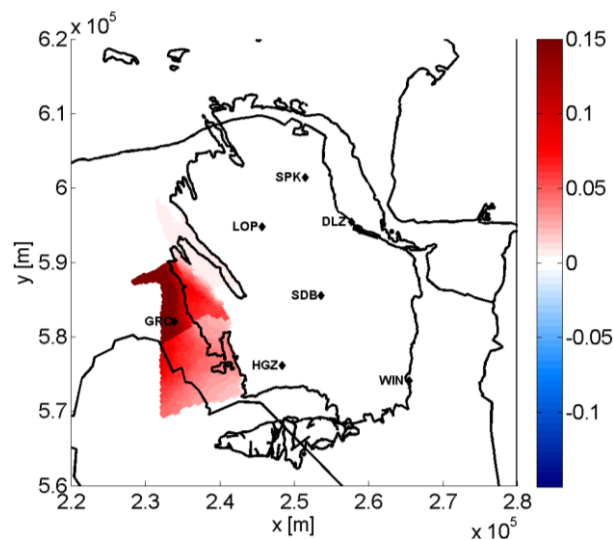


Figure 5-8. Difference in cumulative compaction (m) in January 2014 between the model STR38 (NAM 2014) and the model STR40 (NAM 2014). A positive difference indicates areas where the STR38 model gives more compaction than the STR40 model. The background is similar to Figure 5-4.

5.2.8 Findings for compaction

From our review of the NAM report on the part of compaction in the Eemskanaal area, and based on the TNO analysis of this, TNO notes the following:

- NAM has addressed a range of parameters, that may be responsible for the observed discrepancy between modelled and measured subsidence in this area;
- NAM has constructed two alternative reservoir models (STR38 and STR40), that both fit the observed pressures and water influx better than previous model versions;

- The model STR38 does explain the discrepancy in subsidence significantly better than model STR40; therefore, although STR40 cannot be excluded from a dynamic reservoir behaviour point of view, model STR38 deserves preference for further hazard assessment.
- The solutions presented by NAM primarily rely on modifications of the transmissivity of the aquifer connected to the south-west periphery of the Groningen field;
- These solutions are not unique: other (combinations of) parameters may explain the discrepancy equally well;
- It is therefore recommended to continue looking for improvements to reduce/constrain uncertainties; some suggestions have been made in (TNO 2013), including inversion of subsidence into compaction. We are aware that NAM is working on that.

5.3 Seismic hazard of the Eemskanaal area

5.3.1 Problem statement

Compared to the production plan of 2013, the seismic hazard maps of NAM (2014) are based on different inputs: the compaction and the production scenarios. First of all, the cumulative compaction as per January 1st 2014 has been revised, as has been discussed in paragraph 5.2. Secondly, in the modelling of TNO (2013, 2014a, b) and NAM (2013), it was assumed, that gas production from the Eemskanaal cluster would have stopped in March 2014. The actual production has continued at an average daily rate of some 7 mln Nm³/day (see Figure 5-9). The net result is that in the model predictions the amount of compaction increase in the Eemskanaal area has been underestimated. The question is what the effect on the seismic hazard will be in case of further continuation of the production of the Eemskanaal cluster.

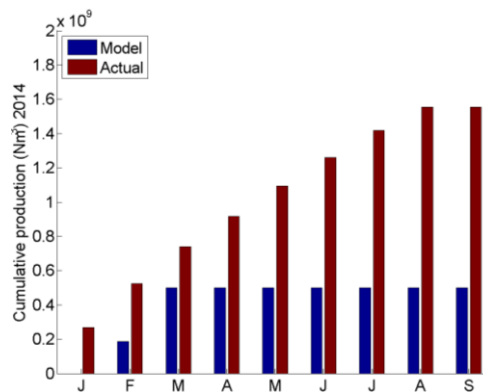


Figure 5-9. Actual and modelled production of the Eemskanaal (EKL) cluster in 2014 per month (January to September).

Since TNO has no access to the tools that have been used to calculate hazard, we have not been able to reproduce or verify the NAM results. We can only comment on the input scenarios that have been run, the calibration of the model and the characteristics of the output.

5.3.2 Scenario's for seismic hazard calculation

NAM has attempted to quantify the effect of changes in compaction and EKL cluster production level on the seismic hazard for the Eemskanaal area. In Appendix B of the NAM report (NAM 2014), a total of 32 scenarios are presented for calculating the seismic hazard.

The model sensitivity has been tested by combining:

- two dynamic reservoir models: model 1=STR40 and model 2=STR38;
- two compaction models: RTiCM (Pruiksma et al. submitted 2014) and Time Decay (TD);
- two seismological models: Strain Partitioning (SP) and Activity Rate (AR);

The production scenarios consider an average daily production rate for the Eemskanaal cluster of

- 3 mln Nm³/day
- 5 mln Nm³/day
- 8 mln Nm³/day

starting at November 1st 2014 (communication NAM). These average daily rates correspond to about 1 bcm, 2 bcm and 3 bcm per year.

Finally, for reference, NAM has presented two field wide production scenarios:

- 'WIPLA': conform the submitted production plan 2013;
- 'Production restriction': based on WIPLA but constrained by the decision of the minister of EZ in January 2014.

TNO considers this range of scenarios sufficient to test the seismic hazard sensitivity within the framework of the seismological models applied. TNO stresses, that this does not necessarily cover the full model uncertainty that exists, such as: the Ground Motion Prediction Equations and calibration of the seismological models on compaction.

5.3.3 NAM Results for seismic hazard

In Appendix B of (NAM, 2014), hazard is expressed in terms of Peak Ground Acceleration (PGA) at 0.2%, 2% and 10%/year chance of exceedance. Values are presented for the scenarios considered and pertain to the Eemskanaal cluster location (Note: in an Addendum to the NAM report a similar table has been provided for two locations in Groningen city).

From the table of results it is clear that the hazard level is strongly dominated by the choice of the relevant probability of exceedance. This choice therefore is crucial for further use in risk assessment, but falls beyond the scope of this report.

Reducing seismic hazard

TNO can only comment on the relative numbers for the various scenarios under the assumption of a certain probability of exceedance. Taking the case of 0.2%/year as a reference, the spread over all scenarios is between 0.29 and 0.38 g. Particularly striking is the fact that the hazard seems hardly (up to maximum 15%) sensitive to the production level assumed for the Eemskanaal cluster. In case of 2%/year

chance of exceedance the difference is even less (< 10%). As was confirmed by NAM, this stems from the fact that the hazard in the south-west periphery is strongly determined by the contribution to the hazard from the central Loppersum area, which is an inherent characteristic of the seismological models applied and the way they are calibrated.

Disaggregation of seismic hazard

At any point on the surface of the Groningen field, the seismic hazard is determined by the number of events, their magnitudes and consequently the peak ground accelerations at this point. A disaggregation of the hazard (NAM 2014c) shows that the hazard, for example, in the city of Groningen consist of a part which is caused by the events in the southwestern part of the Groningen field around Eemskanaal, a part which is caused by the events in the centre of the field and a part which is caused by the events in the south of the field. Reduction of pressure for the EKL clusters would only cause an effect on the hazard of this southwestern part of the hazard. The other parts of the hazard (centre and southern) would still be the same.

5.3.4 Remarks on the calibration of the seismological model

Seismological model

NAM has developed two seismological models: the strain partitioning model (SP) and the activity rate model (AR). Both are developed using the history of seismicity over the whole of the Groningen field. The SP model takes energy as main parameter and the AR model the number of events. In terms of seismic hazard, both models (STR38 and STR40) give similar values of Peak Ground Acceleration (PGA) at the same level of chance of exceedance (NAM 2014). As mentioned in TNO (2013), e.g. local differences in the existence of faults, local stress changes and local heterogeneities play a role (probably secondary) in the occurrence of seismic events. Since the seismological model is based on the history of seismicity, which is occurring mainly in the centre of the field, other parts of the field may not be adequately represented by the current seismological model. Moreover, the uncertainty in the compaction model is not taken into account in the calibration of the seismological model(s): the calibration of the seismological models rely on just one realization of the subsurface model.

Finally, the seismological models (activity rate and strain partitioning) allow for events in the low compaction areas of the field where little or no seismicity has occurred so far. This will smear out the hazard over the field, hiding possible local effects on the hazard.

A reduction in production rate at EKL may lead to a change in the rate of seismicity (as is seen in the centre of the field, due to the reduction of production, see Chapter 2). The lower rate of seismicity per year will at least locally reduce the number of events per year but may or may not (NAM, 2014) influence the hazard. As production in the centre has been decreased since January 17th 2014, the largest reduction of the seismic hazard has already been achieved.

5.3.5 Findings on seismic hazard

From our review of the NAM report on the part of seismic hazard in the Eemskanaal area, and based on the TNO analysis of this, TNO concludes the following:

- TNO considers this range of scenarios sufficient to test the seismic hazard sensitivity within the framework of the seismological models applied.
- TNO stresses, that this does not necessarily cover the full model uncertainty that exists, such as: the Ground Motion Prediction Equations and calibration of the seismological models on compaction.
- From the table of results it is clear that the seismic hazard level is strongly dominated by the choice of the relevant probability of exceedance
- As mentioned in TNO (2013), e.g. local differences in the existence of faults, local stress changes and local heterogeneities (porosity, compaction) play a role in the occurrence of seismic events, which has not been taken into account in the seismological models
- The relative seismic hazard indicator as introduced in March 2014 (TNO 2014a, b) is actually related to seismicity rather than seismic hazard. The value of the indicator is similar to the one calculated in TNO (2014a, b) except for the area around Tjuchem (slight increase) and the area north of Eemskanaal (increase) which is due to the different production model used.

5.4 Overall findings on the NAM (2014) report

NAM presents the following conclusions:

1. The Eemskanaal cluster is located at the western periphery of the field and produces higher calorific gas. This gas needs to be blended to sales specification. Due to the larger subsurface uncertainty at the periphery of the field and the blending requirement forecasting production from the Eemskanaal cluster and compaction/subsidence in the Eemskanaal area is challenging.
2. Using the subsurface model from the production plan 2013 as a base, the History Match for the Harkstede block (produced by EKL-13) has been improved. Two reservoir models capturing the main subsurface uncertainty (aquifer influx) have been prepared in support of the Hazard Assessment for the Eemskanaal Area.
3. For the improved reservoir models, the impact of the compaction model on the hazard is limited.
4. Similarly, the impact of the production level of the Eemskanaal Cluster on the hazard is limited.
5. The impact of the selected improved reservoir model is reflected in a moderate uncertainty in the hazard assessment, mainly to the west of the field.

TNO opinion on these NAM conclusions is:

1. From the geological and reservoir dynamic model as well as the geodesy it is indeed clear that modelling of compaction in the south-west periphery of the Groningen field carries relatively large uncertainty.

2. The solutions presented by NAM (the two proposed models) primarily rely on modifications of the transmissivity of the aquifer connected to the south-west periphery of the Groningen field;
These solutions are not unique: other (combinations of) parameters may explain the discrepancy in subsidence equally well.

And, as to the conclusions 3 to 5, in general:

- TNO has no access to the tools that have been used to calculate seismic hazard, we can only comment on the input scenarios that have been run and the characteristics of the output.
- Seismic hazard is strongly dominated by the choice of the relevant probability of exceedance. All other uncertainties give a much smaller impact on the seismic hazard.
- As mentioned in TNO (2013), e.g. local differences in the existence of faults, local stress changes and local heterogeneities (porosity, compaction) play a role in the occurrence of seismic events, which has not been taken into account in the seismological models.

6 TNOs seismic hazard indicator

Due to the relatively large adjustment of reservoir compaction in the Eemskanaal area (as described in chapter 5), the value of the partitioning coefficient, which determines the proportion of the energy which can seismically be released in the strain partitioning model, has changed as well. In the southwest periphery of the field, the partitioning coefficient is at least doubled and in some areas even one or two orders of magnitude larger for the STR38 model compared to the STR40 model (Figure 6-1).

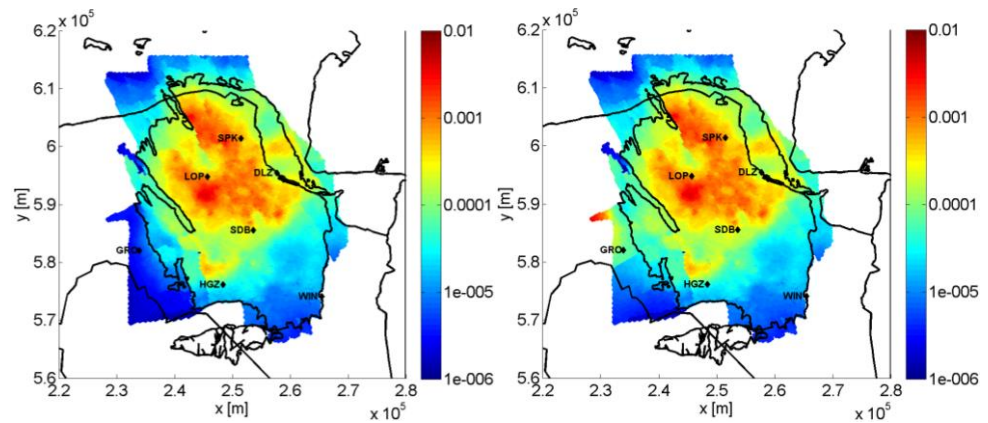


Figure 6-1. Partitioning coefficient for the relationship described in (TNO, 2014b) for the two models of NAM (2014): STR38 (left) and STR40 (right). The background is similar to Figure 5-4.

The seismic hazard indicator is calculated as follows (TNO, 2014a, b).

$$\Delta H(sc1, sc2) = (\alpha_{2017}^{sc2} * h_{2017}^{sc2} - \alpha_{2014}^{sc2} * h_{2014}^{sc2}) - (\alpha_{2017}^{sc1} * h_{2017}^{sc1} - \alpha_{2014}^{sc1} * h_{2014}^{sc1})$$

This indicator is normalized to 1.0 to show relative changes per location in the field. The relative seismic hazard indicator as introduced in March 2014 (TNO 2014a, b) reflects the change in seismic moment, which is more related to event density than to seismic hazard. To allow for comparison with TNO (2014a, Figure 4-4; 2014b, Figure 6-5), we have calculated the seismic hazard indicator for the period January 2014 to January 2017. The models (sc1, sc2) in January 2014 have been replaced by the History Match ('HM') model STR38. This model was chosen because of the better fit to the observed subsidence measurements (Chapter 5).

$$\Delta H(sc1, sc2) = (\alpha_{2017}^{sc2} * h_{2017}^{sc2} - \alpha_{2014}^{HM} * h_{2014}^{HM}) - (\alpha_{2017}^{sc1} * h_{2017}^{sc1} - \alpha_{2014}^{HM} * h_{2014}^{HM})$$

The resulting relative seismic hazard indicator is shown in Figure 6-2 for the history match model STR38 and the 8 million Nm³ production per day scenario for the EKL cluster in comparison to the market demand scenario as proposed in NAM (2013).

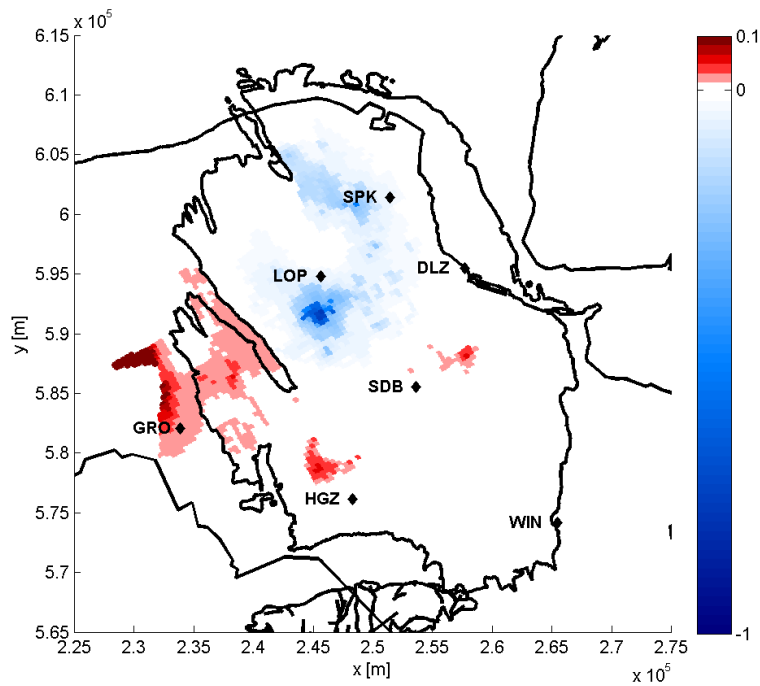


Figure 6-2. Seismic hazard indicator for the STR38 model with 8 mln Nm³/day production of EKL compared to a scenario that follows the market demand.

Comparing the above Figure 6-2 with Figure 6-5 from TNO (2014b), the area where the event density has decreased (blue) due to the production reduction of January 2014 in the centre of the field is the same for both. The indicator value in this area is an order of magnitude larger than in the rest of the field. Additionally, TNO (2014a, b) showed a small increase in seismicity north of Hoogezand. This increase is slightly larger, shown in Figure 6-2. Figure 6-2 shows an increase in the area of Tjuchem, where the SCB cluster has increased production in 2014 (Figure 2-1). The area north of EKL shows an increase in seismicity as well. The cause is twofold: first, the history match model has changed in this specific area which causes larger compaction and hence seismicity; second, the actual production of the EKL cluster has been larger than the previously assumed in the modelling (Figure 5-9).

The spatial distribution of the seismic hazard indicator (Figure 6-2) is similar to the spatial distribution of the difference in earthquake density between the years 2013 and 2014 (Figure 2-6). Both types of information (indicator and observed seismicity) compare a market demand scenario (the observed seismicity in 2013 was due to a market demand production) to the actual production reduction in the centre of the field (observed seismicity in 2014). Remarkably, the indicator is a result of comparing two models based on production scenarios, which is independent of observed seismicity, while the seismicity was observed in 2013 and 2014. Therefore, the seismic hazard indicator suggests a local response in terms of seismicity.

7 Main Findings

Here TNO summarizes the main findings as to the research questions addressed in this report:

Question 1: Are there indications of an effect on seismicity due to the production reduction as imposed on January 17th 2014?

Registered seismic events indicate that the density of seismicity for the Groningen field during 2014 is lower compared to 2013. Analysis of the density of seismicity also shows that during 2014 the spatial pattern has changed compared to 2013. Less seismic events occur in the central part of the field, where production has been reduced since January 17th 2014, while more events are registered in the areas north of Hoogezand and near Tjuchem.

A Bayesian statistical analysis has been performed on the number of seismic events occurring on a yearly basis since the first seismic event in 1991. For the period of 2003 to 2013 this analysis shows that the observed increase of seismic events in the Groningen field is statistically significant and cannot be explained by a stationary model. For the period after 17th of January 2014, the statistical analysis indicates a slight preference for a model that predicts a decrease of seismic events in 2014 over the whole of the field. This is in accordance with the observed lower seismic density in 2014 compared to 2013 mentioned above. The number of observed seismic events, however, is insufficient to make more quantitative statements on this.

Question 2: Analysis of compaction near the Eemskanaal cluster. Is there a geological ground to explain discrepancies between modelled and observed subsidence in terms of porosity and associated compaction coefficients.

The discrepancy between modelled and observed subsidence was circa 7 cm (TNO 2013) in the south-west periphery of the field. The actual reservoir compaction is likely to be larger than calculated so. The south-west periphery of the field has both a fairly high porosity as well as a side aquifer to the west, rendering this part of the field the most uncertain in terms of compaction modelling.

The uncertainty in porosity of the southwest periphery of 1.5 pu, as indicated by NAM, is realistic at the well locations. TNO considers that higher porosity values (1 to 2 pu, maximally 3 pu) in the area between Ten Boer and Eemskanaal cannot be geologically ruled out regarding the absence of well control. Data from compaction experiments of EKL-12 suggest that the value of the compaction coefficient, at a certain porosity level, may be higher in the Eemskanaal area than elsewhere in the Groningen field. Both aspects could, at least partially, explain the discrepancy between modelled and observed subsidence in this area.

The activity of the west aquifer is difficult to model due to the lower well density and scarce data on pressure and water rise. As NAM (2014) indicates both a strong and a weak aquifer could fit the measurements of pressure and water rise. The actual

production of the Eemskanaal cluster is different from the model predictions in 2013 and the beginning of 2014 adding to the uncertainty in compaction.

Based on an analytical estimate, a reduction of production at the Eemskanaal cluster is expected to have a temporary effect (circa 2 years) on the rate of pressure reduction in this part of the reservoir. After this period, pressure decline due to continuing production of surrounding clusters will continue in this area.

Question 3: Review of NAMs (2014) report on the hazard of the Eemskanaal area

TNO opinion on the conclusions of NAM (2014) is:

- From the geological and reservoir dynamical model, as well as geodetical data, it is clear that modelling of compaction in the south-west periphery of the Groningen field carries relatively large uncertainty.
- The solutions presented by NAM (the two proposed models) primarily rely on modifications of the transmissivity of the aquifer connected to the south-west periphery of the Groningen field; These solutions, although certainly plausible, are not unique: other (combinations of) parameters may explain the discrepancy in subsidence equally well.
- Seismic hazard is strongly dominated by the choice of the relevant probability of exceedance. All other uncertainties give a much smaller impact on the seismic hazard.
- As mentioned in TNO (2013), e.g. local differences in the existence of faults, local stress changes and local heterogeneities (porosity, compaction) play a role in the occurrence of seismic events, that have not been taken into account in the seismological models.

Question 4: Actualization of the TNO (2014a,b) report

In TNO (2014a, b), a map of the seismic hazard indicator showed a relatively large decrease in the centre of the field due to the production reduction and a much smaller increase to the north of Hoogezand. In this report, the map of the seismic hazard indicator, as presented in TNO (2014a, b), has been updated for compaction and actual production. Small increases in the indicator value occur in the area north of Hoogezand, the area of Tjuchem and the area north of the Eemskanaal cluster. In the areas north of Hoogezand and the area of Tjuchem, the increase is due to the fact that actual production has been larger than modelled in TNO (2014a, b). The area north of Eemskanaal shows an increase in the indicator as well. The cause is twofold: firstly, the history match model has changed in this specific area which causes larger compaction; secondly, the actual production of the Eemskanaal cluster has been larger than assumed in the previously models.

The spatial distribution of the seismic hazard indicator is similar to the difference in earthquake density for the years 2013 and 2014. The seismic hazard indicator suggests a local response in terms of seismicity (i.e. location of seismic events).

8 References

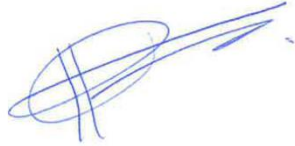
- EZ 2014a Brief van de Minister van Economische Zaken aan de Vaste Kamercommissie (kenmerk: DGETM/ 14008697) 17 januari 2014
- TNO 2012 Toetsing van de belasting op de gebruiksruimte in de kombergingsgebieden Pinkegat en Zoutkamperlaag door bodemdaling ten gevolge van gaswinning onder de Waddenzee. TNO rapport TNO 2014 R11703, 16 maart 2012
- TNO 2013 Toetsing van de bodemdalingsprognoses en seismische hazard ten gevolge van gaswinning van het Groningen veld. TNO rapport 2013 R11953, 23 december 2013.
- TNO 2014a Effecten verschillende productiescenario's op de verdeling van de compactie in het Groningen veld in de periode 2014 t/m 2016. TNO rapport 2014 R10427, 7 maart 2014.
- TNO 2014b Technisch rapport behorende bij "Effecten verschillende productiescenario's op de verdeling van de compactie in het Groningen veld in de periode 2014 t/m 2016". TNO rapport 2014 R10426, 7 maart 2014
- NAM 2003 Groningen Field Review 2003 (GFR2003). Groningen Field Static Modelling and Ultimate Recovery Determination, 2003. NAM Assen.
- NAM 2012 Groningen Field Review 2012 (GFR2012). Static modelling and hydrocarbon volume determination. December 2011, NAM Assen. Document nr.: EP201203204663.
- NAM 2013 Wijziging winningsplan Groningen 2013, inclusief technische bijlage Groningen winningsplan 2013. Versie 29 november 2013.
- NAM 2014 Hazard Assessment for the Eemskanaal area of the Groningen field. Versie 15 november 2014.
- NAM 2014b Continue GPS hoogtemetingen NAM Groningen, rapportage juni 2014.
(http://www.nlog.nl/resources/Meetregisters/Groningen/2014_06%20Continue_GPS_hoogtemetingen_juni_2014_Groningen.pdf)
- NAM 2014 c Addendum to Hazard Assessment for the Eemskanaal area of the Groningen field.

- Pruiksma et al., 2014 J. P. Pruiksma, J.N. Breunese, K. van Thienen-Visser, J.A. de Waal. Isotach formulation of the Rate Type Compaction Model for Sandstone, *submitted to International Journal of Rock Mechanics and Mining Sciences*, October 2014.
- SGS 2013 Independent Review of Groningen Subsurface Modelling. November 2013, SGS Horizon.

9 Signature

Utrecht, 9 December 2014

TNO

A handwritten signature in blue ink, consisting of several overlapping loops and a long horizontal stroke extending to the right.

Ingrid Kroon

Head of department

Karin van Thienen-Visser, Manuel Nepveu, Bart van
Kempen, Marloes Kortekaas, Jenny Hettelaar, Lies
Peters, Serge van Gessel, Jaap Breunese
Authors

A Derivation of relation time-distance of pressure wave

Question

Obtain an analytical equation of the time-distance relation of a pressure wave in the current pressure field of the Groningen gas field.

Basic equations

Reference book Hagoort 'Fundamentals of gas reservoir engineering'

$$d_p = [4 D_h t / \pi]^{1/2} \quad (\text{p. 135 Pressure-penetration distance (radial field)})$$

$$\begin{aligned} > \text{arrival time} \quad t &= \pi d_p^2 / 4 D_h \\ \text{with} \quad D_h &= k / \phi \mu c \quad (\text{p. 131 hydraulic diffusivity}) \end{aligned}$$

Choice of parameters

Temperature $T = 100 \text{ C}$

Pressure $p = 90 \text{ bar}$

Permeability $k = 100 \text{ mD}$ representative for Eemskanaal (EKL) region
 $= 9,9 \cdot 10^{-14} \text{ (m}^2\text{)}$ (p.314 conversion)

Porosity $\phi = 0,2$ representative for Eemskanaal (EKL) region

Viscosity of gas $\mu = 15 \cdot 10^{-6} \text{ (Pa.s)}$ methane @ 90 bar and 100 C
 (Peace software, Berlin)

Compressibility of gas $= (275 / 90) * 0,0286 \cdot 10^{-6} \text{ (Pa}^{-1}\text{)}$ (p.41 and assume $Z = 1$)

Result

$$D_h = 0,38 \text{ (m}^2\text{/s)}$$

$$\begin{aligned} > \text{arrival time} \quad t &= 2,07 * d_p^2 \quad \text{with } t \text{ in [s] and } d_p \text{ in [m]} \\ \text{or:} \quad t &= 0,79 * d_p^2 \quad \text{with } t \text{ in [months] and } d_p \text{ in [km]} \end{aligned}$$

Full penetration of the pressure wave takes longer than the first arrival. The time scale until full penetration will therefore be larger. In the following table a factor 3 is assumed, since the underlying process is exponential and a factor 3 will give the time until 99% of pressure wave has penetrated the medium.

Distance to EKL (km)	Time first arrival (months)	Time (99%) of pressure wave (3*t) (months)
2	3	9
4	13	39
6	28	84
8	51	153
10	79	237

B Bayesian Statistical method

In this appendix we collect background information with respect to the statistical treatment chosen on seismicity at the Groningen field. We will deal here with those elements of Bayesian Statistics that we have actually used. Also, we give an outline of the derivation of the Bayes factor that is central in our investigations. However, we should start with offering some justification of the basis of it all, the Poisson Process.

Poisson Processes

Assume that the probability of an event on the infinitesimal time interval $(t, t+dt)$ is λdt . The proportionality factor λ may depend on time. Further assume that knowledge of (non)-occurrence in any other time interval is irrelevant to the probability of an event on $(t, t+dt)$. THEN it is a mathematical fact that the probability of k events up till time t is given by

$$P(N(t) = k) = m(t)^k / k! \cdot e^{-m(t)} \quad \text{with } m(t) = \int \lambda(t') dt' \text{ over } [0, t] \quad (\text{eq.1})$$

When λ is independent of time we find the usual Poisson distribution; the Poisson process is said to be stationary. Otherwise the Poisson process is called non-stationary.

In this report we will investigate three models. The basic model for seismicity on a chosen time interval is defined as

Stationary Model: $\lambda = a$, **constant**

The second model is chosen to represent an increase in seismicity with time. We have chosen an exponential increase, with a positive time constant τ , and so the model is defined as

Increase Model: $\lambda = a \exp(t/\tau)$

The third model is chosen to represent a decrease in seismicity, and is defined as

Decrease Model: $\lambda = a \exp(-t/\tau)$

Outline of Bayesian Model Comparison.

In our statistical problem we want to investigate whether seismicity data on some interval are best described by a stationary, an increase or a decrease model. In Bayesian Statistics it is possible to attribute a probability (plausibility) to a model *within a given set of* models. This model probability is, denoted as $P(M | D)$, to be read as the probability (plausibility) of model M , conditional on D , the data.

It is easiest to compare two models in the set by computing the quotient

$$P(M | D) / P(M' | D) = [P(M) / P(M')] \times P(D | M) / P(D | M') \quad (\text{eq.2})$$

The quotient in brackets represents the a priori assessment of the models M and M'. To prevent a bias it is chosen to be unity. The other quotient in the equation contains the likelihoods of the data D on assuming model M, resp. M'. This second quotient is known as the **Bayes factor** of the two models. We now see that the odds of the models M and M' is the Bayes factor of these models. Bayes factors will be reported in our investigations.

The models contain parameters that are not known. They are called *nuisance parameters*. The proper way to deal with them in Bayesian Model Comparison is to integrate them out of the problem – a so-called marginalization process. For example, we formally write down $P(D | M, a)$ with some badly / vaguely known parameter 'a'. We invoke a so-called prior $p(a)$, the probability density for parameter 'a' containing the information we have on 'a', *not dependent on the present data set D, i.e. information prior to having seen the data*. The likelihood for model M is then calculated by the relation

$$P(D | M) = \int p(D | M, a) p(a) da \quad (\text{eq.3})$$

It is relevant to choose an appropriate $p(a)$, describing one's state of knowledge. There is quite some literature on how to deal with this (Gregory 2010, Jaynes 2003) especially when one's state of knowledge is poor.

Determining the likelihoods and Bayes factor(s)

We now describe how we determine the likelihood of a given dataset under the general Poisson process in (eq.1). First of all we divide the timeline over a given interval in many small time intervals Δt . We notice in which intervals seismic events have taken place and also in which intervals they did not. The number of intervals with an event be N, without an event be V (void). The probability of NO event is $e^{-\lambda \Delta t}$, the probability of ONE event is $\lambda \Delta t e^{-\lambda \Delta t}$. The time intervals are chosen so small that the probability of more than one event in them is essentially zero. The likelihood of the data set is $P(D | \lambda)$ is the product of the NO-events and the ONE-events at the given times. If the time intervals are taken small any sums in the exponential can be converted into integrals and the final answer becomes

$$P(D | \lambda) = (\Delta t)^N \prod_N \lambda(t_i) \exp(-\int_T dt \lambda(t) dt) \quad (\text{eq.4})$$

Two remarks are in order.

- 1) Not surprisingly the likelihood depends on the choice of the time interval Δt – indeed, each time interval represents an experiment. However, since the Bayes factor of any two models is a quotient of likelihoods the chosen values for Δt drop from the equations. The intervals appear only as logical constructs needed to establish (eq.4); we do not have to worry about them explicitly.
- 2) In (eq.4) only the number of events N seems to feature explicitly. However, this is not quite true: the V time intervals with no event are hidden in the exponential part of the equation. They are essential as they assist constituting the integral in the exponential over the *complete interval* under scrutiny.

The stationary model has one nuisance parameter, the increase and decrease models have two. They must be integrated out as described. Let us first consider

the parameter a . For $p(a)$ we choose a constant distribution over a very large range $[0, a^*]$. That is, we have hardly any prior knowledge about the actual values we will meet in our datasets. It turns out that the integration as shown in (eq.3) can be performed by analytical means; the resulting function of τ is quite complicated – but independent of a^* if that is chosen very large. Next one computes the Bayes factor for an increasing model versus a stationary model by integrating τ out. This operation calls for a different prior probability, the so-called Jeffreys prior. This choice is a mathematical translation of admitting that the expected order of magnitude is not precisely unknown *and* that τ is a so-called scale parameter. (See Gregory, 2010) We still have to choose sensible under and upper limits for τ . We know a priori that values of τ of just a few years are practically excluded, and for the maximum value we choose values slightly over 30 years. The Bayes factor is now given by the integral over this assumed τ -region. We write it symbolically as

$$\text{Bayes factor} = \int f(\tau) g(\tau) h(\tau) d\tau$$

where we have split the integrand into three factors f , g and h each depending on τ

$$\text{With } f(\tau) = \left[\tau \ln \left(\frac{T_{\max}}{T_{\min}} \right) \right]^{-1}$$

$$\text{And } g(\tau) = \exp \left(\frac{\sum (t_i - T_b)}{(T_e - T_b)} \times \frac{(T_e - T_b)}{\tau} \right)$$

$$\text{And } h(\tau) = \left\{ \left[\exp \left\{ \frac{(T_e - T_b)}{\tau} \right\} - 1 \right] / \frac{(T_e - T_b)}{\tau} \right\}^{-(N+1)}$$

- The function $f(\tau)$ is the Jeffreys' prior as explained above. It is the only factor containing the prior information.
- The function $g(\tau)$ is the only factor containing seismic event dates. It shows whether there is a tendency for data to be more concentrated to the beginning of the total time interval under scrutiny $(T_e - T_b)$, or more near the end, or neither. It is easily seen that this function will get very large for N large.
- The function $h(\tau)$ is a kind of regularizing factor taking into account the relation between the total time interval and the value of the time constant τ as well as the number of events recorded. This function arises by the process of integrating parameter 'a' out of the problem. It will tend to become very small for N large.

The Bayes factor for the decrease model is found along the same lines, the formula being the same except for the substitutions $g \rightarrow 1/g$ and $h \rightarrow h \exp \left[\frac{(N+1)(T_e - T_b)}{\tau} \right]$. In the decrease model the 'new' g will tend to be very small, the 'new' h will tend to be very large for N large.

For the numerical evaluation of the integral we used the extended Simpson's rule with a cover M of 500 points. This method is known to have an accuracy of order $1/M^4$.

An interpretation of Bayes factors

In the classical statistical analysis one tests hypotheses and defines a so-called P-value at which a hypothesis is just accepted. In Bayesian statistics the Bayes factor is the probability or plausibility of one model compared to another model. The

following interpretation (due to Harold Jeffrey's, see Wikipedia on Bayes factor) seems to be common.

K	Strength of evidence
< 1:1	Negative (supports M_2)
1:1 to 3:1	Barely worth mentioning
3:1 to 10:1	Substantial
10:1 to 30:1	Strong
30:1 to 100:1	Very strong
> 100:1	Decisive

Whether one calls a strength of evidence decisive at $K=100$, or chooses another criterion is up to one's own standards. The above table, hence, should be considered just a rough guide on how to value the results.

The posterior for τ

Once it has been established that a non-stationary model describes the time distribution of the seismic events better than the stationary model it may appear meaningful to determine the posterior distribution of τ . This posterior $P(\tau | D)$ is equal to the normalized product of the prior $p(\tau)$ and the likelihood $P(D | \tau)$ for τ . But this is equal to the integrand of the Bayes factor divided by the Bayes factor. Hence, we have the posterior at our disposal once we have done the work to obtain the Bayes factor.

From the general form of the graphical display one can infer to what extent the prior information $p(\tau)$ or the likelihood $P(\tau | D)$ dominates the result.

Let us have a look at fig.1. In this figure we see the likelihoods for the three areas pertaining to the seismic events between 1st January 2003 and 17th January 2014. The Bayes factors are (very) large in all three cases. In fig.1 one does not recognize the $1/\tau$ –prior: the three curves are peaked and fall off towards smaller τ -values. Furthermore, especially the two curves of “Central” and “Other” (having the largest Bayes factors) indicate very small values for $\tau > 20$ years. We conclude that the likelihood dominates the posterior. The interpretation is that the occurrence times of the events “speak for themselves”.

The widths of the three curves tell us how strong the data indicate certain values of the scale parameter τ . The larger the Bayes factor of the areas, the more peaked the posterior appears to be. The data discriminate more clearly which values of the time constant fit best. Indeed, in any case where Bayes factors are below one such sharply peaked posteriors are absent.

Additional Results

Period January 2003 up to January 17th 2014

It is worth noticing that if only events with at least a magnitude of 1.5 were regarded for this analysis, the Bayes factors would have been considerably lower see table below. “Increasing” models would still be preferred, but the stationary ones would not be excluded.

Name	Bayes Factor	Number of events
Central	2.67	112
SW	1.61	16
Other	6.72	47

When allowing only events with magnitudes > 2.5 we find that Bayes factors are marginally below one. It is obvious if there is a trend in the data, *more* data do more dramatically expose this trend, if there is any.

Period from January 17th 2014

If we regard all data (i.e. within the original areas instead of "ADAPTED"), the trend of a slight favor of the "decreasing" model is even more clear as appears from the next tables.

Name	Bayes Factor Increase/ Stationary	Number of events
Central + SW + Other	0.83	46

Name	Bayes Factor Decrease/ Stationary	Number of events
Central + SW + Other	1.28	46

This result should come as no surprise, as more data allow more 'discriminatory' verdicts.

References

H.S.Carslaw, J.C.Jaeger, Conduction of Heat in Solids, 1997, Clarendon Press Oxford, p. 261-2

P.C. Gregory, Bayesian Logical Data Analysis for the Physical Sciences, Cambridge University Press 2010, Chapter 3.

E.T. Jaynes, Probability Theory – the Logic of Science, Cambridge University Press 2003, Chapter 12.

C Petrophysical analysis

TNO has evaluated the porosity modelling and petrophysical porosity calculations performed by NAM, focusing on the area in the vicinity of the Eemskanaal cluster.

Available data for petrophysical evaluation

This section presents a description and overview of available data used for this evaluation.

Log data

The Eemskanaal cluster consists of 13 production wells (EKL-01 – EKL-13). The locations of these wells are given in Table D-1 in Appendix D. Table C-1 provides an overview of the available well logs.

Wells EKL-12 (drilled in 1984) and EKL-13 (drilled in 2005) contain the most complete log data sets. Well EKL-13 is strongly deviated over ca. 3 km horizontal distance in South-West direction (see Figure 3-2) and penetrates the Slochteren Sandstone interval 200 m deeper within the Harkstede Block. The other wells have been drilled in the early 1970's and have only limited well log data available.

Table C-1. Available log data for wells in the Eemskanaal cluster

Well	Gamma-Ray	Density	Neutron	Sonic	Resistivity (Deep)	Resistivity (Shallow)
EKL-01	X	X		X	X	X
EKL-02	X	X			X	
EKL-03	X	X			X*	
EKL-04	X	X			X	
EKL-05	X	X			X	
EKL-06	X	X			X	
EKL-07	X	X				
EKL-08	X	X				
EKL-09	X	X				
EKL-10	X	X				
EKL-11	X	X				
EKL-12	X	X	X	X	X	X
EKL-13	X	X*	X*		X*	X

* Slochteren Sandstone interval only partly logged

Core data

Core data is available for wells EKL-1 and EKL-12. In well EKL-1 the Upper Slochteren USS3 and USS2 reservoirs are partially cored over a ca. 27 m along hole interval. The core data of EKL-12 covers the entire Slochteren Sandstone interval. An overview of the core data used for petrophysical evaluation is shown in Table C-2. Figure C-1 shows a distribution of porosity and permeability measurements from plug samples in the Slochteren Sandstone interval.

Besides regular porosity and permeability measurements, the core plug samples of EKL-12 also comprise data from saturation and compressibility experiments. The

analytically determined saturation exponents m and n are used for the petrophysical evaluation. From the compressibility data in well EKL-12 an average *in-situ* correction of ca. 8.3% has been determined.

Table C-2. Overview of core data used for petrophysical evaluation.

Well	Cored interval		Nr. of Samples	Interval Coverage (%)
	Top (MD)	Base (MD)		
EKL-01	2787	2814	88	16.7
EKL-12	2897	3076	451	100

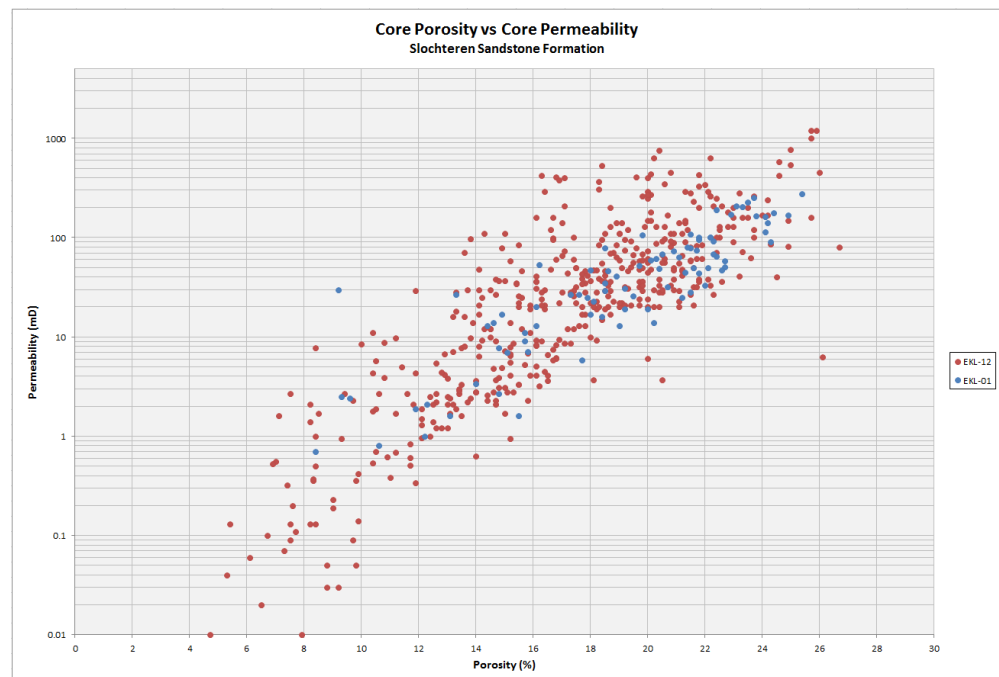


Figure C-1. Porosity vs permeability measured on core plug samples from the Slochteren Sandstone in wells EKL-12

Data provided by NAM

For the evaluation of the Groningen porosity model and the underlying porosity calculations performed by NAM in the Eemskanaal area, a selection of data was provided. The Petrel model that was part of the GFR2012 (NAM 2012), containing the porosity model, all porosity maps, trend maps, and log data of the relevant reservoir units in used wells was available for evaluation, together with the underlying reports of the GFR2003 and GFR2012 (NAM 2003, NAM 2012). Furthermore, the review report of SGS Horizon on the Groningen Field model was available (SGS 2013).

Based on the porosity model, that can be subdivided per reservoir unit, porosity maps were constructed by NAM for each reservoir unit (see Appendix D). These porosity maps are evaluated and compared with porosity data from porosity profiles calculated by NAM. The porosity profiles were extracted from the Petrel model (NAM 2013) and analysed. Below the methods used by NAM to calculate these profiles, and the analysis by TNO is described in detail.

Analysis methods

This section summarizes the petrophysical analysis methods to calculate porosity profiles used by NAM (NAM 2013). Independent petrophysical analyses and porosity calculations performed by TNO are used to evaluate and discuss NAM's methodology and results.

NAM Porosity models

NAM uses two different methods to calculate porosity, depending on the availability of certain well logs.

1. When a density log (possibly in combination with a neutron log) or sonic log and a shallow resistivity log (Rxo log) are available, NAM performs a full petrophysical analysis using a complex iterative Waxman-Smiths Sxo method. For the GFR2003 model (NAM 2003) this method was applied for 125 wells. These results are incorporated in the GFR2012 model (NAM 2013).
2. In case no Rxo log was measured, NAM uses a linear transformation for calculating a porosity profile from the density log. This linear transformation is determined by plotting core porosity measurements against bulk density log measurements at corresponding depths, and matching the resulting correlation line with the matrix- and fluid density at 0% and 100% porosity respectively. The transformation was performed separately for the gas zone and the water zone. The GFR2012 report (NAM 2013) describes a general transform created for the entire Groningen Field. For each individual well this transform was corrected for depth and shale volume, resulting in well-specific transforms. In case no density log was available, NAM applied the same technique to the sonic log. The result is a linear transform to convert sonic slowness to porosity.

From the GFR2003 analysis and modelling NAM deduced that the correlation between density (or sonic) and porosity provides results that are similar to the full Waxman-Smiths petrophysical analysis. Therefore NAM decided to apply this linear correlation technique to an additional set of 240 wells for which limited data are available. These results are incorporated in the GFR2012 model (NAM 2013).

TNO Porosity models

TNO applied a full petrophysical analysis and linear correlation technique on a selection of five wells in the Eemskanaal cluster. One well was analysed by the linear correlation technique only. The evaluation of these analysis results and the comparison to the porosity calculations of NAM, provide an indication of the validity and uncertainty of the porosities used in the model (NAM 2013).

Full petrophysical analyses

Petrophysical analyses were performed for wells EKL-1, EKL-2, EKL-3, EKL-12 and EKL-13. These wells were selected based on the availability of data (see Table C-1), NAM's evaluated porosity ranges and location in the structural model. Well EKL-13 is the most recently drilled and includes an extensive set of logs. Wells EKL-2 and EKL-3 were specifically selected because NAM's work indicates relatively low porosity values compared to the other wells and because these wells are drilled in structurally distinct locations (i.e. within a fault and in a small

intermediate fault block respectively). It was not possible to properly analyse EKL-7 to -11 because resistivity logs are lacking. The analysed porosity values for each reservoir unit are presented in Table C-3 to Table C-6 (column “TNO Petrophysics”).

TNO adopted NAM's upward increasing linear clean sand line method to determine the shale volume in all five wells. NAM applied this technique to correct for the upward increasing feldspar content. TNO considers this method as a valid technique in this study.

For the petrophysical analysis of wells EKL-12 and EKL-13 a neutron-density porosity model was used. For wells EKL-1, EKL-2 and EKL-3 a density porosity model was used, as neutron logs were not available. Saturation calculations were performed using the Indonesian Formula. Gas and formation water properties were obtained from analyses on samples of well EKL-1.

For wells EKL-1 and EKL-12 the calculated porosity profile was calibrated with *in-situ* corrected core analysis measurements. The *in-situ* correction is determined from compressibility measurements on core plug samples of EKL-12. An average porosity reduction factor of 0.917 was applied to correct porosity measurements.

Linear bulk density – core porosity correlation

The determination of the linear relation for converting bulk density values into porosity values requires a bulk density log as well as (*in-situ* corrected) core plug porosity measurements. Well EKL-12 is the only well in the Eemskanaal cluster where both data sets are available for the entire Slochteren Sandstone interval. Although a bulk density log is measured in well EKL-1, TNO does not regard the linear correlation in this well representative for this evaluation as only 27 m of the total 161 m thick Slochteren Sandstone interval was cored.

For each well NAM corrected their general correlation for the entire Groningen field for depth and shale volume. This approach fits the general linear relation to the individual wells. TNO considers their correlation applicable to the area in the vicinity of Eemskanaal as it is directly based on data from well EKL-12. The use of location specific data will reduce the inaccuracy.

In Figure C-2 the *in-situ* corrected core plug porosity measurements of well EKL-12 are plotted against the bulk density log values at corresponding depths (black points). The background colours represent a contour-plot of the data-point density. The contour values clearly show the dominant, linear decreasing trend in the data. Figure C-2 also shows TNO's correlation line which matches with this trend and fits through the data points (black line). This correlation line is used by TNO to convert the bulk density log values to porosity values in the Eemskanaal area.

TNO calculated porosity profiles for six wells using this linear correlation method. The average porosity per reservoir unit can be found in Table C-3 to Table C-6 (column “RHOB-CPOR”).

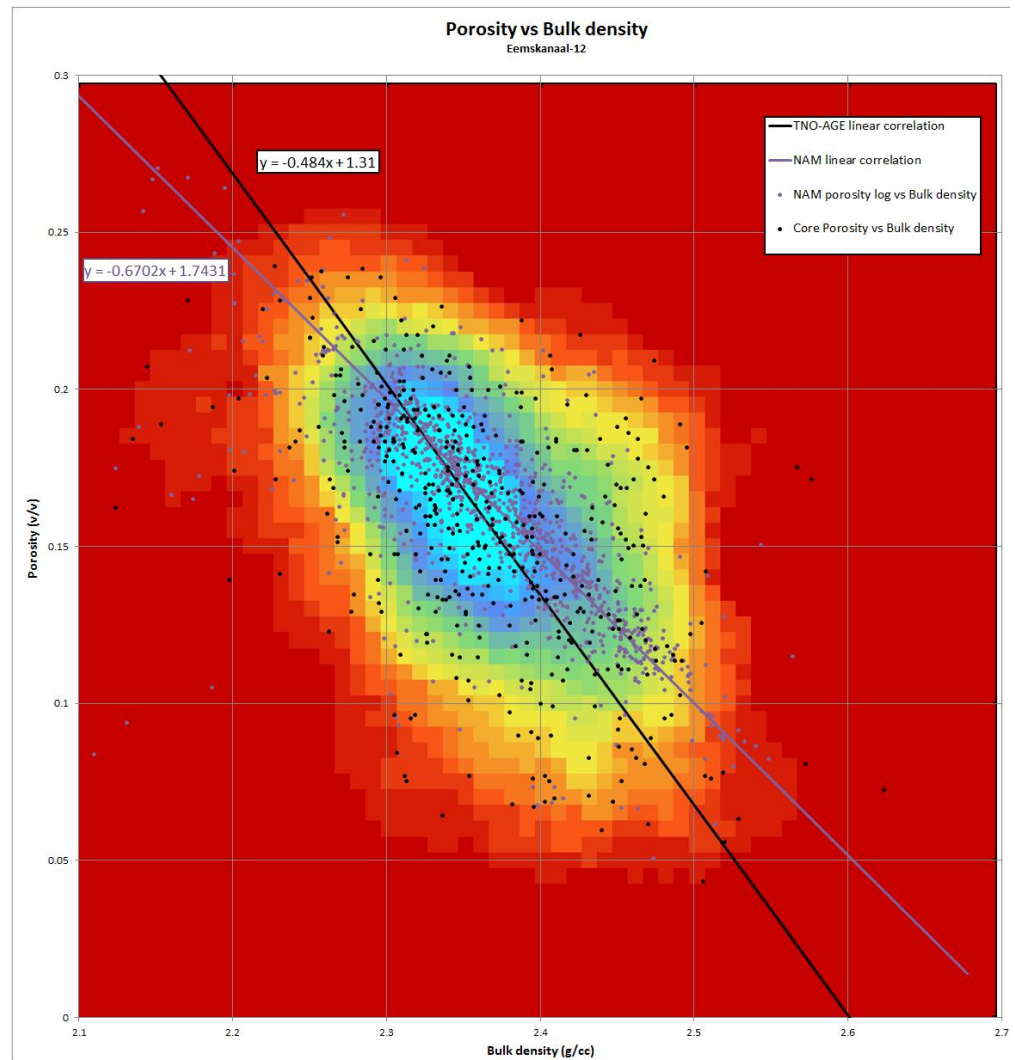


Figure C-2. Contour plot of data-point density based on black data points. Black point set represents EKL-12 core porosity measurements versus bulk density. The black line is defined by TNO and represents the linear trend through this set. The purple point set represents porosity values from NAM's porosity profile versus bulk density. The purple line, defined by NAM, represents the trend through this set.

Results of petrophysical analysis

In Table C-3 to Table C-6 a summary of the available porosity data for all thirteen wells in the Eemskanaal cluster is provided. This includes map derived porosities, average porosities of NAM's porosity profiles, petrophysical analysis results from TNO, and porosities calculated with the linear RHOB-CPOR relation by TNO. Most of the porosity profiles by NAM are calculated with their RHOB-CPOR relation.

Table C-3. Overview of determined and calculated porosity values for the USS3.res reservoir interval.

USS3.res						
Well	Top (mTVD)	Base (mTVD)	Porosity (%)			
			NAM maps	NAM logs	TNO Petrophysics	RHOB-CPOR
EKL-1	2761.79	2789.52	17	14.6	14.3	12.8
EKL-2	2802.07	2832.37	13	12.2	12.2	11.8
EKL-3	2749.61	2780.15	16	15.7	16.2	16.0
EKL-4	2722.19	2753.61	18	18.2		
EKL-5	2753.92	2782.72	18	18.4		
EKL-6	2752.29	2781.84	18	18.2		
EKL-7	2718.54	2748.59	18	18.5		19.5
EKL-8	2724.32	2752.32	18	17.2		
EKL-9	2727.51	2752.07	17	18.9		
EKL-10	2727.62	2753.66	16	15.3		
EKL-11	2730.62	2756.94	16	16.3		
EKL-12	2750.00	2777.76	17	17.8	17.9	18.8
EKL-13	2937.23	2968.07	16	16.5	17.6	15.7

Table C-4. Overview of determined and calculated porosity values for the USS2.res reservoir interval.

USS2.res						
Well	Top (mTVD)	Base (mTVD)	Porosity (%)			
			NAM maps	NAM logs	TNO Petrophysics	RHOB-CPOR
EKL-1	2792.12	2834.63	18	17.5	17.4	15.1
EKL-2	2834.35	2875.31	12	10.6	10.7	9.8
EKL-3	2783.33	2825.72	17	15.0	15.3	14.9
EKL-4	2756.46	2797.94	20	20.8		
EKL-5	2785.6	2827.61	20	19.5		
EKL-6	2785.2	2827.09	18	18.7		
EKL-7	2751.55	2794.87	19	19.7		20.8
EKL-8	2755.06	2801.34	20	18.7		
EKL-9	2755.56	2801.51	19	20.7		
EKL-10	2756.25	2803.15	17	16.9		
EKL-11	2759.68	2805.95	18	18.7		
EKL-12	2780.33	2827.97	18	17.6	17.8	18.0
EKL-13	2971.17	3021.01	17	17.0	17.2	14.6

Table C-5. Overview of determined and calculated porosity values for the USS1.res reservoir interval.

USS1.res						
Well	Top (mTVD)	Base (mTVD)	Porosity (%)			
			NAM maps	NAM logs	TNO Petrophysics	RHOB-CPOR
EKL-1	2837.53	2875.47	16	15.0	14.5	14.1
EKL-2	2877.44	2917.6	13	12.6	12.5	12.1
EKL-3	2829.51	2868.19	15	13.7		13.9
EKL-4	2800.19	2837.77	17	17.8		
EKL-5	2829.44	2866.33	16	14.4		
EKL-6	2829.53	2868.54	16	16.5		
EKL-7	2797.1	2833.77	18	18.0		19.1
EKL-8	2805	2840.48	16	17.3		
EKL-9	2804.85	2840.82	16	16.9		
EKL-10	2806.2	2841.83	15	14.2		
EKL-11	2808.99	2843.22	15	15.5		
EKL-12	2830.84	2866.64	15	14.8	14.8	14.0
EKL-13	3024.18	3072.98	13	12.9		

Table C-6. Overview of determined and calculated porosity values for the LSS2.res reservoir interval.

LSS2.res						
Well	Top (mTVD)	Base (mTVD)	Porosity (%)			
			NAM maps	NAM logs	TNO Petrophysics	RHOB-CPOR
EKL-1	2877.76	2922.87	11	14.1	11.7	11.8
EKL-2	2919.73	2921.7	11	7.1	6.6	
EKL-3	2871.38	2894.15	11	9.9		13.2
EKL-4	2841.38	2886.15	12	13.3		
EKL-6	2871.13	2896.88	11	11.1		
EKL-7	2837.48	2884.97	12	12.2		12.5
EKL-8	2845.05	2884.94	12	13.9		
EKL-9	2845.68	2895.68	12	13.3		
EKL-10	2845.33	2897.25	11	10.7		
EKL-11	2846.87	2898.27	11	12.0		
EKL-12	2869.21	2915.09	14	15.1	13.1	13.4

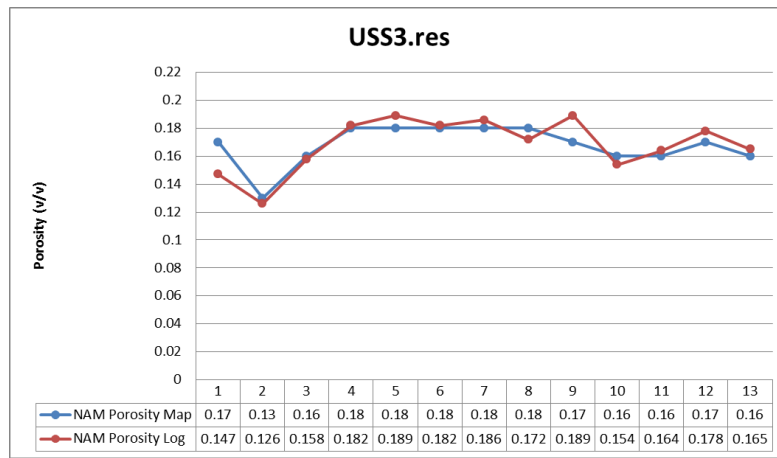


Figure C-3. NAM Porosity from maps at well locations (blue) and average porosity from NAM's porosity logs (red) for the USS3 reservoir.

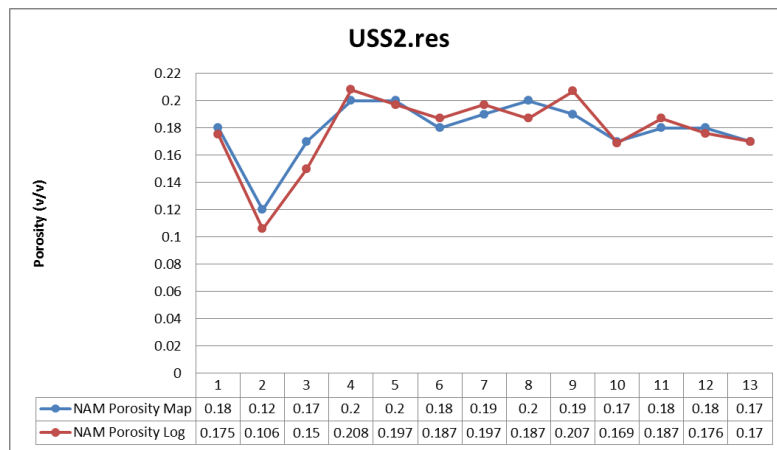


Figure C-4. NAM Porosity from maps at well locations (blue) and average porosity from NAM's porosity logs (red) for the USS2 reservoir.

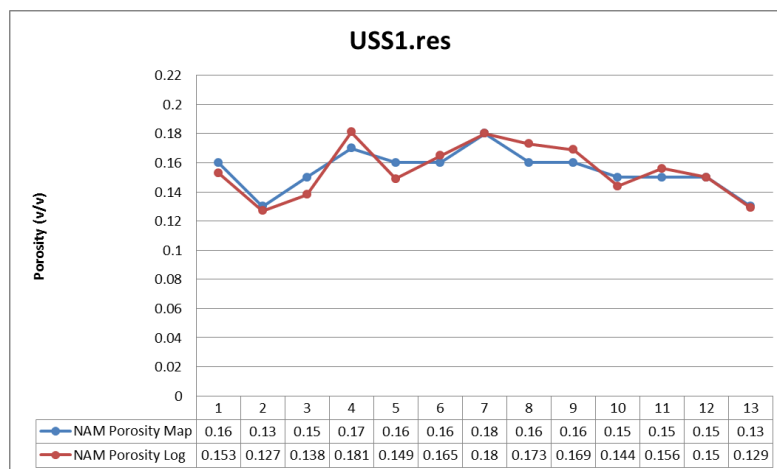


Figure C-5. NAM Porosity from maps at well locations (blue) and average porosity from NAM's porosity logs (red) for the USS1 reservoir.

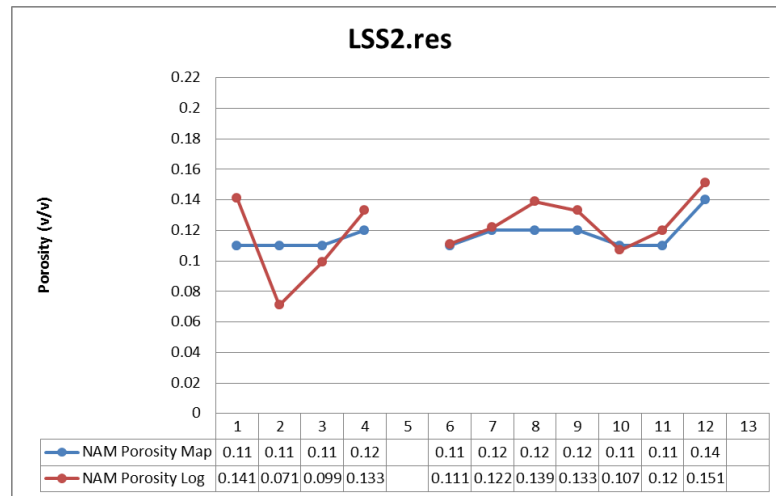


Figure C-6. NAM Porosity from maps at well locations (blue) and average porosity from NAM's porosity logs (red) for the LSS2 reservoir

Evaluation of porosity models

This section evaluates the analyses results from TNO and the porosity model, porosity maps, and porosity calculations performed by NAM focusing on the area in the vicinity of Eemskanaal. The objective is to scan whether average porosities in the GFR2012 model are valid or not, since small differences in porosity can possibly explain observed higher compaction rates than modelled compaction rates.

Comparison between NAM porosity profiles and petrophysical analyses by TNO

Table C-3 to Table C-6 show the compared values from TNO's and NAM's porosity values for each reservoir unit.

For the three Upper Slochteren Sandstone units only minor differences are observed between results from the porosity profiles of NAM and analyses of TNO. This consistency supports the validity of the results of NAM.

For all three wells in which the Lower Slochteren Sandstone unit was encountered, TNO's porosity values are significantly lower than those calculated by NAM (Table C-6). An explanation of this difference can be a difference in analysis method. NAM calculated most porosity profiles by using their RHOB-CPOR method, while the compared values by TNO are results from petrophysical analyses. In fact, TNO's values are closer to the values in NAM's porosity maps, thereby supporting the validation of the porosity maps at the well locations.

In summary the porosity profiles by NAM – except for LSS2.res – show a good match with the results from petrophysical analyses by TNO.

Comparison of the linear correlation method

This section discusses NAM's and TNO's linear correlation methods used to calculate porosity profiles and checks their applicability for the wells in the Eemskanaal cluster area.

Figure C-2 shows two different point sets for well EKL-12. The black points represent bulk density values versus the corresponding core porosities. The purple points represent bulk density values plotted versus the corresponding porosities

from NAM's porosity profile. A clear difference in the trend of both point sets can be observed. The black line has a slightly steeper slope than the purple line. This difference is probably caused by the application of a general relation for the entire Groningen Field (although corrected for depth and shale volume) to the density log of EKL-12.

The review of SGS on this method states that the mean error is about 0.5 pu (SGS 2013). Because this concerns an average value, the error of individual wells may be higher than 0.5 pu which apparently is the case in Well EKL-12.

The difference in slope for both trend lines in Figure C-2 is expressed in the average porosities calculated for other wells. Determined RHOB-CPOR values above ca. 18% porosity are generally higher than the NAM log porosity, and lower than NAM's porosity profile when below 18%.

When evaluating the porosities calculated by NAM, the difference at lower porosities is less interesting because its effect on compaction is relatively low. More interesting however are the differences at higher porosities. Because there is some uncertainty in the correlation defined by TNO, it is probably not suitable to calculate highly accurate porosities. However, the difference in the relations of NAM and TNO indicate there is a range of uncertainty over the entire porosity range. At porosities higher than 18% the relation of TNO calculates higher porosities than NAM's relation, up to 1-2 pu difference.

Comparison between porosity maps and log porosities

NAM calculated average porosity maps for each reservoir unit by co-kriging the log based reservoir porosities from all available profiles with average porosity trend maps. The porosity modelling and construction of the trend maps by NAM is further explained in (NAM 2013).

In order to validate the results of the interpolation process, the calculated porosity profile values were averaged for each reservoir unit identified by NAM. Similar to NAM, TNO used a cut-off of 0.41. The average porosity profile values and the mapped porosity values at the well locations are presented in Table C-3 to Table C-6.

Except for the Lower Slochteren reservoir unit LSS2.res, the log average porosity values in the wells closely resemble the average mapped porosity values of all other reservoir units. From this resemblance TNO concludes in overall that NAM's porosity interpolation methodology properly honors the input data.

It is not clear from the report (NAM 2013) what causes the overall higher log porosity compared to mapped porosity in reservoir unit LSS2 (Well EKL-02 shows a strong negative difference which is probably caused by an inaccurate log average due to a small reservoir thickness of about 2 m). Although observed, this difference is not considered to affect the modelled compaction significantly because at porosities lower than 17% the compaction coefficient is hardly sensitive to porosity. In fact, the map porosities at well locations in LSS2 are closer to the porosities calculated by petrophysical analyses by TNO, which supports the validity of the porosity maps at well locations.

Compaction coefficient

In addition to the evaluation of NAM's porosity model in the area of the Eemskanaal cluster, TNO performed a sensitivity analysis of the effect of porosity and small scale porosity changes on the value of the compaction coefficient.

Compaction coefficient logs

In order to visualize the effect of porosity variations on the compaction coefficient, TNO constructed compaction coefficient logs. This was done by converting NAM's porosity profiles using the formula for Groningen core samples only (p. 86 in TNO 2013). The resulting log magnifies the intervals with high porosities that are especially susceptible to compaction. In a continuous log even the small scale variations and depth intervals highly sensitive to compaction can be identified. This gives much more detailed information than only a reservoir average. An example is given in Figure C-7 where the calculated compaction coefficient log of EKL-9 is shown.

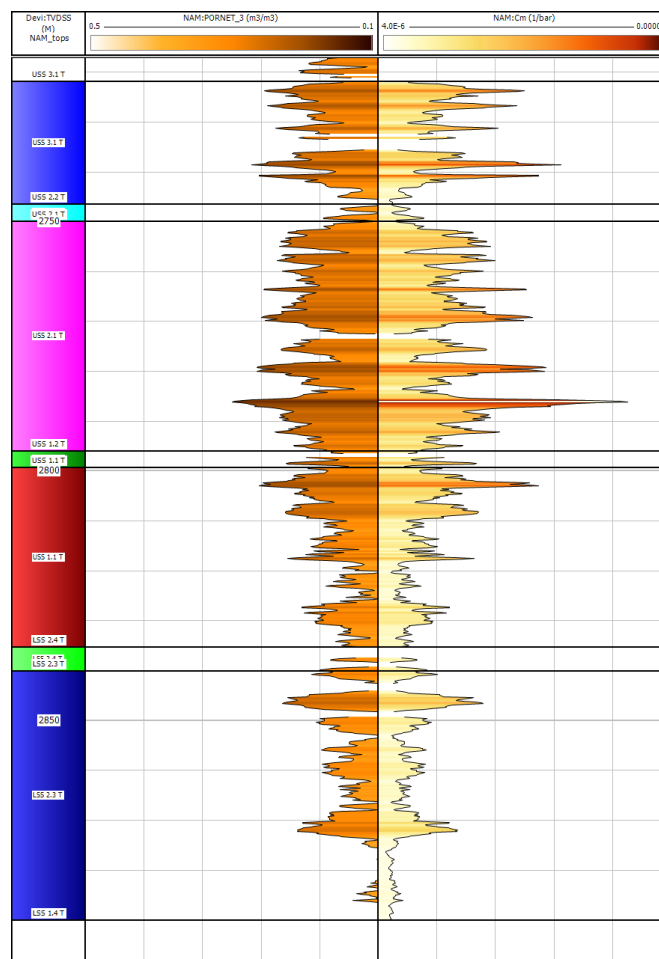


Figure C-7. EKL-09 porosity log (left) and compaction coefficient log (right). Above about 17-18% porosity the compaction coefficient increases significantly.

Compaction, and especially differential compaction generates buildup of (differential) stress that can easily be released resulting in an earthquake. By using a well panel of compaction coefficient logs depth intervals with probably a high differential compaction on a small lateral scale can be identified. TNO created such a panel for the wells in the Eemskanaal cluster in order to analyse differential compaction. Figure C-8 shows a well panel of 6 wells from West to East through the cluster; crossing two faults (see Figure 3-2).

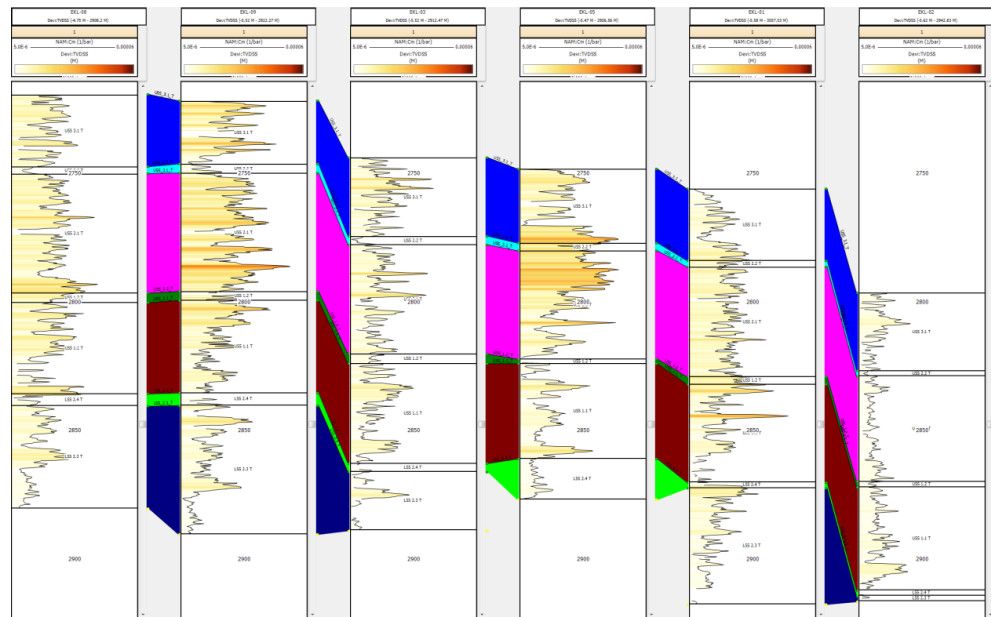


Figure C-8. Well panel from West to East through 6 wells in the Eemskanaal cluster, representing Cm logs.

Sensitivity of compaction coefficient to porosity changes

There is always a degree of uncertainty in the average porosity calculated for a reservoir unit, which inherently also results in a degree of uncertainty in the calculated compaction coefficient. Because the relation between porosity and compaction coefficient exhibits an exponentially increasing trend, the degree of uncertainty becomes even more significant at higher average porosities.

Table C-7. Calculations of the relative increase of compaction coefficient with respect to 1% and 2% porosity increase for well EKL-09.

EKL-09					Phi + 1 pu		Phi + 2 pu	
Interval	Phi	Cm	Cm + 1 pu	Cm + 2 pu	Phi increase	Cm increase	Phi increase	Cm increase
USS3.res	18.9	1.45E-05	1.61E-05	1.79E-05	5.3%	11.1%	10.6%	23.6%
USS2.het	13.1	8.00E-06	8.64E-06	9.40E-06	7.6%	8.0%	15.3%	17.5%
USS2.res	20.7	1.68E-05	1.88E-05	2.09E-05	4.8%	11.5%	9.7%	24.4%
USS1.het	17.7	1.21E-05	1.34E-05	1.49E-05	5.6%	10.9%	11.3%	23.2%
USS1.res	16.9	1.15E-05	1.27E-05	1.41E-05	5.9%	10.4%	11.8%	22.4%
LSS2.het	14.5	8.95E-06	9.77E-06	1.07E-05	6.9%	9.2%	13.8%	19.9%
LSS2.res	13.3	8.65E-06	9.38E-06	1.02E-05	7.5%	8.4%	15.0%	18.3%
LSS1.het	6.1	5.63E-06	5.79E-06	5.97E-06	16.4%	2.8%	32.8%	6.0%

TNO quantified the effect of small average porosity variations on the average compaction coefficient of a reservoir unit by increasing the porosity with 1 and 2 pu. Results of these calculations on well EKL-9 are given in Table C-7 This table clearly shows that the relative increase in compaction coefficient is much higher compared

to the relative increase in average porosity at higher porosities (e.g. USS2.res). An increase of 1 or 2 pu on low porosity reservoirs (e.g. LSS1.het) results in a significantly smaller increase in compaction coefficient. From these results it can be concluded that, depending on the average porosity of an interval, an increase of porosity of 1 or 2 pu can lead to a significant increase in calculated compaction.

Summary of Results

These are the results of the independent evaluation by TNO and the comparison with the evaluations by NAM:

- Results from petrophysical analyses performed by TNO match with NAM's porosity profiles in the Upper Slochteren interval. A difference in porosity occurs in the Lower Slochteren reservoir LSS2. However, the results of TNO match properly with NAM's porosity maps. This generates more confidence in the validity of the porosity maps.
- The linear correlation between bulk density and porosity used by NAM is a general relation, corrected for well specific depth and shale volume. A similar relation is defined by TNO, based on well data from a well in the Eemskanaal cluster. Although this relation has a higher uncertainty because it is based on data of a single well, it will give a more location specific porosity estimation.
- Because there is some uncertainty in the correlation defined by TNO, it is probably not suitable to calculate highly accurate porosities. However, the difference in the relations of NAM and TNO indicate there is a range of uncertainty over the entire porosity range. At porosities higher than 18% the relation of TNO calculates higher porosities than NAM's relation, up to a difference of 1-2 pu.
- The porosity model and maps created by NAM show, at well locations, a good match with averages from their porosity profiles. Except for the Lower Slochteren interval, where most of NAM's porosity profiles give higher porosity values at the well locations.
- Compaction coefficient logs show that already a slight increase in porosity (1-2 pu) possibly has a relatively large effect on (differential) compaction, especially in the high porosity range.

D Geological information at location Eemskanaal based on static model GFR2012

Eemskanaal cluster well information

Table D-1. List of wells in the production cluster Eemskanaal with their location (RD reference system) and top Rotliegend in True Vertical Depth (TVD in m) and measured depth (MD in m along hole).

Well	X	Y	TVD	MD
EKL-01	241629.6	584395.3	2737.1	2744.0
EKL-02	241666.6	584654.8	2747.8	2754.5
EKL-03	241560.3	584485.4	2690.9	2702.8
EKL-04	242403.9	584608.9	2659.1	2840.0
EKL-05	241529.4	584196.6	2689.3	2721.5
EKL-06	241555.0	584392.9	2692.6	2699.1
EKL-07	241363.9	584166.5	2654.3	2716.9
EKL-08	241423.0	584300.9	2662.5	2693.0
EKL-09	241409.2	584384.1	2662.6	2693.4
EKL-10	241353.8	584529.7	2664.1	2695.3
EKL-11	241345.6	584663.2	2666.2	2697.3
EKL-12	241028.7	585199.1	2684.4	2838.0
EKL-13	239568.7	582119.0	2870.8	4371.0
TBR-04	238869.0	586648.0	2733.5	2752.0
BDM-01	233582.0	591079.0	2819.0	2960.0
BDM-02	233598.0	591120.0	2830.0	2959.0
BDM-03	233601.1	591081.5	2862.1	3285.0
BDM-04	233580.2	591137.7	2850.0	3253.0

Structural information

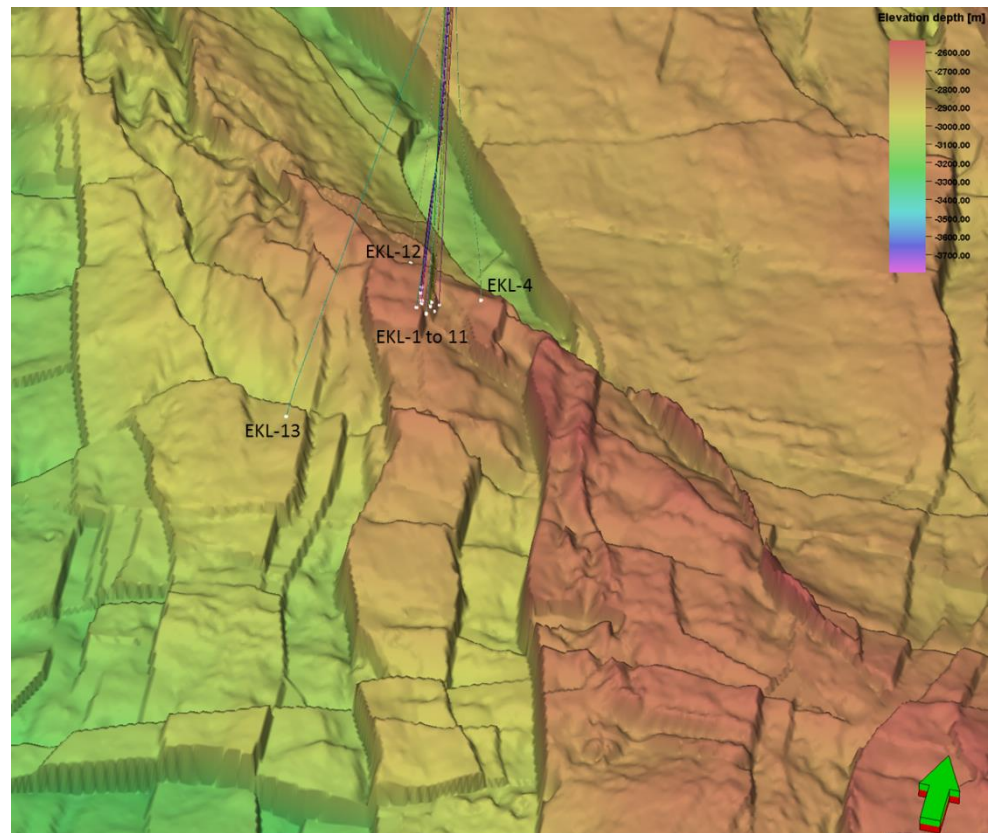


Figure D-1 Position of Eemskanaal cluster wells on Top Rotliegend depth surface (GFR2012).

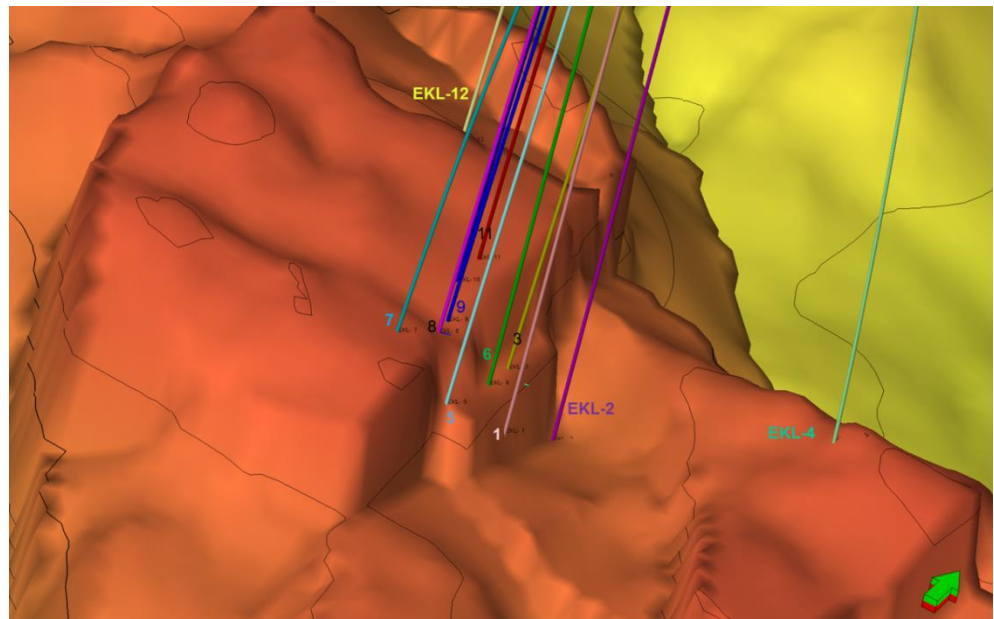


Figure D-2 Close-up of position of Eemskanaal cluster wells EKL-1 to EKL-12 on Top Rotliegend depth surface (GFR2012).

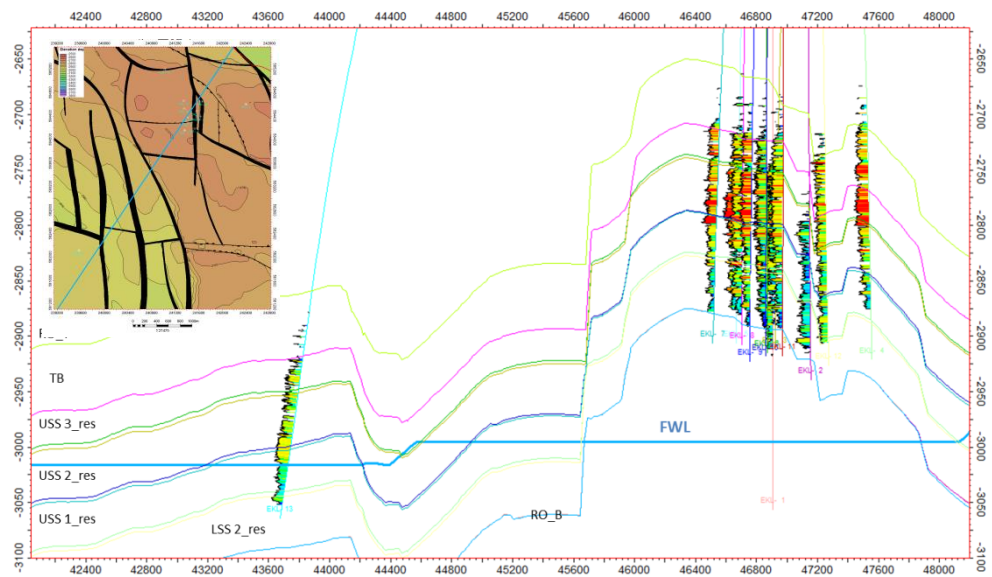


Figure D-3 Transect showing the different FWL at the EKL-13 location (Harkstede block) at 3016 mTVD in the Upper Slochteren 1 zone vs the 2995mTVD at the Eemskanaal cluster location (FWL in the Carboniferous).

Porosity information Eemskanaal

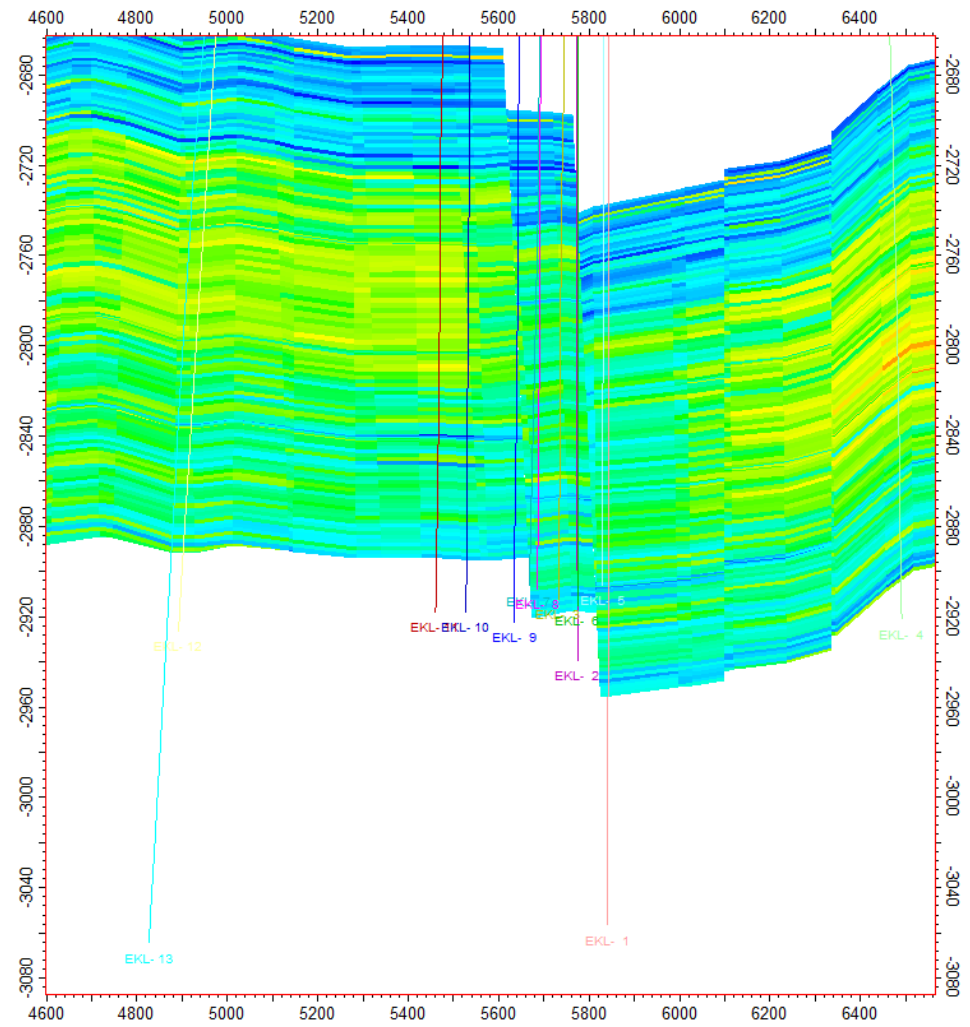


Figure D-4 Transect through Eemskanaal cluster shows lower porosity in downthrown blocks.

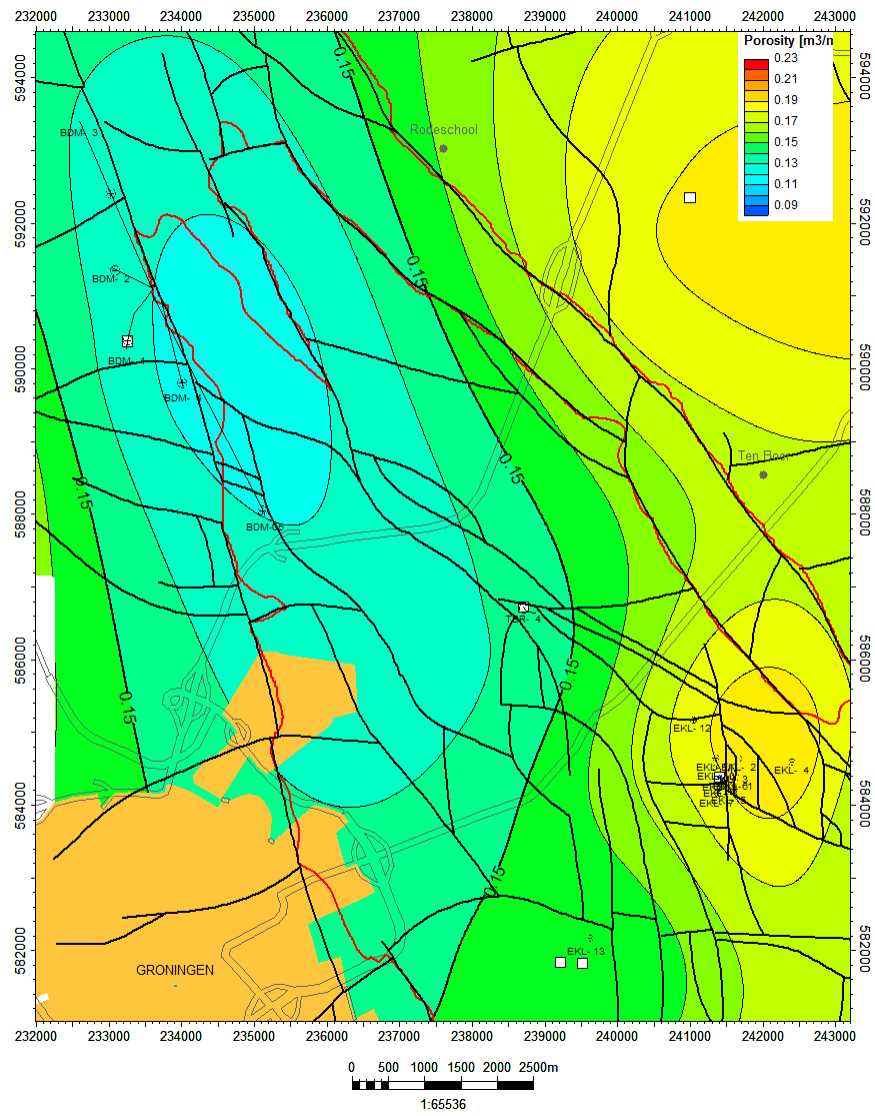


Figure D-5 Porosity trend map for the Upper Slochteren 3 reservoir zone (USS3.res). The white squares indicate the wells NAM considered to be relevant to create the trend map (GFR2012). From the GFR2012 report it is unclear which Eemskanaal was chosen apart from the EKL-13 well.

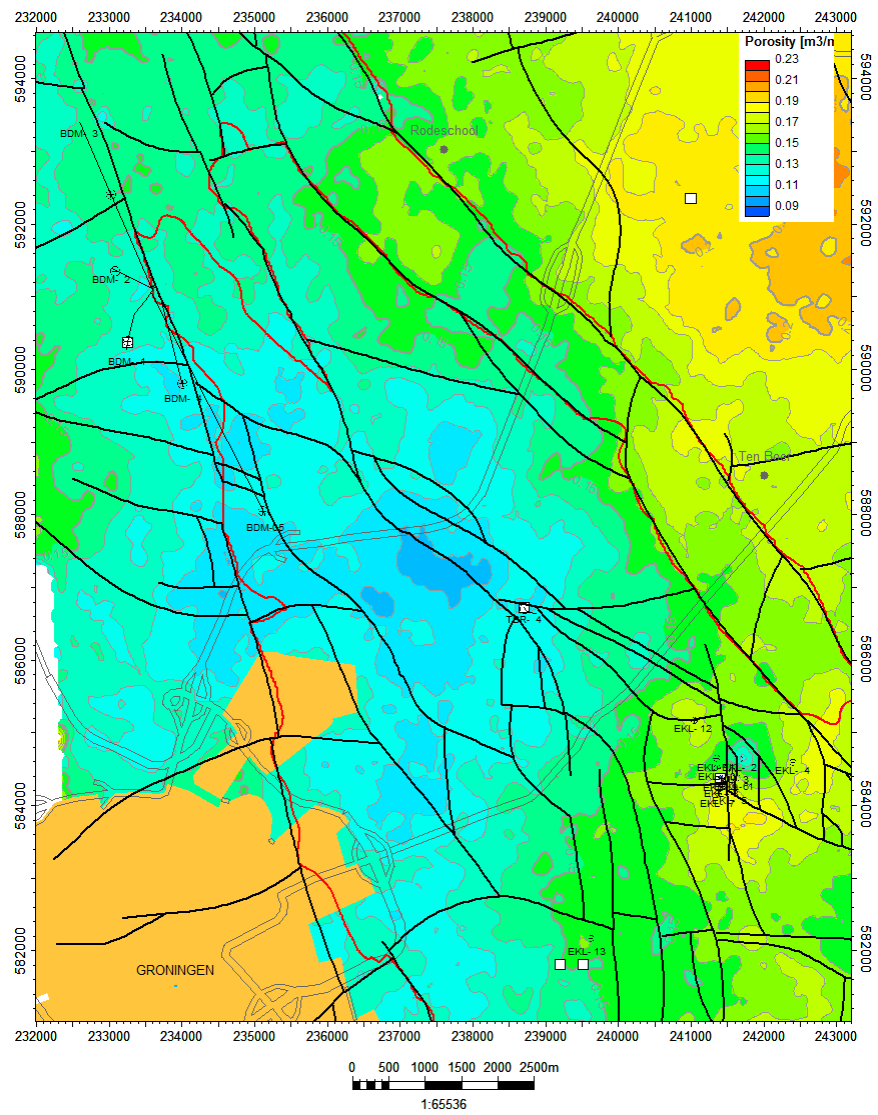


Figure D-6 Average porosity map for the USS3.res zone based on the GFR2012 porosity model at the Eemskanaal location.

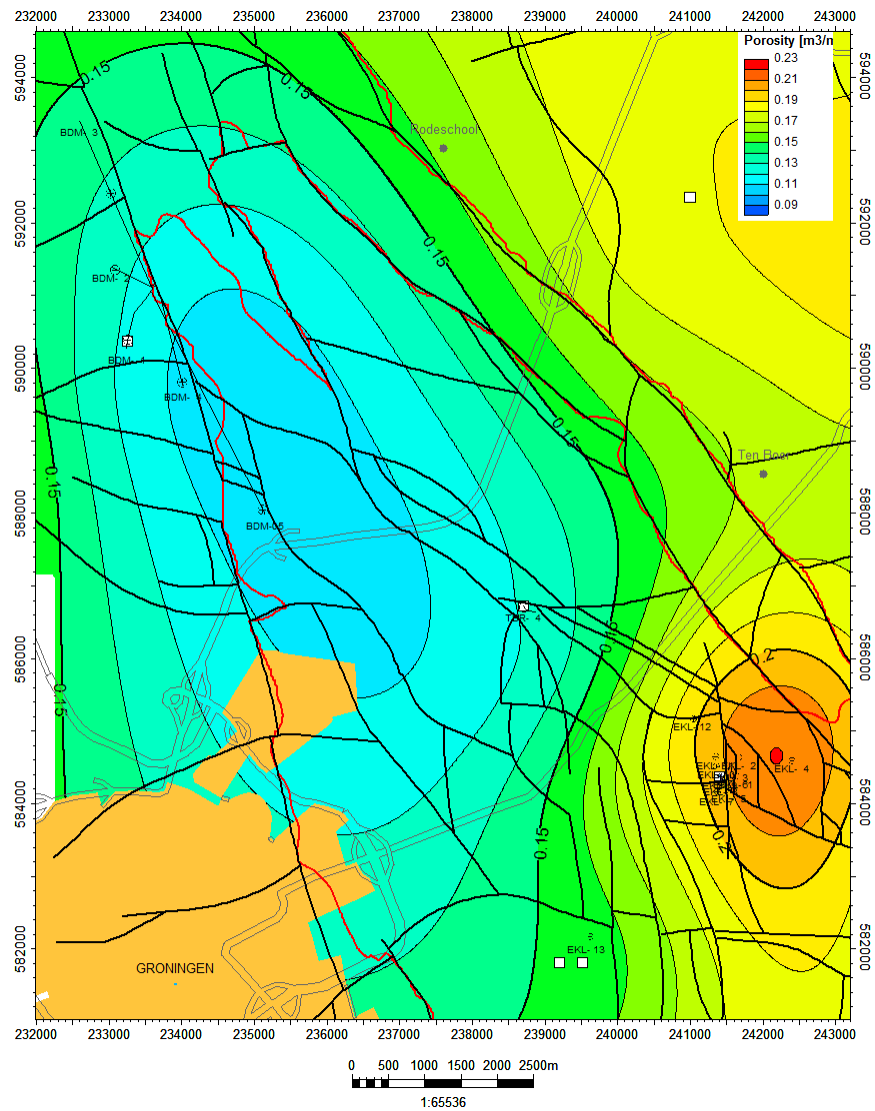


Figure D-7 Porosity trend map for the Upper Slochteren 2 reservoir zone (USS2.res). The white squares indicate the wells NAM considered to be relevant to create the trend map (GFR2012). From the GFR2012 report it is unclear which Emskanaal was chosen apart from the EKL-13 well.

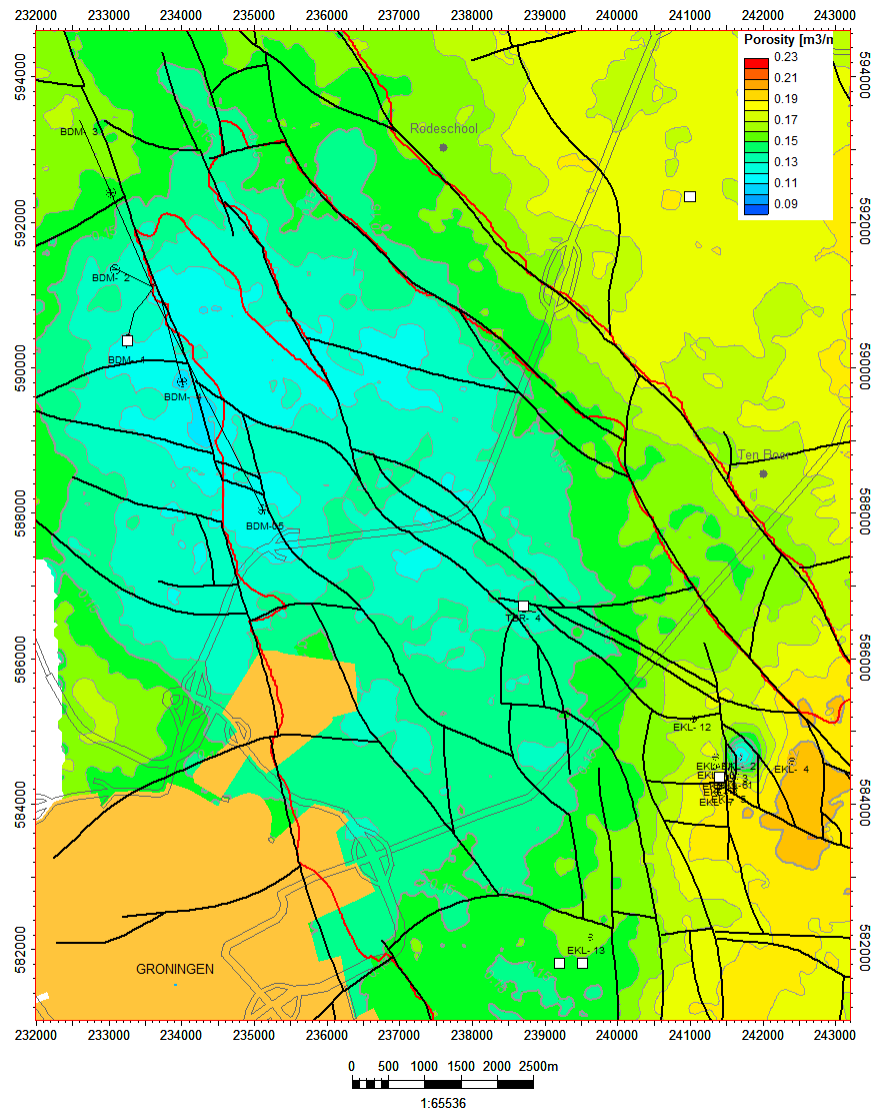


Figure D-8 Average porosity for the USS2.res zone based on the GFR2012 porosity model at the Eemskanaal location.

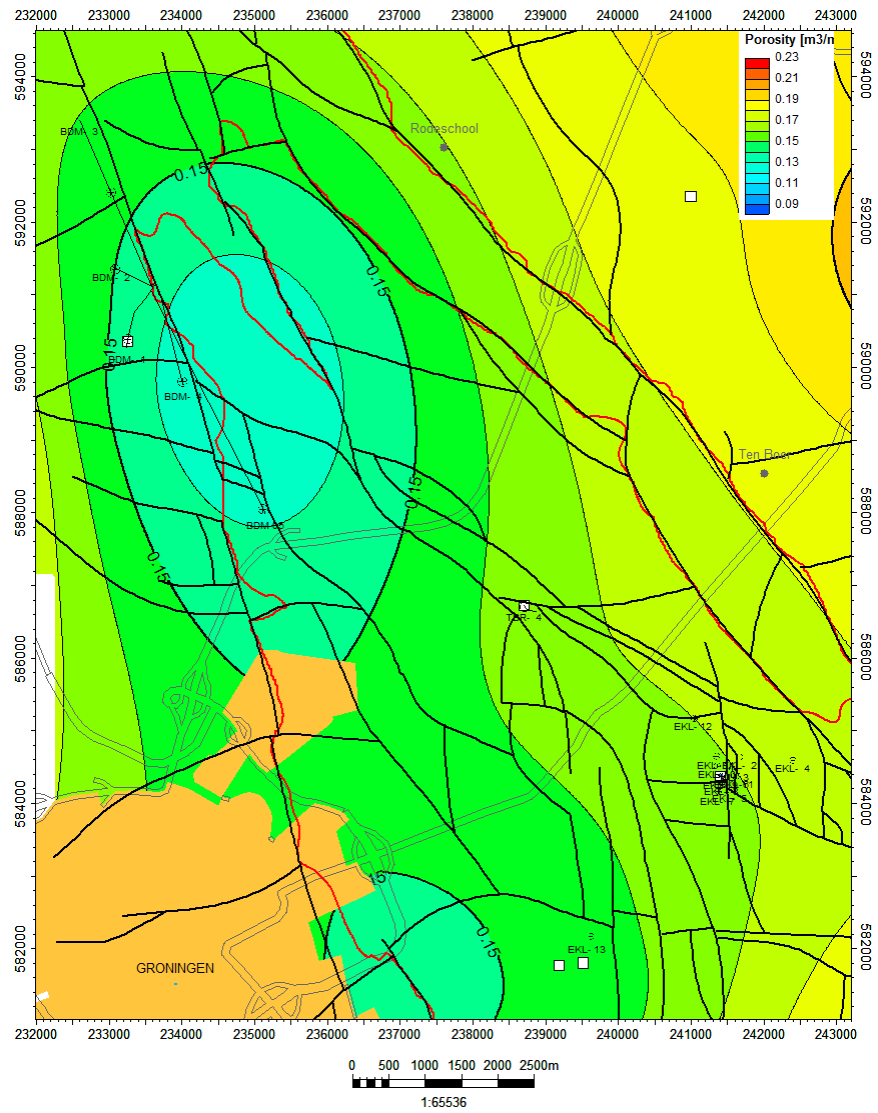


Figure D-9 Porosity trend map for the Upper Slochteren 1 reservoir zone (USS1.res). The white squares indicate the wells NAM considered to be relevant to create the trend map (GFR2012). From the GFR2012 report it is unclear which Eemskanaal was chosen apart from the EKL-13 well.

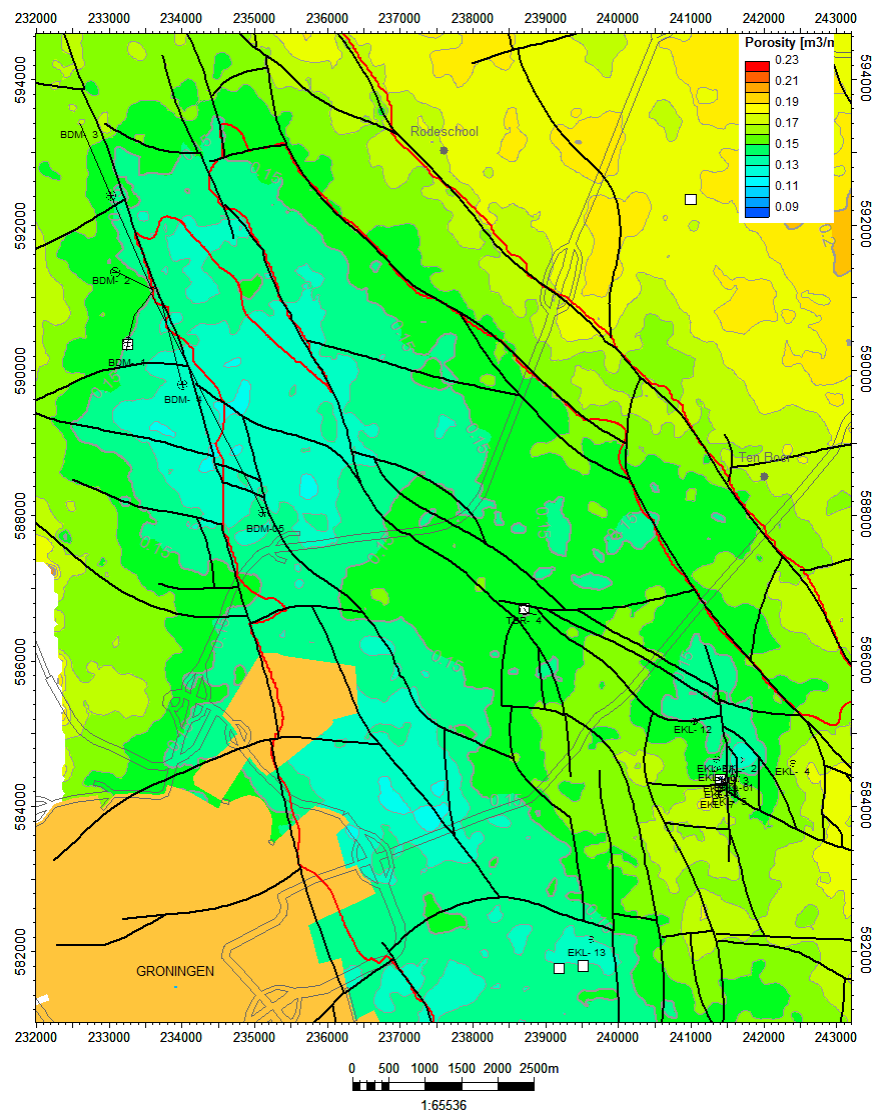


Figure D-10 Average porosity for the USS1.res zone based on the GFR2012 porosity model at the Eemskanaal location.

E Reservoir dynamics

Figure E-1 shows the pressure distribution in the top of ROSLU in October 2014 for three models: the production plan model, STR38 and STR40. For the production plan model the pressures are shown on 1-1-2014. For STR40, the pressure support in the south-west corner of the model is very clear.

Figure E-2 and Figure E-3 illustrate the effect of the changed viscosity of the Lauwersee aquifer. This shows that the high pressure in the south-west corner in STR40 is the result of a combination of reduced permeability below FWL and the decrease in viscosity of the analytical Lauwersee aquifer. The extra support from the lower viscosity of the aquifer improved the fit considerably in the Harkstede block (Figure E-3).

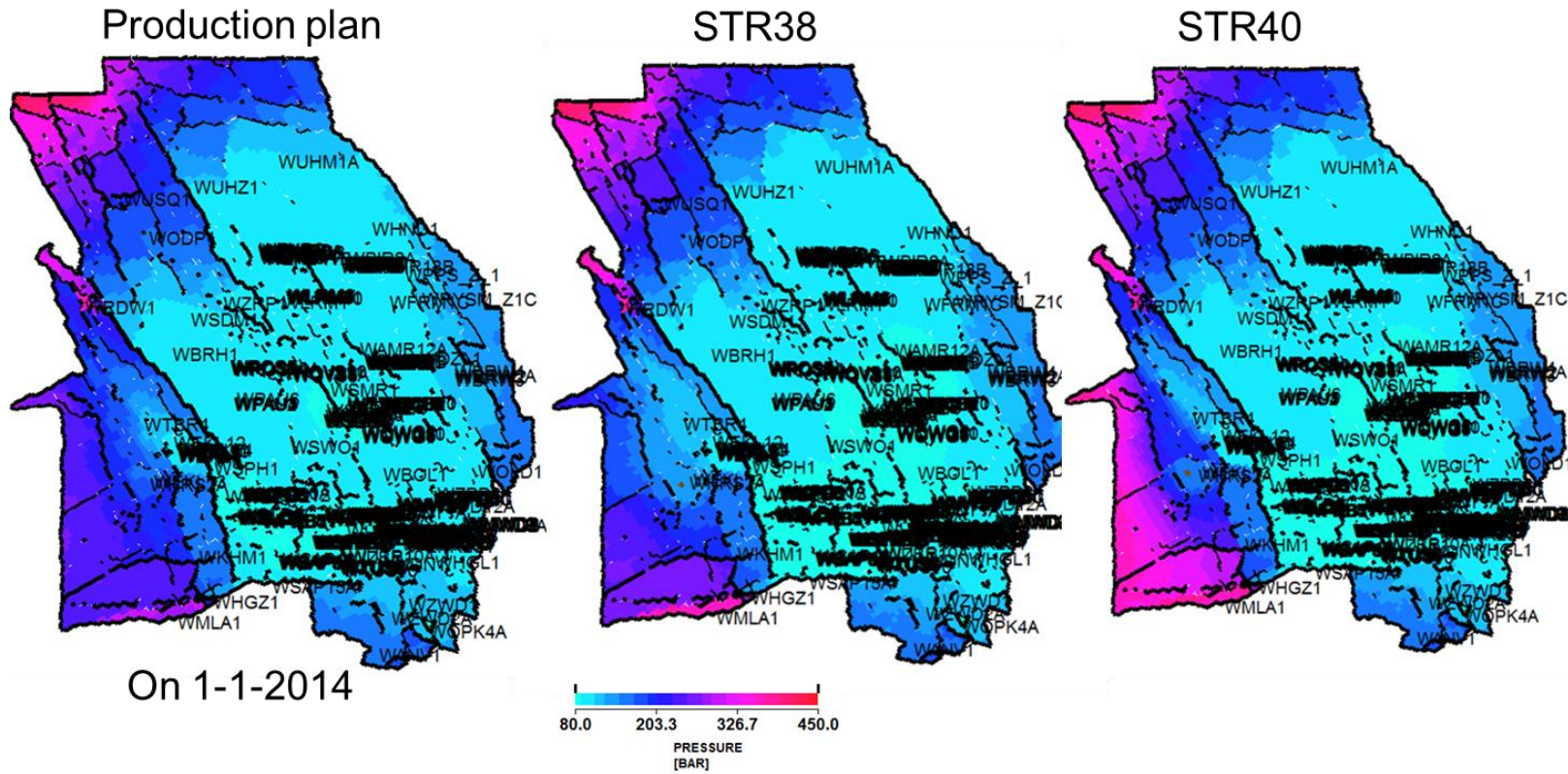


Figure E-1. Pressure in the top of the Upper Slochteren formation (ROSLU, model layer 4) showing the effect of the aquifer in Oct 2014

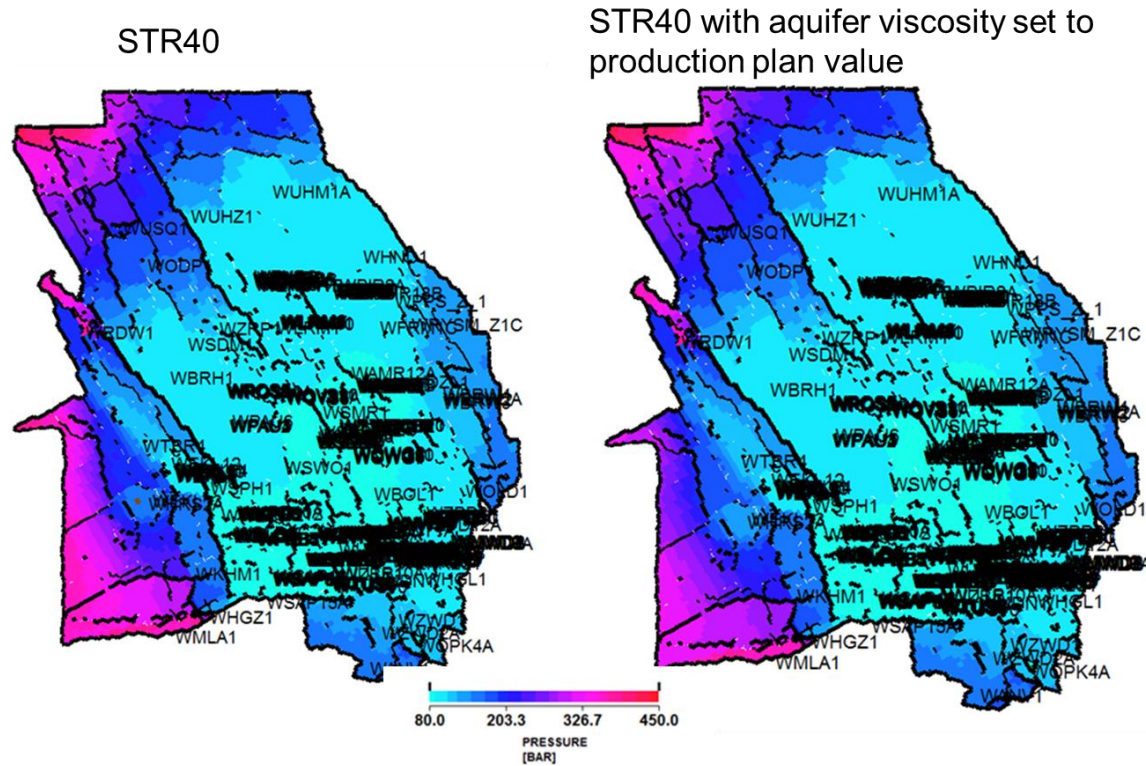


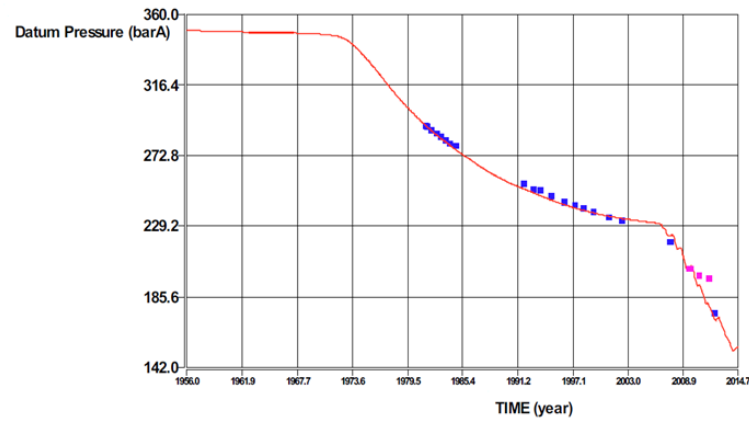
Figure E-2. Pressure on 1 Oct 2014 in the top of Upper Slochteren formation (ROSLU, model layer 4), for STR 40 (left) and STR40 with viscosity of the Lauwersee aquifer from the production plan model (right).

STR40

Runfile: BestMatch_v31_Prod2014octSTR40_SubCorrection_SodM.run



Table Name: WHRS2A_PRES
Plot Name: SPTG_WHRS_plot
Time=2014.744011 [YEAR]



STR40 with aquifer viscosity set to production plan value



Table Name: WHRS2A_PRES
Plot Name: SPTG_WHRS_plot
Time=2014.744011 [YEAR]

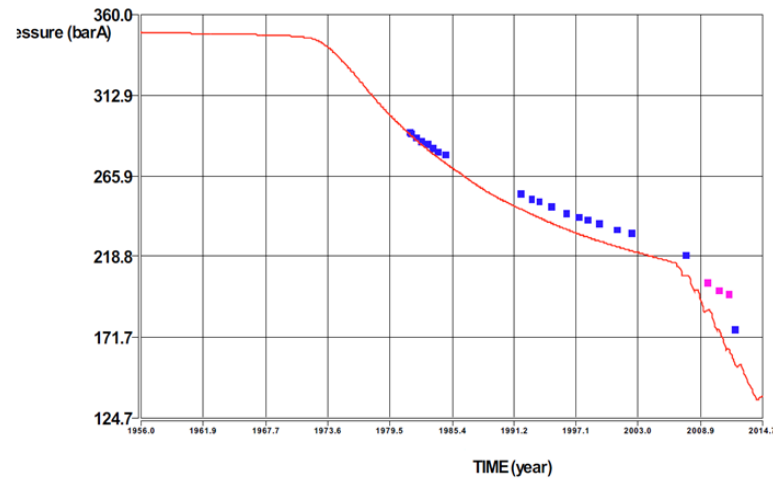


Figure E-3. Pressure history match for well HRS-2A for STR40 (left) and STR40 with the viscosity of the Lauwersee aquifer from the production plan model (right).

F Earthquake density maps for 2003 to 2012

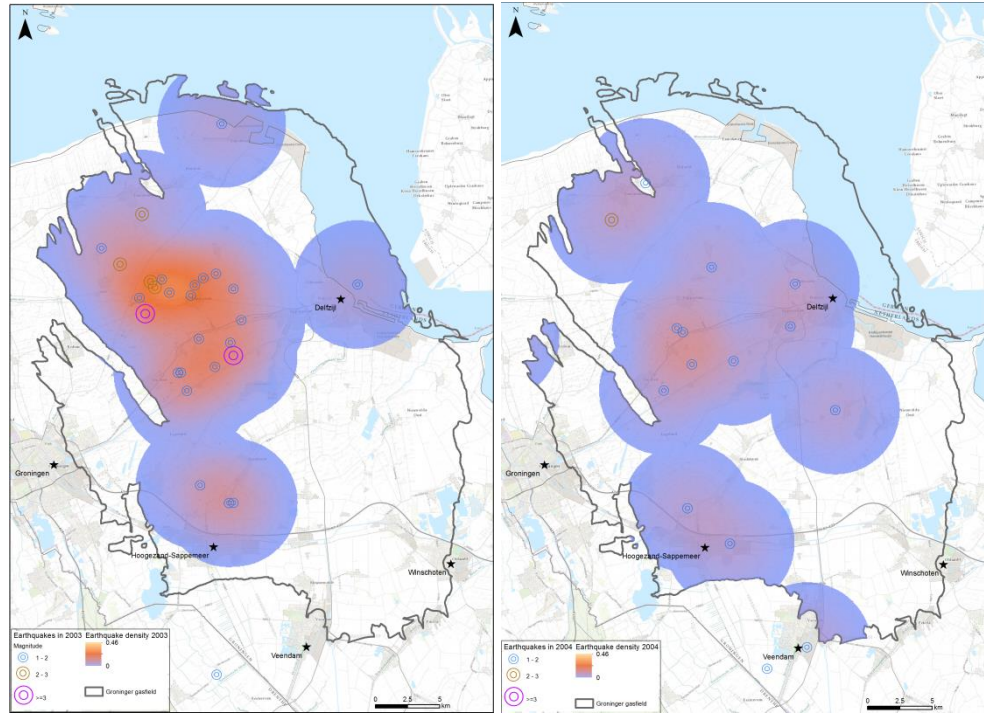


Figure F-1. Earthquake density (number of events per km²) in 2003 (left) and 2004 (right).

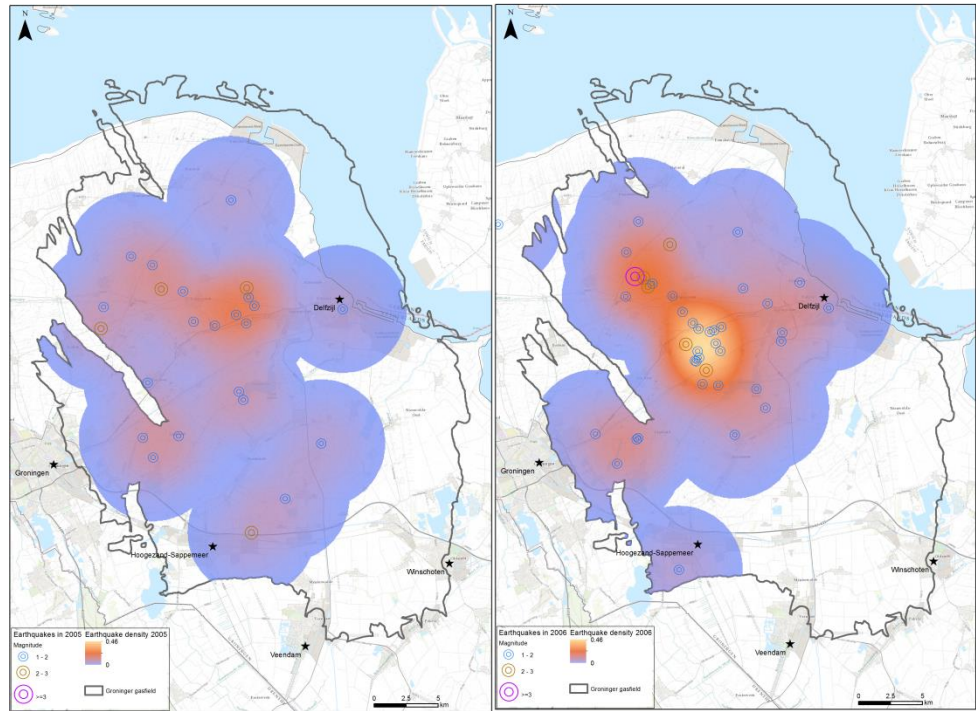


Figure F-2. Earthquake density (number of events per km²) in 2005 (left) and 2006 (right).

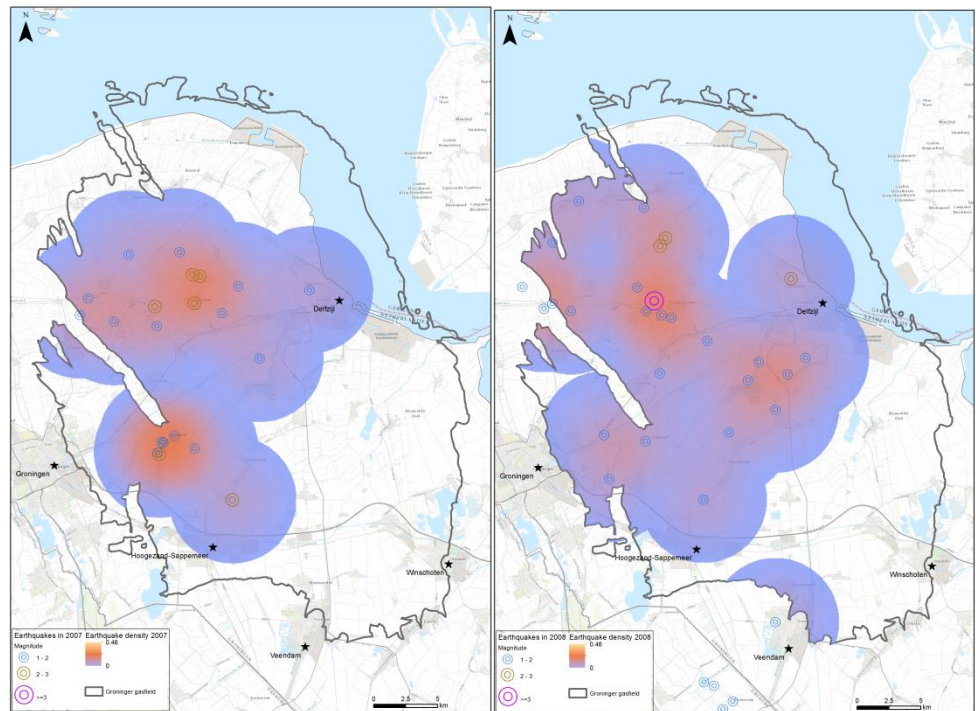


Figure F-3. Earthquake density (number of events per km²) in 2007 (left) and 2008 (right).

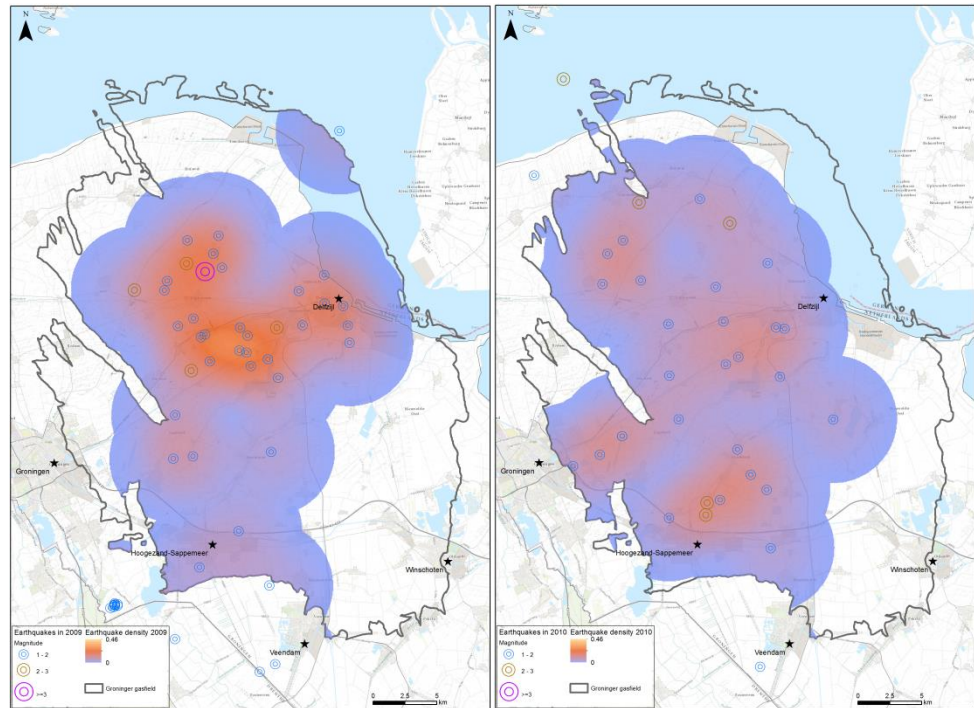


Figure F-4. Earthquake density (number of events per km²) in 2009 (left) and 2010 (right).

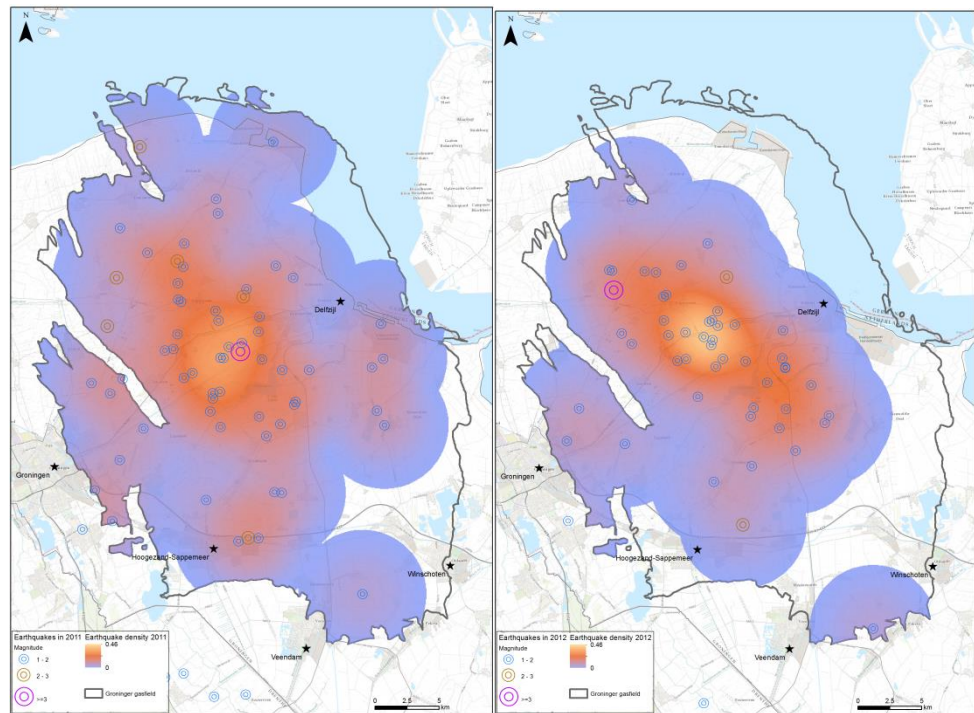


Figure F-5. Earthquake density (number of events per km²) in 2011 (left) and 2012 (right).